Technische Universität München

Fakultät für Medizin

Klinikum rechts der Isar

Klinik und Poliklinik für Plastische Chirurgie und Handchirurgie

(Direktor: Prof. Dr. Hans-Günther Machens)

Superficial Burns & Secondary Burn-Injury Progression: A Rat Model for Topical Application of Tissue Protective Agents

Fabian Dominik Weiß

Vollständiger Abdruck der von der Fakultät für Medizin der Technischen Universität München zur Erlangung des akademischen Grades eines Doktors der Medizinischen Wissenschaften (Dr. med. sci.) genehmigten Dissertation.

Vorsitzender: apl. Prof. Dr. Klaus-Peter Janssen

Prüfer der Dissertation:

1. apl. Prof. Dr. Yves Harder
2. Priv.-Doz. Dr. Alexander Konstantinow

Die Dissertation wurde am 05.03.2020 bei der Technischen Universität München eingereicht und durch die Fakultät für Medizin am 07.10.2020 angenommen.

für
meine Eltern

1 Contents

2 Figure Legends

3 Table Legends

4 Overview of Abbreviations

%	percent
%TBSA	percentage of total body surface area
°C	degrees Celsius
a.U.	arbitrary unit(s)
approx.	approximately
b.i.	burn induction
bw	bodyweight
BWP	burn wound progression
CCD	charged-coupled device
cm	centimeter(s)
d	day(s)
d1	measurement point at one day after burn induction
d10	measurement point at ten days after burn induction
d14	measurement point at fourteen days after burn induction (two weeks)
d2	measurement point at two days after burn induction
d4	measurement point at four days after burn induction
d7	measurement point at seven days after burn induction (one week)
DNA	deoxyribonucleic acids
DSMO	dimethyl sulfoxide
E-collar	Elizabethan collar
FDA	Food and Drug Administration
g	gram(s)
G	gauge
GABA	gamma-Amino butyric acid
h	hour(s)
h1	measurement point at one hour after burn induction
h8	measurement point at eight hours after burn induction
HE	haemotoxylin and eosin staining
i.e.	id est; Latin “that is”
i.p.	intraperitoneal
i.v.	intravenous
I°	first-degree burn; superficial / epidermal burn
ICG	indocyanine green
IIa°	second-degree burn, superficial partial-thickness burn
IIb°	second-degree burn, deep partial-thickness burn
III°	third-degree burn, full-thickness burn
IV°	fourth-degree burn, subdermal burns
IVC	individually ventilated cages
kg	kilogram(s)
l	liter(s)
LDI	Laser Doppler Imaging
LSCI	Laser-Speckle-Contrast-Imaging
min	minute(s)
ml	milliliter(s)
mm	millimeter(s)
n	size of the statistic sample
n.a.	not available
O_2	oxygen
pH	potential of hydrogen
ROI	region of interest
ROS	reactive oxygen species
SD	standard deviation
sec	second(s)
SEM	standard error of the mean
TBSA	total body surface area
TNFα	tumor necrosis factor alpha
UV	ultraviolet
V	Volt(s)
VEGF	vascular endothelial growth factor
w	week(s)
ZPF	Zentrum für Präklinische Forschung

5 Summary

5.1 English Abstract

Background: Due to secondary burn wound progression (BWP), a burn injury extends in depth and surface within 48-72 hours, thus augmenting morbidity and mortality. Today, there is no standardized approach to prevent BWP despite numerous pre-clinical tests of tissue protective agents. Adverse effects of mainly systemic administration often limit the tested substances. A commonly used animal model to investigate BWP and tissue protective agents is the "burn comb model" by which a full-thickness burn with intercalated unburned interspaces is induced on a rat's back.

Goal: The aim of this animal study was to establish a modified burn comb injury that progresses to the intermediate dermis if left untreated and allows macroscopic, microscopic and perfusion data collection; and to design a sparsely restricting frame dressing that enables safe and reproducible topical drug application.

Methods: After preliminary trials with 12 Wistar rats, 17 rats' dorsa were burned with 10 seconds application of a preheated metal stamp, resulting in an injury of 8 20x10mm burn fields and 6 unburned 20x5mm interspaces. A manifold varied 8-components aluminium frame was sutured onto the back of 12 animals and combined with an Elizabethan collar. At defined time points over a 14-day course, photo documentation and Laser-Speckle-Contrast-Imaging (LSCI) was performed. Frame durability was assessed with an originated score. Selective histopathological burn depth was evaluated. The results of the 10sec burn group were compared to 9 rats burned for 60 seconds.

Results: Histopathologically, the 10sec group showed a maximum wound depth in interspaces and burn fields to the intermediate dermis after an untreated progression within the first 24 hours.

In the 10sec group, interspace LSCI-perfusion was significantly higher than in the burn fields. Post-burn interspace perfusion was increased only after the 10sec burn. 10sec interspace perfusion was significantly higher and reached levels above baseline earlier - already on day 1 - than the 60sec group.

Macroscopically, a significant extension of necrosis in interspaces was seen between days 1 and 2 in both groups. Interspace necrosis was distinctively higher in the 60sec group.

The frame dressing was durable in ⅔ of the animals up to day 4. However the use of Elizabethan collars and re-suturing seemed inevitable.

Conclusion: The presented burn comb model combined with a frame dressing showed first promising results for further investigations of topical agents onto BWP. The 10sec burn comb model induced an injury to the intermediate depth, differing significantly from deeper burns in horizontal and vertical necrosis extent as well as in LSCI-perfusion.

5.2 Deutsche Zusammenfassung

Hintergrund: Durch die sekundäre Brandwundenprogression (BWP) kommt es nach Verbrennungen innerhalb von 48-72 Stunden zu einer Tiefen- und Oberflächenausdehnung der ursprünglichen Brandverletzung, was Morbidität und Mortalität erhöht. Aktuell gibt es kein standardisiertes Verfahren zur Prävention der BWP trotz vieler präklinischer Versuche mit gewebeprotektiven Wirkstoffen. Oft sind Nebenwirkungen der meist systemisch verabreichten Substanzen für eine mögliche Anwendungsmöglichkeit limitierend. Ein häufig genutztes Tiermodell zur Untersuchung der BWP und gewebeprotektiver Substanzen ist das „Burn Comb Modell“, mit dem eine allschichtige Verbrennung mit zunächst unversehrten Zwischenräumen am Rücken der Ratte induziert wird.

Zielsetzung: Ziel dieser tierexperimentellen Studie war die Etablierung einer modifizierten „Burn Comb Verbrennung“, bei der es unbehandelt zu einer Tiefenausdehnung bis in die mittlere Dermis kommt und bei der makroskopische, mikroskopische und Perfusions-Parameter bestimmt werden können; und die Etablierung eines wenig-einschränkenden Rahmenverbands zur sicheren und zuverlässigen topischen Wirkstoffapplikation.

Methodik: Nach Vorversuchen an 12 Wistar Ratten, wurde bei 17 Ratten am Rücken mittels 10-sekündiger Applikation eines erhitzten Metallstempels eine Verbrennung induziert. Es resultierte eine Verletzung von 8 20x10mm Brandflächen und 6 unverbrannten 20x5mm Zwischenräumen. Ein mehrfach modifizierter 8-Komponenten-Aluminium-Rahmen wurde auf den Rücken von 12 Tieren genäht und mit Halskrause kombiniert. Zu definierten Zeitpunkten über 14 Tage erfolgte die Fotodokumentation und Laser-Speckle-Contrast-Imaging (LSCI). Die Rahmenhaltbarkeit wurde mittels eines entwickelten Schemas beurteilt. Die Bestimmung der histopathologischen Verbrennungstiefe erfolgte zu ausgewählten Zeitpunkten. Die Ergebnisse dieser 10-sekündigen Verbrennungsgruppe wurden mit 9 Ratten verglichen, bei denen eine 60-sekündige Verbrennung durchgeführt wurde.

Resultate: Histopathologisch zeigte sich bei 10-sekündiger unbehandelter Verbrennung nach Tiefenzunahme innerhalb von 24h eine maximale Schadensausdehnung in den Zwischenräumen und Brandflächen bis in die mittlere Dermis. In der 10sec Gruppe war die Zwischenraum-LSCI-Perfusion signifikant höher als die der Brandflächen. Nur nach 10sec Verbrennung zeigte sich ein Zwischenraum-Perfusionsanstieg. Die 10sec Zwischenraum-Perfusion lag signifikant höher und

signifikant früher - bereits an Tag 1 - oberhalb des Ausgangswertes als die 60sec Zwischenraumperfusion.

Makroskopisch zeigte sich in beiden Verbrennungsgruppen ein signifikantes Fortschreiten der nekrotischen Areale in die Zwischenräume zwischen Tag 1 und Tag 2. Das Ausmaß der Zwischenraum-Nekrose der 60sec Gruppe lag signifikant oberhalb der 10sec Gruppe.

Der Rahmenverband war bei ⅔ der Tiere bis Tag 4 stabil. Jedoch zeigte sich das Anbringen einer Halskrause sowie regelmäßiges Nachnähen unabdingbar.

Schlussfolgerung: Das vorgestellte „Burn Comb Modell“ mit Rahmenapplikation zeigte erste gute Ergebnisse zur weiteren Untersuchung von Effekten topischer Wirkstoffe auf die BWP. Das 10-sekündige „Burn Comb Modell“ induzierte eine Verbrennung intermediärer Tiefe, die sich signifikant in vertikaler und horizontaler Nekroseausdehnung, sowie in LSCI-Perfusion von tieferen Verbrennungsverletzungen unterscheidet.

6 Introduction

6.1 Overview

Burn injuries are common throughout the world. Alone in the US, every year approximately 2 million people suffer from burns (Singh et al. 2007), out of which more than 450.000 receive medical treatment, 40.000 are hospitalized and more than 3.000 die (American Burn Association 2016). Burns account for up to 1% of all emergency department visits; thereof roughly 10% are admitted to the hospital (Wilkinson 1998, Taira et al. 2010).

The majority of burns are superficial and minor (Evers et al. 2010), not needing any secondary medical providers. Deeper, severe burns necessitate extensive surgeries and therapy including intensive care in specialized multi-disciplinary burn centers (Arbeitsgemeinschaft der Wissenschaftlichen Medizinischen Fachgesellschaften 1999).

Burns have a great effect onto quality of life, morbidity and mortality (Jeschke et al. 2015). Often, burn injuries require protracted medical care and patients do not suffer only from direct disabilities like scarring, contractions or systemic impairments (Jarrett et al. 2008) but also from subsequent aesthetic deformations, psychological stress and social withdrawal (Wiechman and Patterson 2004).

Even though recent research has further broadened treatment options, both with surgical and conservative approaches, burn injuries are still a relevant problem (Tenenhaus and Rennekampff 2012, Sheridan and Chang 2014, Rowan et al. 2015). Therefore, further research is required to foremost improve patient care but also to reduce high health-care expenses (Hop et al. 2014).

6.2 Burn Injury Definition

According to the American Burn Association (Kagan et al. 2013), a burn is defined as

> *"….an injury to the skin or other organic tissue primarily caused by thermal or other acute trauma. It occurs when some or all of the cells in the skin or other tissues are destroyed by hot liquids (scalds), hot solids (contact burns), or flames (flame burns). Injuries to the skin or other organic tissues due to radiation, radioactivity, electricity, friction or contact with chemicals are also identified as burns."* (Kagan et al. 2013)

Burns are sudden processes resulting in acute wounds. Burns impair the skin's physiologic protection from environmental influences plus its thermo- and fluid regulation. Thus a burn patient is exposed to heat, cold, wind, radiation or bacterial colonization and infection (Pallua and von Bülow 2006). Severe burns lead to serious systemic reactions known as burn disease including excessive immune response, sepsis, hypovolemic shock, hypothermia or cardiovascular impairment (Pallua and von Bülow 2006, Spies and Vogt 2008, Daigeler et al. 2015).

While age, gender, accompanying traumatic injuries or preexisting impairments such as obesity, diabetes mellitus, hypertension, cardiopulmonary or vascular diseases also play a role in the pathophysiology of a burn wound (Kagan et al. 2013), the prognostic evaluation of morbidity and mortality, as well as the decision for treatment options and necessities mainly stem from two entities: Burn depth and extent (Shupp et al. 2010, Kolokythas and Aust 2011).

6.3 Burn Depth

The morbidity of a cutaneous burn injury predominantly derives from its depth, thus how far the cell damage ranges vertically through the skin (Devgan et al. 2006). The depth of a thermal burn wound depends on the inflicted skin temperature which itself results from the heat source's temperature and the exposure time. This is known as the time-temperature relationship (Martin and Falder 2017). Protein denaturation and loss of membrane stability begins when the skin's temperature rises above 40-44°C (Evers et al. 2010, Martin and Falder 2017). Cell damage at this temperature may be reversible while at higher temperature levels, skin damage may be irreversible (Jauch et al. 2013). Dependent on the inflicting temperature, the skin heating takes different time spans: At 44°C, it takes 3600 seconds to damage the skin, while temperatures >70°C require an exposure time of less than 1 second for irreversible damage (Moritz and Henriques 1947).

6.3.1 Burn Depth Determines Therapeutic Approach

Burn depth is the primary determinant of skin regeneration potential which guides the decision between conservative or surgical therapeutic approach (Papini 2004, Devgan et al. 2006, Tiwari 2012, Hop et al. 2013, Tobalem et al. 2013, Daigeler et al. 2015). Wound healing depends on the integrity of keratinocyte cell reservoirs in skin appendages like hair follicles, sweat and other skin glands (Papini 2004, Kolokythas and Aust 2011) which lie in the deep, reticular part of the dermis. These cells can

repopulate the skin's upper layers and are able to regrow fully functional skin (Shupp et al. 2010). Since these structures are not damaged in superficial burns, these injuries are self-limiting and can re-epithelialize within 14-21 days without any later loss of function or remaining scars (Papini 2004, Jaskille et al. 2009). Any burns expanding to the deep partial-thickness layer, harm the skin appendages in the reticular dermis and thus limit the capacity for re-epithelialization. Wound healing in the deep dermis results from fibroblastic collagen accumulation (Kolokythas and Aust 2011), ensued by hypertrophic scarring, contraction, loss of function and a prolonged healing period (Papini 2004, Singh et al. 2007, Kagan et al. 2013). This reasons the clinical recommendation for reconstructive surgery in deep burns (Papini 2004, Jaskille et al. 2009, Daigeler et al. 2015).

6.3.2 Burn Depth Degrees

Burns are categorized into three main depths (Spies and Vogt 2008, Evers et al. 2010, Kagan et al. 2013), underlining different treatment options:

- Superficial (I°)
- Partial-thickness (II°) and
- Full-thickness (III°) & Subdermal (IV°)

The following details in burn depth classifications, summarized in Table 1, are adapted from several publications (Johnson and Richard 2003, Spies and Vogt 2008, Evers et al. 2010, Shupp et al. 2010, Jannasch and Lippert 2012, Kagan et al. 2013, Daigeler et al. 2015).

6.3.2.1 Superficial Burns (I°)

Strict superficial burns are classified as first-degree (I°) burn injuries. Only epidermal skin structures are damaged while dermal appendages are vital. Erythema, light edema and sensation of pain characterize I° burns. They appear dry and red, however upon slight pressure, the skin blanches. When testing with a pinprick, the damaged skin bleeds because main vessels are not clotted. Superficial burns heal without scar formation in 3-7 days. Dead skin tissue can exfoliate and itching may occur. No surgery is required; instead frequent use of skin care is proposed to support the healing process.

6.3.2.2 Partial-Thickness Burns (II°)

Partial-thickness burns are classified as second-degree (II°) or grade 2 burns. Due to differing clinical aspects and therapeutic strategy, superficial partial-thickness (IIa°) burns are distinguished from deep partial-thickness burns (IIb°).

6.3.2.2.1 Superficial Partial-Thickness Burns (IIa°)

In superficial partial-thickness burns (IIa°), the epidermis and only the underlying superficial papillary layer of dermis are injured. Patients suffer pain while the skin appears red and blanches under pressure. Moist blisters may form between epidermis and dermis. Pinprick testing reveals painful bleeding. Most of the skin appendages are intact as well as capillary blood flow. Superficial partial-thickness burns have the potential to heal spontaneously and do not require surgical intervention. The main therapeutic goal is to avoid bacterial colonization through aseptic bandages to allow complete wound healing within 2-3 weeks.

6.3.2.2.2 Deep Partial-Thickness Burns (IIb°)

In deep partial-thickness burns (IIb°), the complete epidermis and dermis - including the papillary and the deeper, reticular layers - are damaged. The majority of skin appendages are destroyed while the subcutaneous fat is intact. Pain sensation is less distinct than in more superficial burns, examined with an insensitive pinprick test and little bleeding. The damaged skin is dry and white, without blanching under pressure. While IIb° wounds can possibly heal secondarily if bacterial contamination is prevented, the healing period lays between 3-9 weeks and is accompanied by hypertrophic scarring and contraction. Therefore, deep partial-thickness burns are treated surgically.

6.3.2.3 Full-Thickness Burns (III°) and Subdermal Burns (IV°)

Full-thickness burns (III°) extend through the complete skin with all its layers and can reach the underlying subcutaneous fat. There is neither pain nor any sensory sensation. Hair and nails are loose and can be extracted without any resistance. The pinprick test can be performed painless and without any bleeding. The subcutaneous vessels are mostly damaged or clotted. The skin usually presents as dry, white with a leather-like appearance. Denatured dermis stands out as burn eschar. The wound cannot heal without extensive contraction and exposing a broad, deep bed of

granulation tissue. Therapy requires surgery with necrosectomy and reconstruction procedures.

Sometimes, deep full-thickness burns (III°) which damage not only the skin, but also the underlying tissues such as fascia, muscle, tendons, bones or organs are classified as fourth-degree (IV°) or subdermal burns (Arbeitsgemeinschaft der Wissenschaftlichen Medizinischen Fachgesellschaften 1999). However, the differences between III° and IV° burns are clinically irrelevant, since both necessitate surgery.

Table 1: Overview of Burn Degrees
Burn Injury Degrees and their characteristics.
Table assembled according to Kagan et al. (2013), Evers et al. (2010), Shupp et al. (2010), Johnson and Richard (2003), Daigeler et al. (2015), Spies and Vogt (2008) and Jannasch and Lippert (2012).

Burn degree	**I°**	**IIa°**	**IIb°**	**III°**	**IV°**
	Superficial	Superficial Partial-Thickness	Deep Partial-Thickness	Full-Thickness	Subdermal Burns
Involved Skin Layers	only epidermis	epidermis and superficial (papillary) dermis	epidermis, superficial (papillary) dermis AND deep (reticular) dermis	full skin (all layers) and underlying fat tissue	full skin (all layers) and underlying fat tissue AND other subdermal structures (fascia/muscle/ bone/ligament/tendon)
Skin Appendages	intact	intact	variable, but most skin appendages are lost	loss of all skin appendages	
Aspect	Erythema (red) moist	Erythema (red) blanching under pressure moist	white non-blanching dry	white, red or charred leathery dry	varying, mostly charred
Blisters	none	moist blisters	moist blisters	none	none
Pain Sensation	moderate-severe	severe	minimal	minimal - none	usually none
Healing (If Infections Are Prevented)	spontaneously in 3-7 days	spontaneously in 2-3 weeks; pigmentation can change	might heal with scarring & contraction within 3-9 weeks	does not heal without intervention	
Scarring and Contraction	none	none	hypertrophic scarring and contraction; joint functionality often impaired	extensive scarring and contraction	extensive scarring and contraction
Treatment	conservative	conservative	surgery	surgery	extensive surgery

6.3.3 Burn Depth Assessment

Assessing the burn depth is made by clinical judgment since no objective imaging technique has been established as the gold standard (Jaskille et al. 2009, Kolokythas and Aust 2011). Most human burn injuries create heterogeneous wounds with varying depths (Kaiser et al. 2011, Nguyen et al. 2013). Thus, when assessing burn depth, not all areas might be evaluated correctly, limiting the rate of accurate diagnosis and resulting therapy (Heimbach et al. 1992). Especially in partial-thickness burns, correct burn depth assessment ranges from 50% in inexperienced physicians to 76% in experienced surgeons (Heimbach et al. 1984, Jaskille et al. 2009).

Techniques like obtaining histological punch biopsies, fluorescent dyes, thermography and ultrasound have been tested for a more objective and dynamic evaluation of burn depth, but all of them have proven insufficient for clinical use (Heimbach et al. 1992, Jaskille et al. 2009). Only Laser Doppler assisted burn depth assessment has shown better results than exclusive clinical examination, but still it is not widely used in clinical routine due to practicability, scanning time and other shortcomings (Johnson and Richard 2003, Monstrey et al. 2008, Jaskille et al. 2010, Eriksson et al. 2014). This might change in a growingly economic driven healthcare system, since using the Laser Doppler assisted burn depth evaluation might be cost-saving (Hop et al. 2016).

6.4 Burn Extent: Affected Total Body Surface Area

Besides burn depth and the deducted therapy, burn extent - expressed in percentage of total body surface area (%TBSA) - is still the major factor for prognosis, mortality and complications (Jarrett et al. 2008, Enoch et al. 2009, Keck et al. 2009, Jeschke et al. 2015, Rowan et al. 2015). In burns with great extent, threats like fluid shifts, as well as infections, hypothermia or limited grafting areas are higher. Burns in adults affecting more than 20 %TBSA are considered severe, regardless of burn depth (Kolokythas and Aust 2011, Rowan et al. 2015), and require care in specialized burn centers (Arbeitsgemeinschaft der Wissenschaftlichen Medizinischen Fachgesellschaften 1999).

6.4.1 Assessment of Burn Extent

While software-assisted %TBSA estimation has been validated as reliable but is not widely used (Kolokythas and Aust 2011, Parvizi et al. 2016), there are three major clinical approaches to assess injury extent (Hettiaratchy and Papini 2004, Spies and Vogt 2008, Enoch et al. 2009):

The Rule of Nines (Wallace 1951), helps to gauge %TBSA by dividing the whole body area of an adult into parts of 9% as shown in Figure 1. Head and arms represent 9% TBSA each. Each of the anterior and posterior trunk as well as each leg represent 18% TBSA. Hand, feet and genital region each represent 1% of TBSA (Spies and Vogt 2008).

The Palm Method takes into account that palm and fingers of each individual's hand approximately represent 0.8-1% of the total body surface area (Hettiaratchy and Papini 2004, Enoch et al. 2009, Jauch et al. 2013). Overlaying the burn victim's palm and fingers over the burned area approximates the injury extent.

The Lund-Browder chart allows assessing the %TBSA by using age-group matched tables as pictured in Figure 2 (Wachtel et al. 2000, Enoch et al. 2009, Jauch et al. 2013). Using the charts is supposed to be the most accurate but most time-consuming approach for assessing burn extent (Wachtel et al. 2000, Hettiaratchy and Papini 2004).

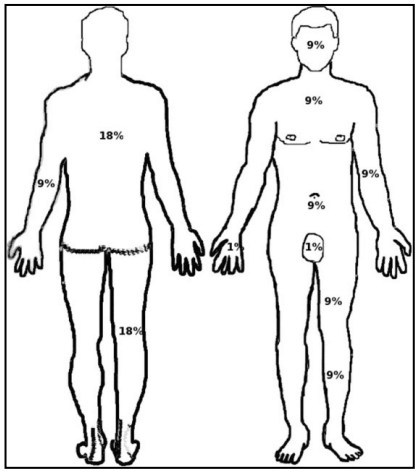

Figure 1: Wallace Rule of Nines
Figure from Alharbi et al.: Treatment of burns in the first 24 hours: simple and practical guide by answering 10 questions in a step-by-step form. World Journal of Emergency Surgery 2012 7:13. (Alharbi et al. 2012). Originally published by BioMed Central Ltd. Permission for use granted under the terms of the Creative Commons Attribution.

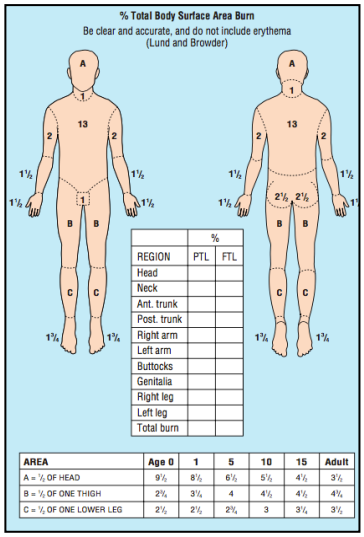

Figure 2: Lund-Browder Chart
Figure from Hettiaratchy, S. and R. Papini (2004). "Initial management of a major burn: II--assessment and resuscitation." Bmj 329(7457): 101-103. (Hettiaratchy and Papini 2004) Permission for use in this work was kindly granted by Copyright Clearance Center for the BMJ Publishing Group.

6.5 Secondary Burn Wound Progression

Although burns are acute injuries, the wounds are not static but steadily evolving. A relevant phenomenon is secondary “burn wound progression”, also known as “burn-injury progression“ or „burn wound conversion“: In the first 48 – 72 hours, burn wounds further progress in depth and extent (Hinshaw 1968, Knabl et al. 1999, Singh et al. 2007). Through this burn wound progression (BWP), initially unburned areas around and below the original burn wound are damaged (Singh et al. 2007). BWP causes continuing tissue damage without any new thermal insult. Burns advance vertically from superficial to deep skin layers as well as horizontally, increasing the surface extent (Salibian et al. 2016). This results in higher morbidity and mortality (Singh et al. 2007, Jeschke et al. 2015). Particular critical is the progression from superficial partial-thickness to deeper burns (Singh et al. 2007) where wound healing is deemed unlikely and instead requires surgical intervention. But especially those injuries are regarded as susceptible (Evers et al. 2010).

6.5.1 No Clinical Standard to Prevent Burn Wound Progression

Current burn therapy includes emergency treatment with stabilizing the cardiovascular status, cooling and pain management before proceeding with further treatment, either conservatively or surgically, in an appropriate care setting. But

there is no standardized procedure in order to avoid, prevent, minimize or even predict burn wound progression (Singh et al. 2007, Salibian et al. 2016).

6.5.2 Jackson Burn Wound Model

Already in 1953, Jackson classified three distinct zones in burn wounds (Jackson 1953). This "Jackson Burn Wound Model" is widely accepted throughout the literature (Devgan et al. 2006, Singer et al. 2013, Tobalem et al. 2013, Schmauss et al. 2014) and is used to explain BWP. Jackson divided the burn wound as shown in Figure 3: The inner coagulation zone, the surrounding zone of stasis and the peripheral hyperemic zone (Jackson 1953, Hettiaratchy and Dziewulski 2004).

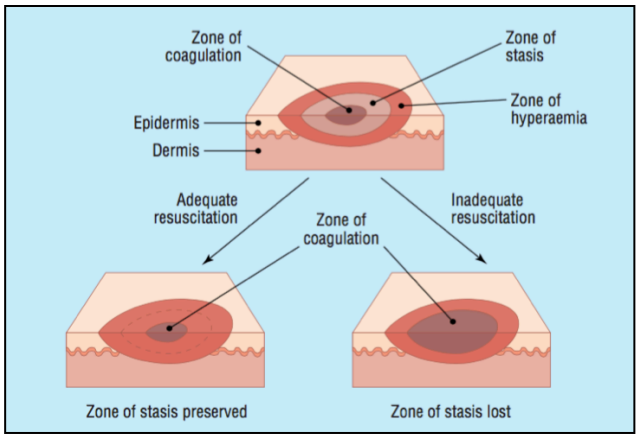

Figure 3: Jackson Burn Wound Model
Jackson burn wound model schema and the effects of adequate or inadequate resuscitation.
Figure from Hettiaratchy, S. and P. Dziewulski (2004). "Pathophysiology and types of burns." BMJ: British Medical Journal 328(7453): 1427-1429. (Hettiaratchy and Dziewulski 2004)
Permission to use was kindly granted by Copyright Clearance Center for the BMJ Publishing Group.

In the innermost zone, the tissue is non-vital following the burn. This tissue in the coagulation zone is exposed to the maximum thermal insult which leads to direct protein denaturation, cell membrane destruction and cell death (Singh et al. 2007). This core zone is irreversibly damaged beyond repair (Schmauss et al. 2015) and the tissue will develop ischemic necrosis notwithstanding any therapy. Since thermal burns turn into coagulation necrosis, this zone is also called coagulation zone.

Around this core zone, there is a zone of stasis where burn wound progression takes place (Schmauss et al. 2015, Salibian et al. 2016): The tissue is regarded as still vital after the burn, however its metabolism is critically impaired and at risk for necrosis. Inflammation and hypoperfusion is present in this zone even though the vasculature is still patent after the injury (Jackson 1953, Shupp et al. 2010, Tobalem et al. 2013). If this compromised tissue is not adequately treated, the zone of stasis will undergo cell

death (Evers et al. 2010, Schmauss et al. 2015). However, the exposed tissue has potential for complete regeneration following the burn if adequate treatment is initiated for resuscitation and the ongoing impairment reduced (Battal et al. 1996, Knabl et al. 1999, Hettiaratchy and Dziewulski 2004, Singh et al. 2007, Rowan et al. 2015).

The most peripheral zone around the burn wound is called zone of hyperemia, which is vital after burns and will fully recover spontaneously (Xiao et al. 2013). Circulation is elevated: This zone appears reddish and with occurring edema but histologically no damage to dermal structures is apparent (Shupp et al. 2010).

6.5.3 Pathophysiology of Burn Wound Progression

Even though BWP has high clinical relevance - due to its high impact onto patient's morbidity and mortality, and has been in the research focus in the last sixty years - the pathophysiology has not been completely understood. BWP develops as a result of complex and cross-linked events in the zone of stasis and is regarded as a second step mediated through tissue responses. A broad consensus supports four main physiopathologic pathways, which contribute to injury-progression (Singh et al. 2007, Shupp et al. 2010, Xiao et al. 2013, Salibian et al. 2016). These pathways are closely intertwined and affect each other (Figure 4):

1. Inflammation (systemic response and cell infiltration)
2. Perfusion alterations (hypoperfusion, ischemia and edema)
3. Formation of free radicals (and lipid peroxidation)
4. Necrosis & programmed cell death (including apoptosis and autophagy)

6.5.3.1 Inflammatory Response

The damaged cells and the thereby activated macrophages and neutrophils release an abundance of inflammatory mediators like interleukins, tumor necrosis factor α (TNFα) and matrix metalloproteinases (Ipaktchi et al. 2006, Shupp et al. 2010). These cytokines lead to collagen degradation, apoptosis, adherence of neutrophils to the endothelium which itself leads to hypoperfusion by venule occlusion, and the production of free radicals (Shupp et al. 2010). The inflammatory environment aggravates already impaired micro-hemostasis and deteriorates thrombotic mechanisms (Salibian et al. 2016) through release of histamine, vascular endothelin growth factor (VEGF), bradykinin, prostaglandins and thromboxane (Singh et al.

2007). Inflammation leads to edema, fluid shifts and complement activation (Singh et al. 2007).

6.5.3.2 Perfusion Changes

Resulting from imbalance between vasoconstriction and vasodilatation, microthrombosis, fluid shifts and edema (Salibian et al. 2016), burn damage impairs the blood flow, leading to hypoperfusion in the tissue at risk (Singh et al. 2007). Insufficient perfusion is followed by clotting, edema and release of free radicals (Singh et al. 2007, Shupp et al. 2010). As a result of this interrupted microcirculation, delayed ischemia and cell death occurs (Schmauss et al. 2015). Through inflammatory cytokines, microthrombosis arises. Neutrophil activation with venule occlusion is one factor, destroyed vascular endothelium with resulting hypercoagulability another. Furthermore fibrinolysis is reduced. Resulting thrombus formation and coagulation causes hypoperfusion, hypoxia and cell damage (Isik et al. 1998, Singh et al. 2007).

Through heat-induced changes of vascular permeability, fluid shifts result in decreasing intravascular pressure and edema formation in the surrounding tissue, known as capillary leak. This excessive fluid in the extravascular space increases the pressure onto the vasculature, again leading to decreased perfusion. Vascular integrity is further impaired by elevated levels of histamine, bradykinin, leukotrienes, VEGF, substance P, and nitric oxide (Shupp et al. 2010).

6.5.3.3 Free Radicals

As a result of neutrophil activation, direct endothelial damage, thermal cell damage and depletion of antioxidants, toxic free radicals are released (Salibian et al. 2016). These free reactive oxygen species (ROS) include hydrogen peroxide, superoxide radicals, hydroxyl radicals besides other oxygen-free radicals (Shupp et al. 2010, Salibian et al. 2016). This results in oxidative stress, which compromises cells by lipid peroxidation, protein denaturation and DNA damages (Horton 2003, Shupp et al. 2010). Again through ROS, mediators are set free, worsening the inflammatory milieu.

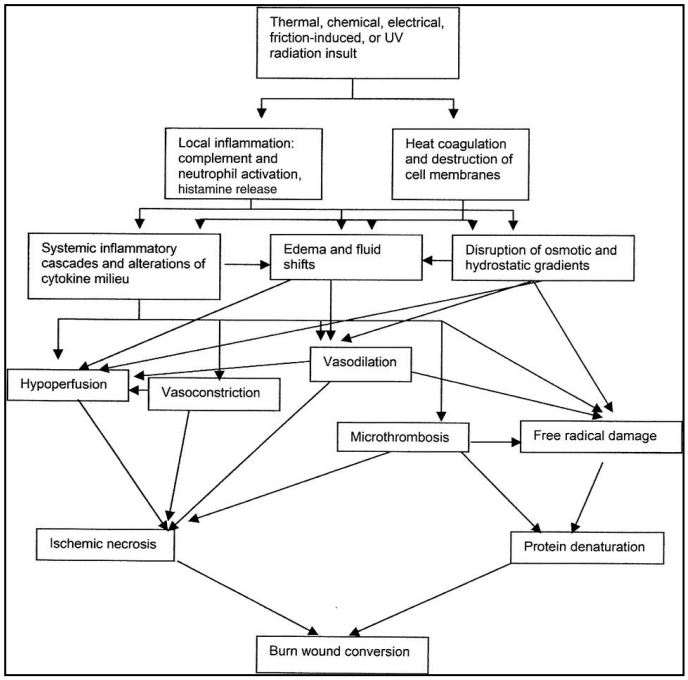

Figure 4: Pathways of Secondary Burn Wound Progression
Complex physiopathologic mechanisms lead to an ischemic milieu with protein denaturation, impaired perfusion and cell death.
Figure from Singh, V., L. Devgan, S. Bhat and S. M. Milner (2007). "The pathogenesis of burn wound conversion." Ann Plast Surg 59(1): 109-115. Permission for re-use kindly granted by Wolters and Kluwers.

6.5.3.4 Cell Death

While the initial thermal insult leads to direct cell death in the coagulation zone, the described mechanisms trigger further damage and promote cell death through secondary processes in the zone of stasis (Singh et al. 2007). Three different cell death mechanisms have been reported in burn wounds: Necrosis ("oncosis"), apoptosis and autophagy (Shupp et al. 2010, Salibian et al. 2016).

Oncosis is the process of non-programmed cell death with preceding cell swelling and the sequela of an inflammatory response (Shupp et al. 2010). Oncosis, formerly known as cellular necrosis (Majno and Joris 1995), is not only apparent in burn injuries through the initial direct heat damage, but also through secondary mechanisms as shown with attested elevated oncosis parameters in the ischemic zone up to 48 hours after the injury (Singer et al. 2008). Ischemia-induced cell death occurs (Deniz et al. 2013).

Apoptosis, programmed cell death, has been observed in burns as well (Gravante et al. 2006). Induction or time-dependent delay in apoptosis is hypothesized to interact with oncosis (Singer et al. 2008, Shupp et al. 2010).

Autophagy - housekeeping recycling in lysosomes (Reggiori and Klionsky 2002, Glick et al. 2010) - is a process only recently found in burn wounds (Salibian et al. 2016).

Up to now, it is unclear whether increased autophagy aggravates (Tan et al. 2013, Guo et al. 2015) or hinders BWP (Xiao et al. 2014) but it contributes to the evolving character of burn wounds.

Through the different cell death mechanisms BWP leads to further tissue damage.

6.6 Experimental Approaches to Burn Wound Progression

A lot of research has been conducted to expose contributing pathogenetic mechanisms and to develop therapeutic or prophylactic strategies against BWP (Shupp et al. 2010, Schmauss et al. 2014, Salibian et al. 2016). Animal models play a major role in research targeting BWP. A systematic analysis of experiments examining BWP throughout 2010-2014 stated that all conducted studies in this period have used animal models (Salibian et al. 2016). Beyond that, a lot of burn research has been targeted with in vivo animal models since in vitro experiments are limited in the possibility to assess the complex interactions between the involved pathogenetic factors, even more when examining systemic reactions of severe burns (Abdullahi et al. 2014). Since different animal models have various advantages, drawbacks and certain price disparities, none can cover every aspect of the molecular and cellular pathways. The kind of animal used in certain studies depends on hypothesis, budget restrictions, availability, similarity to humans, preliminary tests and the researcher's experience (Dorsett-Martin 2004, Abdullahi et al. 2014). Animal models for burn wounds should be safe, reliable, reproducible and have a high validity at a preferably low cost. (Dahiya 2009). The three main species used for burn research and especially for BWP in recent years have been rats, mice and pigs (Abdullahi et al. 2014, Schmauss et al. 2014, Salibian et al. 2016).

Recently rats were the most commonly used animals in burn research (Dahiya 2009). In exploring BWP regarding cellular mechanisms and preventive agents, rat models have proven to be predominantly feasible (Schmauss et al. 2014, Salibian et al. 2016) since a wide variety of techniques for burns in rats have been described; and in the last years, the most commonly used burn model regarding BWP has been the "burn comb model" (Schmauss et al. 2014, Salibian et al. 2016).

6.6.1 Burn Comb Model

The burn comb model has been originally described in 1992 (Regas and Ehrlich 1992) where the authors introduced a rectangular brass bar with transverse notches. They used this bar - also known as stamp, burn template or burn comb - to create four

burn sites with intercalated bands of uninjured skin by placing the heated metal onto a rat's dorsum. The interjacent uninjured skin bands were labeled interspaces and represented the zone of stasis (Regas and Ehrlich 1992). Since then, variations of this metal bar have been commonly used and standardized for various applications (Abdullahi et al. 2014, Salibian et al. 2016). The principle of a heated burn comb with integrated notches to create distinct areas representing different wound zones has stayed the same. Alterations to the original design have been made to metal material (Tobalem et al. 2013), size (Tobalem et al. 2012), application pressure (Macri et al. 2013, Crouzet et al. 2015) or exposure time (Singer et al. 2013, Ponticorvo et al. 2017). With varying these factors, both burn depth and burn extent can be controlled. The burn comb model variants have been used to study drug effects, perfusion alterations, histological and biochemical outcomes and anti-coagulatory or anti-inflammatory parameters in rodents (Schmauss et al. 2015). It has furthermore been adapted to other animals such as mice (Bohr et al. 2013) and pigs (Singer et al. 2009). Since 2010, the major half of studies elucidating BWP has used a burn comb model (Salibian et al. 2016). However, most of these burn comb models in rats induced full-thickness burns (Tobalem et al. 2012, Tobalem et al. 2013, Guo et al. 2015, Reddy et al. 2015).

This preference for deeper and full-thickness burns is not limited to the burn comb model: In a review identifying 116 burn studies in rats between 2008-2011 (Mitsunaga Junior et al. 2012), out of 86 experiments which described burn depth, 30 studies employed models for second-degree burns and 54 used third-degree burns. While deeper burns account for higher morbidity and mortality, the neglect of less severe burns surprises, considering that world-wide the majority of burns is supposed to be superficial (Waitzman and Neligan 1993). Evers et al. estimate mild burns at a rate of 600/100000 inhabitants while severe burns are estimated at 5/100000 (Evers et al. 2010). II° burns account for half of the burns treated in secondary medical care in the US where less than 5 percent were III° (Taira et al. 2010). With the burn comb model being a popular research tool in burns, there is an under-representation of superficial burn depths in BWP studies.

6.6.2 Wound Protection Devices in Rats

A known limitation in studies with imposed wounds is the ability of rats to get rid of dressings and to manipulate the wound area (Pfurtscheller et al. 2013). Rats damage the wound site mainly with their teeth, hind- and forelegs (Macionis 2000). This manipulation is unfavorable in wound healing studies, sometimes even limiting the evaluable parameters (Singer et al. 2011). Despite the common use of rats in burn and wound healing research, there are few descriptions of wound protection or topical application devices. Different attempts to protect wounds from manipulation, gnawing and self-mutilation have been made throughout the years:

In 1980, Fox and Frazier have described the first wound protection dressing when testing anti-microbiological agents (Fox and Frazier 1980). Their dressing, an Orthoplast saddle, was fastened over the wound area with wire sutures. This allowed a single researcher to change dressings without the need for anesthesia.

In a study on flap survival in rats, McGrath applied a dressing, fastening it with a wire hook and safety pin (McGrath 1981). The hook was sutured on the animal while the dressing itself was fastened to the hook with the safety pin. The dressing was changed every 12 hours through opening of the safety pin.

Ueda et al. used a vinyl chloride tube around the rat's body for a week (Ueda et al. 1981). With using a transparent tube, they could inspect the wound area. The tube with a diameter of 5cm was put over the rat's body and thorax, a gap cut into the tube and adjusted with a tape. This device had only protective reasons and they did not perform any dressing changes or use any topical treatment.

Pynn and coworkers addressed the problem with a protective rat vest out of X-ray film over the forelegs (Pynn et al. 1983) but not over the wound. With using their vest in over 200 rats, they were able to reduce self-mutilation. Another group later stated problems with ulcers stemming from the thin X-ray film (Fujimori et al. 1990). They changed the design of the vests in 50 rats while using a transparent vinyl chloride plate. Both type of vests have in common that they do not cover the wound area itself (Pynn et al. 1983, Fujimori et al. 1990).

The use of a protective vest and collars were compared to shortening of the rat's teeth in 1999 (Komorowska-Timek et al. 1999). The study concluded that simple shortening of the teeth every 3-4 days successfully hindered rats from gnawing. The gap between upper and lower teeth seemed sufficient to obviate aimed biting. The results shown were more desirable than with collars or vests. However, Macionis

showed in his work that rats use not only their teeth, but also fore- and hindlegs to remove any disturbing object from their body (Macionis 2000). He proposed to limit rats in their ability to manipulate wound areas by restricting neck movements with gluing splints from mandibular bone to the breastbone, applying a vest on the forelegs with immobilizing one foot and neutralizing hindleg manipulation by taping the distal feet in a fixed position. Despite Macionis' reported successful results, the suggested technique poses questions from an animal welfare perspective, since it heavily constrains the rat's movement (Macionis 2000).

Another attempt to introduce a protective device was made with mounting a clear shield onto the rat's dorsum (Martineau and Chua Chiaco 2000). A transparent polycarbonate was shaped into a dome that was then mounted with hook and loop fasteners on the rat. This protective shield was used in larger rats up to 475g and completely assembled weighted 16g. The researchers showed a possible duration of up to 28 days and the rats tolerated the transparent mount well.

Pfurtscheller and his group introduced the most recent wound protection armor (Pfurtscheller et al. 2013). They combined a scalding model in 250-350g rats with armor out of thermoplastic material shaped in half cylindrical form. The material was then fixated onto the animal's back by using steel sutures. A wound cover was sutured on top of the carved-out thermoplastic material. The authors proposed enhancing the armor with adding aluminium components to the thermoplastic material as underlying stabilization. 10 mounted armors in 14 animals lasted for a month (Pfurtscheller et al. 2013).

Even though wound manipulation and self-mutilation in rats have been described as a limiting factor for more than 35 years in animal research literature and various protective dressing devices have been introduced since, we were not able to find an existing suitable device for our experiment, allowing for regular wound inspection, assessing perfusion parameters over 2 weeks without dismounting the armors and simultaneously allowing the application of topical treatments.

6.7 Tissue Protective Agents to Reduce Burn Wound Progression

According to Uygur and coworkers,

> *"…an ideal pharmacological agent for saving the zone of stasis should have the following features: safety, clinical availability, easy administration, reproducibility of effective results, feasibility of postburn treatment, cost-effectiveness, known mechanism of action, established bioavailability, and protective effects on the zone of stasis".* (Uygur et al. 2009)

Such an agent has not yet been found. Several research groups have tested agents and treatment procedures to reduce BWP as reviewed recently (Schmauss et al. 2014, Schmauss et al. 2015).

6.7.1 Systemic Agents Pose Systemic Risks and Adverse Effects

A lot of the selected agents have shown promising results attenuating BWP when used after the burn injury (Schmauss et al. 2015). Most of the tested agents were applied systemically via oral, intravenous, intraperitoneal or intramuscular route. When administered in this fashion, higher doses could lead to systemic adverse reactions that limit, impair or even negate therapeutic effects. The adverse effects and risks of a systemically BWP-decreasing agents depend on the mechanism of action and include infection, bleeding or cardiovascular events.

As shown in former research, agents targeting the inflammatory response by antibody-mediated inhibition of leucocyte adherence in burn wounds (Mileski et al. 1992, Bucky et al. 1994, Choi et al. 1995) may lead to infection (Sharar et al. 1991), fever or even myocardial infarction (Enlimomab Acute Stroke Trial Investigators 2001). Immunosuppressive Rapamycin was shown to attenuate BWP (Xiao et al. 2013) but again systemic application increases the risk for infections. An agent effective in inhibiting inflammasome activation and therefore attenuating systemic immune activation (Xiao et al. 2016) has also been shown to exert anti-platelet activity and thus carrying the risk of bleeding (Wang et al. 2007). Hemorrhagic complications also diminish possible use of recombinant tissue-type plasminogen activator (Isik et al. 1998) or other anti-coagulatory drugs (Singh-Joy and McLain 2008, Yuhua et al. 2012). Hemorrhage or even heparin-induced thrombocytopenia is a risk when using heparin or derivates systemically (Oremus et al. 2007, Uraloglu et al. 2018).

Pro-rheological agents such as Beraprost sodium, TAK-044 or the pleiotropic Erythropoietin have side effects like symptomatic tachycardia (Battal et al. 1996),

hypotension (Battal et al. 1997), or compromised blood rheology through increased hematocrit levels (Tobalem et al. 2012, Tobalem et al. 2013). Certain agents with anti-oxidative properties, successfully reducing BWP (Choi and Ehrlich 1993, Taira et al. 2009), have not been FDA-approved and might carry an increased risk for cardiovascular events (Nissen and Wolski 2007).

6.7.2 Tested Topical Agents to Reduce Burn Wound Progression

Many agents have reduced BWP, but few have proven as versatile regarding safety, clinical availability and easy administration (Kayapinar et al. 2015). A standardized, targeted method to prevent BWP without the risk for systemic complications has not been accomplished (Sun et al. 2012). Regarding these limitations, especially topical applied agents might be able to avert systemic adverse effects. While most research focuses on deep burns, also patients suffering from minor and superficial burns, not needing in-patient care, might profit from topical drugs. If applied as creams, lotions, hydrogels or nanoparticles; topical agents could also promote wound healing, pain relief and ameliorate cosmetic results (Hayati et al. 2018). Topical antibacterial wound dressing are already routinely used in burn treatment and could be supplemented by tissue protective drugs (Ipaktchi et al. 2006, Stone Ii et al. 2018). Consequently, few scientists have yet shifted towards the topical application of tissue protective agents. However the research is still quite limited, as noted by Poranki in 2016:

> *"Topical application of an efficacious therapeutic agent targeting cell survival in the zone of stasis in burns represents a simplified, local treatment modality, but little work has been published toward this goal."* (Poranki et al. 2016)

Nonetheless, few groups reported successful results with topical drugs preventing BWP, reducing vertical and/or horizontal burn wound extension (Schmauss et al. 2015):

Tobalem et al. showed that the application of cold water (17°C) and even more warm water (37°C), applied for 20 minutes after the burn induction, could reduce perfusion impairment and delay BWP in rats (Tobalem et al. 2013). Similarly, Rizzo and his colleagues reported hypothermic therapy with water circulating blankets at 33-34°C as an effective measure to decrease burn wound depth (Rizzo et al. 2013). Sun and his group showed reduced BWP and alleviated overall inflammation in rats through

topical application of Infliximab (Sun et al. 2012), an antibody antagonistic to tumor necrosis factor α (TNFα). Systemic complications of Infliximab like infections, cancer, tuberculosis or inflammatory diseases (Scheinfeld 2004) could potentially be avoided through the topical use, but further research is needed (Friedrich et al. 2014). Cerium nitrate showed tissue protective properties when used as a topical antiseptic in a rat full-thickness burn comb model (Eski et al. 2012). Topical use of EDTA as an iron-chelator reduced histological burn depth and macroscopic surface extension in a full-thickness rat burn comb model (Wang et al. 2015). While the main goal was to promote wound healing in a pig burn study conducted by Poranki et al., they were also able to show that local keratin biomaterial hydrogel with extracted keratin proteins reduced BWP (Poranki et al. 2016). Another study by Singer et al. conducted in a pig model could show that topical enzymatic debridement with a bromelain-derived debriding agent reduced tissue necrosis in the zone of stasis (Singer et al. 2010). Fu and coworkers showed that topical applied hydrogel with granulocyte-macrophage colony-stimulating factor (GM-CSF) exerts protective effects in the zone of stasis in a rat burn comb model (Fu et al. 2017). Recently, a carbomer 940 hydrogel was shown to ameliorate perfusion in a full-thickness rat burn comb model (Hayati et al. 2018).

In summary, topical administration of tissue protective agents have showed promising results (Schmauss et al. 2015). With this application route, systemic adverse effects could be avoided and potentially higher doses could be targeted at the burn wound. Prevention of increasing burn depth could be relevant for all burn patients, but especially in superficial burns which could then be treated in outpatient settings. Therefore further research, especially with topical agents and adequate dosage in vivo burn models, is required.

6.8 Laser-Speckle-Contrast: Technique and Imaging

Altered blood flow and microcirculation in burn wounds contribute to BWP (Singh et al. 2007, Shupp et al. 2010). Thus, various techniques have been used to analyze skin perfusion, including invasive techniques like intravital microscopy (Harder et al. 2004), indocyanine green (ICG) fluorescent angiography (Fourman et al. 2014), Xenon-clearance (Proano et al. 1997) or radionuclide imaging (Eski et al. 2012); besides non-invasive methods like near-infrared spectroscopy (Kaiser et al. 2011), videomicroscopy (Eriksson et al. 2014), spatial frequency domain imaging (Nguyen et

al. 2013) or Laser Doppler Imaging (LDI) (Tobalem et al. 2013, Eriksson et al. 2014, Hayati et al. 2018). A relatively young method to assess blood flow is Laser-Speckle-Contrast-Imaging (LSCI) (Briers 2001). The technique originally described in 1982 to exemplify microcirculatory blood flow in the retina (Briers and Fercher 1982), has been continuously enhanced to allow real-time perfusion imaging with high spatial and temporal resolution (Briers and Webster 1996, Eriksson et al. 2014).

6.8.1 Technical Principles of Laser-Speckle-Contrast-Imaging

In LSCI, a coherent laser is used to illuminate the wound area (Sen et al. 2016). The light is backscattered from the subject in a random, irregular pattern due to biological tissue morphology and properties. The diffracted backscattered interference pattern is called laser speckle, which can be recorded using a camera (Ponticorvo and Dunn 2010, Eriksson et al. 2014) (Figure 5).

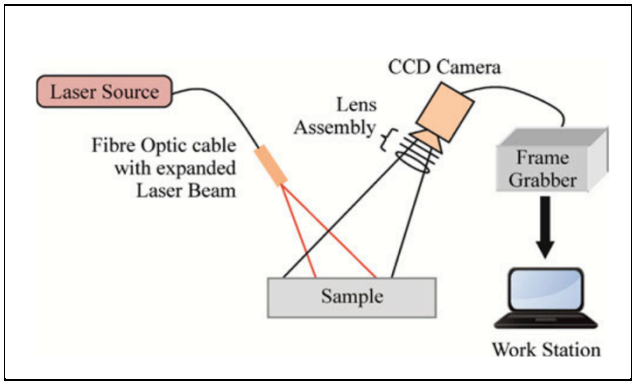

Figure 5: Schematic Laser-Speckle Contrast-Imaging
In Laser-Speckle-Contrast-Imaging, a laser is used to illuminate the sample and the backscattered interference pattern is detected by a charge-coupled-device (CCD-) camera.
Image originally published in Basak, K., M. Manjunatha and P. K. Dutta (2012). "Review of laser speckle-based analysis in medical imaging." Med Biol Eng Comput 50(6): 547-558. (Basak et al. 2012). Permission for re-use kindly granted by Rightslink Copyright Clearance Center.

The speckle pattern consists of dark and bright superposed interference areas where light waves are cancelled or reinforced. In static tissue with still particles, the obtained diffracted speckle pattern is high in contrast. But if motion is present within the observed tissue, the laser speckle is instead fluctuating and blurred (Ponticorvo and Dunn 2010, Lindahl et al. 2013). The amount of blurring can be quantified in relation to the exposure time and used to create the speckle contrast (Senarathna et al. 2013, Eriksson et al. 2014). Since motion in dormant biological tissue mainly stems from erythrocytes and particles in the blood stream (Senarathna et al. 2013), increased blood flow leads to intensified blurring and therefore to a reduced speckle

contrast. Through statistically analyzing the speckle contrast and its deviations from standard grayscale intensity in the observed tissue, perfusion can be deduced (Basak et al. 2012, Eriksson et al. 2014). The contrast image is used to create a color-coded intensity image, correlating to the vascular flow, expressed in arbitrary units (Sen et al. 2016).

6.8.2 Differences in Laser Doppler and Laser-Speckle-Contrast-Imaging

Laser Doppler (LDI) and Laser-Speckle-Contrast-Imaging (LSCI) are related methods but use different physical theories for data sampling (Eriksson et al. 2014). Both methods share their non-contact, non-invasive properties and perfusion values are linearly related and highly correlated (Millet et al. 2011), despite the more superficial tissue penetration of 0.3mm-1mm in LSCI (Briers 2001, Senarathna et al. 2013, Eriksson et al. 2014). Laser Doppler devices send out laser beams with a certain wavelength onto the subject. In static tissue, the light is reflected with the same wavelength. When blood cells travelling through the observed tissue are hit by laser beams, the wavelength is changed through the Doppler effect (Micheels et al. 1984, Schabauer and Rooke 1994). The backscattered light is scanned by the device and analyzed for the amount of Doppler-shifted light beams. Higher amounts and frequencies permit conclusions of blood flow and velocity (Micheels et al. 1984). Since LSCI avoids scanning like LDI, image acquisition is faster and covers a larger area (Eriksson et al. 2014). Another advantage of LSCI is the non-impairment onto perfusion evaluation from environmental light, camera distance and angle (Lindahl et al. 2013, Zötterman et al. 2017). While in clinical settings, LDI is more commonly used, LSCI and its time-saving data acquisition might prove more feasible in the future (Zötterman et al. 2017).

7 Purpose of this Study

More research in topical tissue protective agents in non-full-thickness burns is needed. For this reason, the purpose of this study was two-fold:

1. The first goal was to establish a rat burn comb model where BWP leads to damage extending to the intermediate dermis. In our model, the burn wound should only spread to the intermediate skin layers and therefore be defined as a non-full-thickness burn. Measured parameters should include flowmetry using the LSCI-technique, burn wound progression through histological evaluation and quantification of resulting gross interspace necrosis. These determinants should be monitored in short time intervals over at least 2 weeks, subsequently comparing them to a formerly used, standardized full-thickness burn.

2. The second aim was to establish a flexible, durable and easy to mount frame or bandage for rats in order to be able to use topical agents. The dressing should meet animal welfare requirements, not hinder the rats and allow administering of topical agents while concurrently preventing rats from wound manipulation. Furthermore it should facilitate evaluation of flowmetry and gross wound assessment, possibly on a daily basis.

8 Material & Methods

8.1 Animals & Housing

All experiments were conducted according to European FELASA guidelines, German Animal Welfare Act and approved by the Regierung von Oberbayern. A total of 38 male Wistar rats (Charles River Laboratories, Sulzfeld, Germany) were used for this study. On arrival at the study site (Zentrum für Präklinische Forschung ZPF, Klinikum rechts der Isar, Technische Universität München, Munich, Germany), the animals were checked for proper health status. Animals were given at least 14 days to adapt for housing conditions before commencing procedures. The study site facilities had restricted personal access, daily animal care, automatic climate control and a 12-hour day-night-rhythm with twilight phases. Animals were kept in individually ventilated cages (IVCs) with up to 2 rats stored in one cage (Type IV; base 60x38cm), respecting size and weight. Autoclaved food (Altromin Spezialfutter, Lage, Germany) and water was offered without any restrictions at their disposal „ad libitum“. Additionally autoclaved oat flakes were served up to a body weight of 400g for ensuring sufficient weight at the beginning of the experiments. Wood pellets were used as litter. Water bottles and wood pellets were replaced twice weekly. Autoclaved wood pulp, cardboard or plastic houses were offered for nest-building.
After burn induction, the enrolled animals were kept individually in IVCs. For the following three days, while animals were treated with Buprenorphine, autoclaved hay was used instead of wooden pellets and nest-building material was removed.

8.2 Preparation For Burn Induction

Only healthy rats between 435-535g were enrolled in the experiments. We used a complete antagonizable bodyweight-adapted combination anesthesia consisting of Midazolam (Hexal®, Holzkirchen, Germany), Medetomidin (Sedator, Albrecht, Auendorf, Germany) and Fentanyl (Fentadon®, Albrecht, Auendorf, Germany). A table of applied doses is attached (chapter 14). The anesthesia was injected intraperitoneally in the lower right abdominal quadrant after nuchal grab fixation. Following injection, rats were put into darkened cages individually and respiration was closely monitored. Anesthetic depth was verified after 5 minutes by checking lid and toe pinching reflexes. If the anesthesia was sufficient, we began preparations for burn induction. The eyes were protected with ointment (Bepanthen® Augen- und

Nasensalbe, Bayer Vital GmbH, Leverkusen, Germany). If the applied dose was insufficient or additional dosages were required later, one third of the original dosage was injected similarly until adequate narcosis was achieved.

Then, the animals were placed on a 37°C-warm electric heating mat (Medax, Neumünster, Germany) which was covered with sterile drapes. Using a nosecone, the anesthetized animals were treated with 100% Oxygen ("O_2") at a flow rate of 2l/min. For preemptive pain prophylaxis 0.05 milligrams per kilogram bodyweight (mg/kg bw) Buprenorphine (Buprenodale®, Albrecht, Auendorf, Germany) was injected subcutaneously. We shaved the animal's back and applied depilatory cream (Balea, dm, Karlsruhe, Germany). Next, the rat's spine and the burn comb stamp dimensions were outlined on the dorsal skin with a felt tip (Figure 6). Stamp placement was planned with a distance of 5mm to the spine. After preparation and outlining, we took digital photos and measured the baseline Laser-Speckle-Contrast-Imaging (LSCI) flowmetry. Before proceeding, anesthetic depth was rechecked.

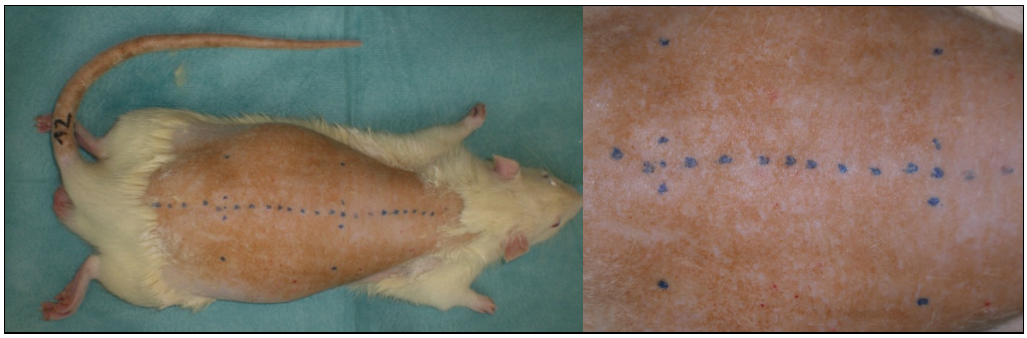

Figure 6: Stamp Position Outlining
Marked rat with outlining of the spine and stamp application positions on both sides. The marking shows a 5mm distance to the spine on both sides.

8.3 Burn Induction

All burn procedures were conducted after application of systemic anesthesia and preemptive subcutaneous analgesia. For burn induction we used a 136g chrome-nickel template with a length of 55mm and a width of 20mm as the "burn comb stamp". Four rectangular 20x10mm planes were separated by three 20x5mm indentions (Figure 7).

Figure 7: Burn Comb Template
The used chrome-nickel template was 55mm long and 20mm wide. Four rectangular 20x10mm planes were separated by three 20x5mm notches. The stamp had a total weight of 136g.

Two identical stamps were put into boiling water at 100°C for 15 minutes until temperature equilibration. The stamp was applied without any additional pressure onto the previously marked rat dorsum for the desired time burn time (see 8.3.1). First the right side of the rat's dorsum was burned. With the second stamp, the left side was burned immediately afterwards. Four 20x10mm rectangular burn wounds resulted on each side with three 20x5mm unburned intercalated interspaces between them (Figure 8).

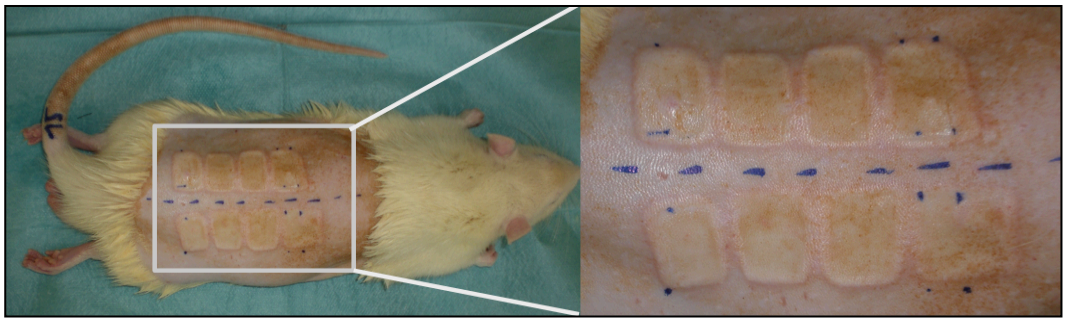

Figure 8: Rat Dorsum after Burn Induction
The stamps were applied consecutively without any pressure. The right image shows the enlarged wound area. Picture taken at the time point "post-burn" after a 10sec burn. The stamp's burn imprints can be distinguished.

After the burn induction, we took digital photos and measured perfusion with the LSCI device for post-burn data collection.

After photographing and measuring again at the time point 1 hour, we antagonized the narcosis: After completed burn induction and first measurements, the anesthesia was completely antagonized combining Atipamezol (Antisedan®, Elanco, Bad Homburg, Germany), Flumazenil (Hexal®, Holzkirchen, Germany) and Naloxon (B. Braun, Melsungen, Germany). A table of detailed dosage is attached (chapter 14). The body-weight-adapted antagonization was applied subcutaneously into the nuchal skin fold and the animals woke up under cardio-respiratory monitoring.

Subsequently, the burned rats were treated with a subcutaneous injection of 0.05mg/kg bw Buprenorphine each 8-12 hours for the next 3 days.

8.3.1 Burn Time

Burn time was measured with a stopwatch. We induced a burn wound in 12 preliminary animals with different burn times ranging from 5 to 60 seconds. The histology obtained by these preliminary animals was used to assess a burn time in order to create a superficial to intermediate burn wound, but not a full-thickness burn. Data from these preliminary animals was not used for the analysis.

In the study group we inducted a ten second (10sec) burn in 17 rats. This 10sec burn time had been deemed as appropriate in the preliminary animals after discussion with the histopathologists. Twelve of the animals on which we applied the template for 10 seconds received a frame dressing (see chapter 8.5.2). Rats that were sacrificed at early time points did not receive a frame. 13 animals were included in the perfusion and histology analysis. Nine animals were burned with the burn comb for sixty seconds (60sec) as a control group with a standardized full-thickness burn as formerly described (Tobalem et al. 2012, Tobalem et al. 2013).

8.4 Measurements: Digital Photo Documentation and Perfusion-Flowmetry

We repeatedly observed and measured the animals in the experiment. Each measurement consisted of digital photo documentation and LSCI flowmetry. As depicted in Figure 9, time points of analysis were: “Baseline” (before the burn induction), shortly after burn induction (“post-burn”), 1 hour (“h1”), 8 hours (“h8”), Day 1 (“d1”), Day 2 (“d2”), Day 4 (“d4”), Day 7 (“d7”), Day 10 (“d10”) and Day 14 (“d14”). After 2 weeks, measurements were performed once a week.

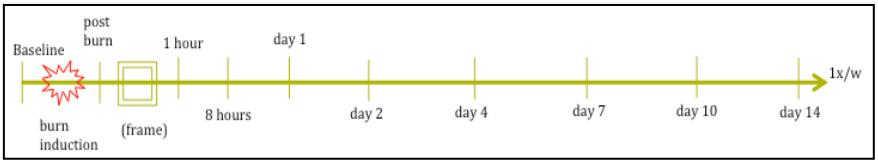

Figure 9: Measurement Points
The timeline marks time points where analysis was performed according to the protocol. See text for further information. Timeline is not drawn to scale.

If we mounted a frame, this was done between post-burn and 1 hour. Animals burned for 60 seconds were not measured on day 10 since none of the animals received a frame.

8.4.1 Inhalation Narcosis for Measurements

Except for the time points baseline, post-burn and 1 hour, when the animals were still under antagonizable injection anesthesia; we used an Isoflurane inhalation narcosis: After checking health status weight, we placed the animals in an anesthesia induction box. We used an anesthesia device (MDS matrx®, Völker, Kaltenkirchen, Germany) for the narcosis and flooded the animals with 5% Isoflurane (Isofluran CP®, CP-Pharma, Burgdorf, Germany) at an oxygen-flow (O_2-flow) of 6l/min. After loss of positional reflexes, we reduced the inhalation dosage to 1-2% Isoflurane at an O_2-flow of 2l/min using a nosecone to maintain the sedation. If animals had an E-collar, we removed it before reducing the Isoflurane dosage. If the animals showed any signs of pain or if frame materials or sutures were not intact, we applied 0.05mg/kg bw Buprenorphine subcutaneously into the neck skin fold before proceeding with any measurements or re-suturing.

8.4.2 Photo Documentation

The anesthetized rat was put onto a sterile cover and the wound area cleaned and macroscopically inspected. If any hair was re-growing, it was shaved to ensure adequate wound inspection. For photo documentation we used a digital camera (Exilim EX-Z75 7.2MP; Casio; Casio Europe, Norderstedt, Germany) and took 3 photos of every rat at each time point (Figure 10): One overview picture of the whole animal (no zoom, focal length 6.3), one picture zoomed-in onto the rat's dorsum (zoom-level 2, focal length 10.4), one close-up shot of the wound area and frame (zoom level 5, focal length 16.51). All photos were taken with the same camera and light settings, triggering the internal camera flash. The camera was mounted on a tripod stand with a fixed position.

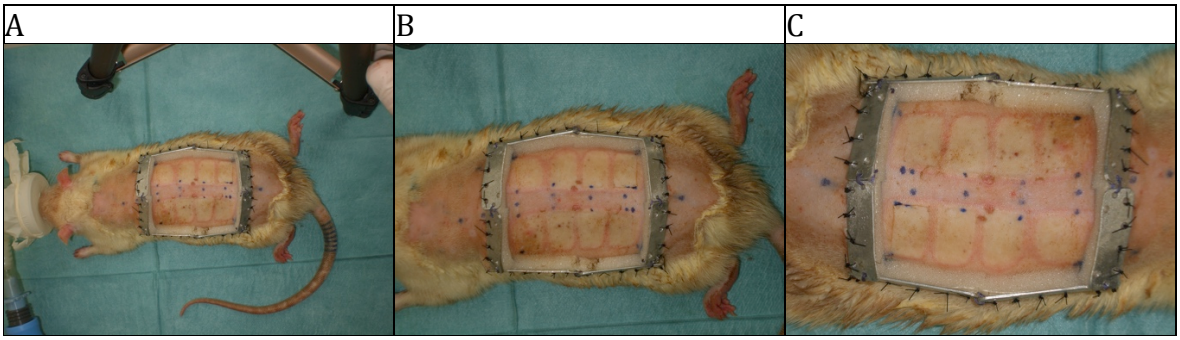

Figure 10: Example of Photo Documentation
Shown are 3 photographs of the same rat on the same time point. Notice the 3 different zoom levels for animal overview (A), rat's dorsum (B) and wound area (C). Animal with mounted frame.

8.4.3 Flowmetry with Laser-Speckle-Contrast-Imaging

Subsequently, we performed non-invasive perfusion measuring with a Laser-Speckle-Contrast-Imaging flowmetry device (moorFLPI-2; Moor Instruments, Sinzig, Germany) and corresponding software (moorFLPI-2Measurement Version 1.0; Moor Instruments Ltd., Devon, England). The full-field imaging device was calibrated according to the manufacturer. A laptop (Lenovo G500s; Lenovo Deutschland, Stuttgart, Germany) with Windows 7 (Microsoft Corporation, Unterschleißheim, Germany) was used for data storage and processing.

The animal was mounted in spread prone position on a soft black surface. The LSCI-device was installed in a defined distance over the wound area and we used the software tool to focus. On every measurement point, we took 2 flowmetry recordings, each 60 seconds with a frame rate of one image per second: One “macro” shot of the wound area and surrounding non-burned tissue and one “micro” shot with an enlarged wound area, using the software’s zoom function (Figure 11).

After completing the measurements, the Isoflurane and O_2 inflow was turned off. The animals were put back in their individual cages. If the rats had a mounted frame, we re-attached the E-collar at this point. The rats woke up under monitoring of vital functions.

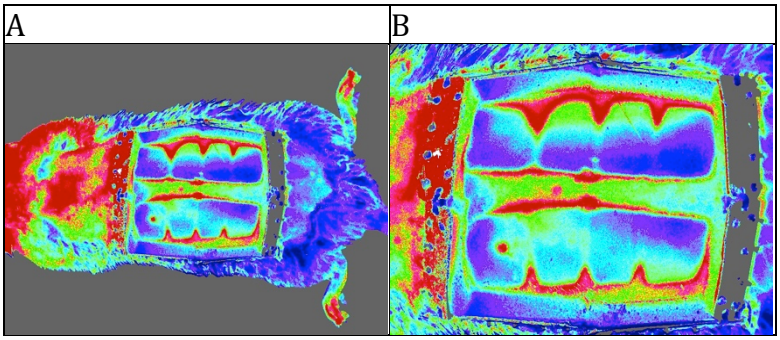

Figure 11: Example of LSCI Measurement
At each time point, we recorded one “macro” (A) and one “micro” (B) sequence, 60sec each with a frame rate of 1 frame per second. The sequences were software-processed for flowmetry averaging.

8.5 Frame Dressing

Throughout the experiment we tested different preliminary frame dressings before deciding to use a self-developed aluminium frame with 8 double-layered components.

8.5.1 Preliminary Frames

In 12 preliminary animals, we mounted different frame types in order to establish a suitable frame to be used over the experiment's time span. Each preliminary frame was mounted in at least two animals and observed for a minimum of 2 days to examine restrictions and limitation of the frame.

8.5.1.1 First Preliminary Frame: Soft Frame

The first frame was made out of Varihesive® (ConvaTec, Munich, Germany) hydrocolloid bandaging material. The material seemed flexible and soft enough to avoid animal restriction. A scalpel was used to cut out a one-piece framing to enclose the burn wound area (Figure 12). The rest material of the cut Varihesive® bandage was turned upside down and used as a cover sheeting. We used transparent foil (Opsite Flexigrid, Smith-Nephew, Hamburg, Germany) to drape the wound area.

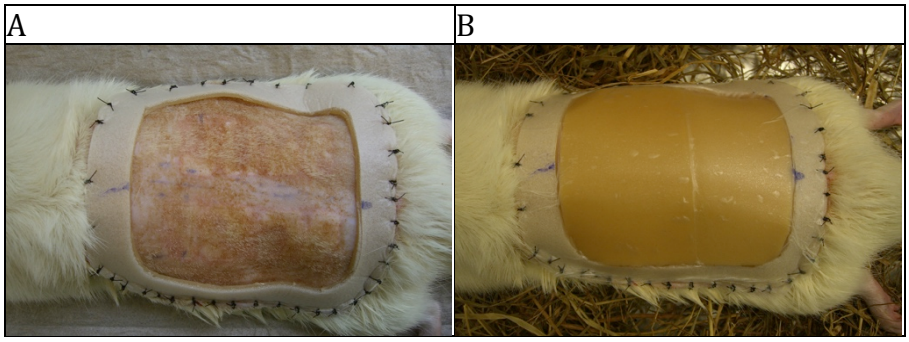

Figure 12: First Preliminary Frame
Mounted Varihesive® hydrocolloid bandaging soft frame (A). The burn wound was covered with Varihesive® bandage material turned upside down (B).

8.5.1.2 Second Preliminary Frame: Thermoplastic Strengthening on Lateral Sides

For the next design, we applied thermoplastic material onto the lateral frame sides. The material offered small holes through which stitches could be placed and allowed quick assembly. To facilitate fitting to the shaped rat's dorsum, we inserted a joint into the thermoplastic material by cutting the plastic in half and reconnecting the single parts with two stitches (Figure 13). The plastic lateral sides were connected to the soft cranial & caudal parts of the frame with sutures on the corresponding ends after the outside corners were rounded off to avoid sharp plastic rims.

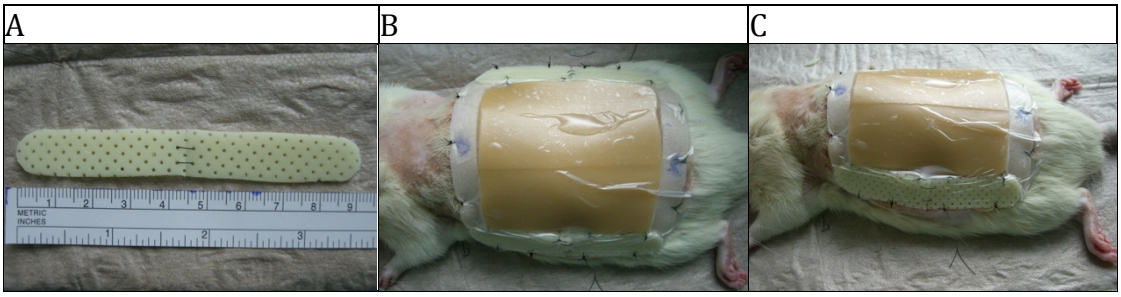

Figure 13: Second Preliminary Frame with Thermoplastic Material
Split design of the thermoplastic lateral frame sides after re-connecting them with sutures and rounding off the outside edges (A). Mounted frame with soft cranial and caudal components and with thermoplastic enhanced lateral sides. Wound sealing with reversed Varihesive® bandage material and transparent foil (B & C).

8.5.1.3 Third Preliminary Frame: Single Layer Aluminium Frame

In a next step, we moulded an aluminium metal frame light enough to avoid compromising weight load. In order to suture the frame onto the rat, we punched several holes in the single aluminium parts with a distance of 4-6mm between each other (Figure 14). The single aluminium parts had a width of 15mm.

Originally we planned to use one long aluminium component for the lateral parts of the frame. However we preferred an 8-component design instead in order to allow a tight fitting and to enclose the burn area with the frame. The cranial and caudal parts of the frame were bent according to the shape of the rat's dorsum to further increase tightness of the mounted frame (Figure 14). For sealing and cushioning the rat from the metal parts, we taped self-adhesive fixing foam onto the metal.

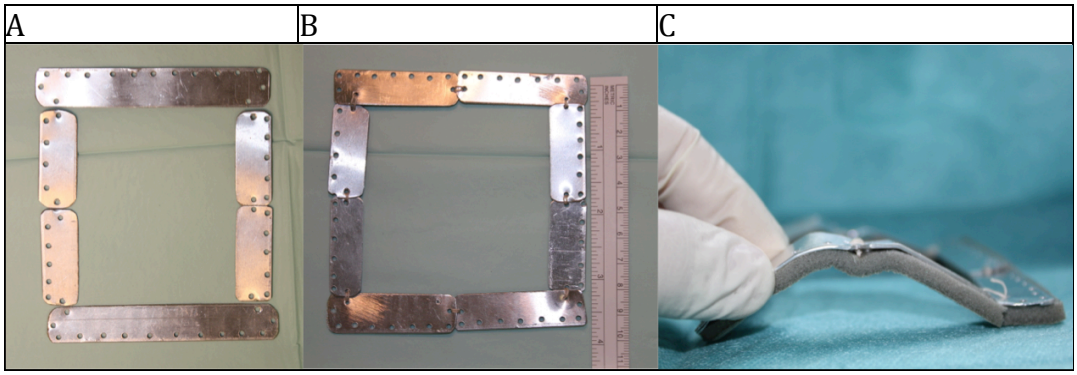

Figure 14: Single Layer Aluminium Frame
The first aluminium frame was assembled from 6 different parts: 2 long bars for the lateral frame sides and 2 shorter parts for each cranial/caudal side (A). Altered broad aluminium frame with 8 single components and changed frame dimensions (B). The cranial and caudal components were further bent to improve fitting to the dorsum's shape and self-adhesive foam was taped to the bottom (C).

8.5.1.4 Further changes on the preliminary Aluminium Frame

After the results with the single layer aluminium components, we further altered the frame design. Due to the width of the single components and the assembled frame, we aimed to reduce the frame size by folding the sides of the individual frame parts. Double-layered single components had a width of 10mm. Narrowing of the frame was done by changing the components' length. We abstained from mounting the frame with wire sutures since no efficient frame fixation could be achieved. We stuck to single suture technique and resolved to use frames only in combination with an Elizabethan collar (E-collar).

8.5.2 Final Aluminium Frame with Eight Double-Layered Components

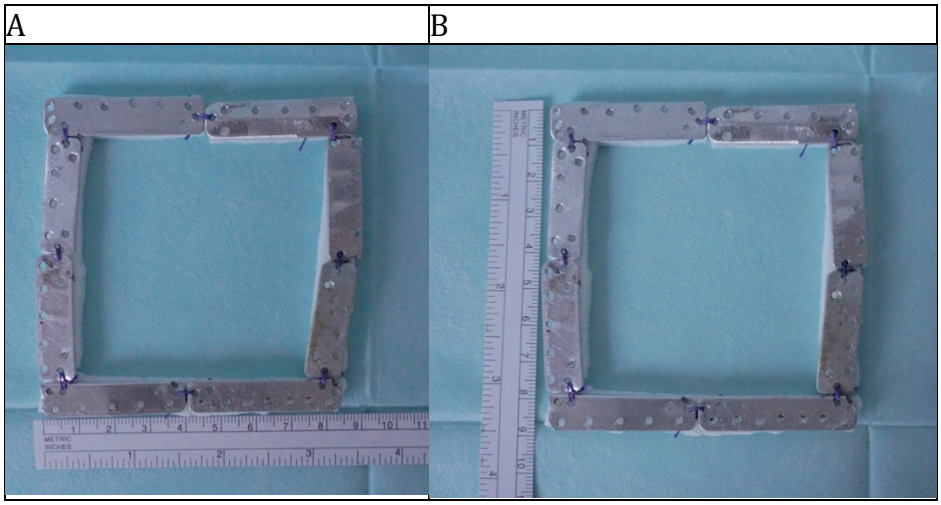

Figure 15: Assembled Final Aluminium Frame
The upper part and lower parts are 84mm long (A). They were placed parallel to the rat's spine as the lateral frame sides. Left and right sides of the frame on the picture are cranial and caudal sides of the frame. They had a length of 88mm (B). Eight sutures can be seen where single components of the frame were connected.

We used an aluminium frame with eight double-layered aluminium components as our final frame in a collective of 12 animals, each burned for 10 seconds and equipped with an E-collar. The complete frame dimensions were 84mm laterally and 88mm cranially/caudally (Figure 15). Completely assembled the frame weighted 5g and enclosed the burn comb wound area. The lateral frame sides consisted out of two components, each with a length of 42mm and a width of 10mm. Through the aluminum components, we punched 1mm holes with a distance of 5mm. Each lateral frame component had 5 to 6 holes for fixation plus additional ones at the joint areas. The two lateral components were connected to each other in a flexible joint by using 2-0 Vicryl® (Ethicon, Johnson & Johnson Medical GmbH, Norderstedt, Germany) sutures. The cranial and caudal components were 34mm long and 10mm wide each

and connected in the same manner as the lateral ones. They had 4 to 5 holes plus additional ones at the joint ends. Side, cranial and caudal frame sides were also connected with 2-0 Vicryl® sutures and therefore flexible. White self-adhesive foam dressing (*Mepilex® safetac*, Mölnlycke Health Care, Düsseldorf, Germany) was used for padding.

8.5.2.1 Frame Mounting

The frames were mounted after burn induction and post-burn measurements while the animals were still anesthetized and sedated. We used 3-0 Ethilon® (Ethicon, Johnson & Johnson Medical GmbH, Norderstedt, Germany) suture material in single button technique for mounting the frame by utilizing all punched holes in the aluminum to fixate the frame. The frame was mounted onto the back with up to 12, respectively 8 sutures on each frame side (Figure 16). Attention was paid to avoid tension on the rat's skin.

We analyzed the frame durability in twelve animals equipped with the final double-layered frame. A frame was considered mounted and durable if no complete cranial, caudal or lateral side was gnawed open and no more than 15 sutures needed re-suturing. Re-fixation was performed as required by re-suturing the frame when the animals were anesthetized with Isoflurane and after subcutaneous 0.05mg/kg bw Buprenorphine application. When the frame was fully un-mounted, no re-suturing was done. On day 10 all remaining frames were dismantled while the rat was still anesthetized. The individual frame parts were re-used after disinfection.

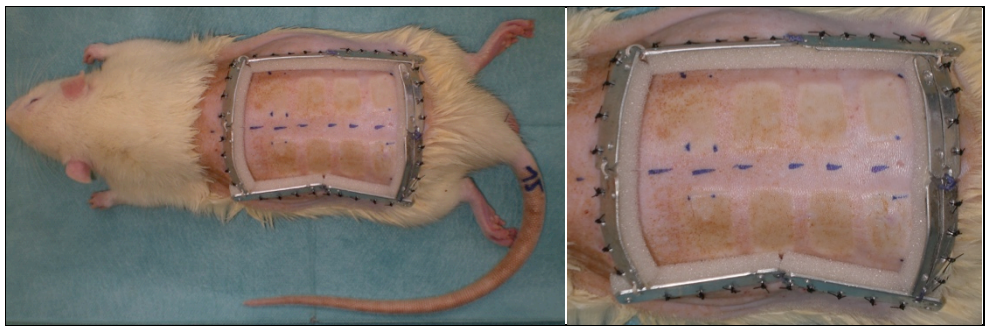

Figure 16: Mounted Double-Layered Aluminium Frame
Rat at 1 hour after burn induction. Complete mounted frame in single button technique. The wound area was enclosed by the frame.

8.5.2.2 Elizabethan Collar for Animal with Final Aluminium Frame

All 12 study animals for frame evaluation were equipped with Elizabethan collars („E-collars") made of soft, thin plastic. 8 animals were treated with a short E-collar and 4

with a long model. Short and long collars had an outer radius of 75mm or 85mm respectively and both versions had an inner cut out part with a radius of 25mm. We removed approximately 30° of the collar in order to size it individually to each rat (Figure 17). We taped the inner rims with Mepilex® safetac foam dressing (Mölnlycke Health Care, Düsseldorf, Germany). To attach the E-collars tightly around the neck, we incised 2mm holes and applied brass fasteners (Figure 17). Careful regard was paid not to constrict the neck, while maintaining a satisfactory tightness. The rats were monitored for changes in movement, signs for distress or behavioral alterations. During in-lab observation and while performing measurements, all E-collars were temporarily removed in order to allow grooming. After finishing the measurements, the E-collars were re-attached.

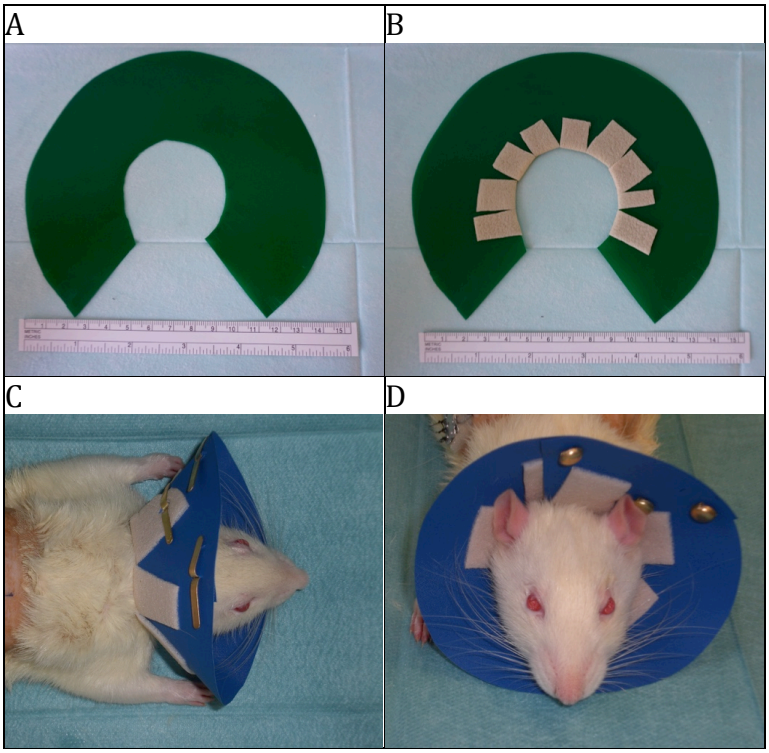

Figure 17: Elizabethan Collar for Wound and Frame Protection
Animals with mounted frames were equipped with an Elizabethan collar (E-collar).
The small E-collar had a 75mm outer-rim-radius and a 25mm inner-rim-radius. A small portion of the collar was excised and small incisions were made for fastening (A) and the collar prepared with foam padding (B). Applied E-collar with brass fasteners (C&D). After each collar attachment, constriction of the neck was precluded.

8.6 Euthanasia, Histology and Burn Depth Score

8.6.1 Euthanasia and Tissue Harvesting

After the observation period, euthanasia was performed with a threefold overdose of Pentobarbital (150mg/kg bw; Narcoren®, Merial, Hallbergmoos, Germany). The lethal injection was performed under Isoflurane sedation.

Sacrificing experiment animals was done on different time points to analyze evolving burn depth histologically. There was no repeated tissue harvesting from the same animal. In the 10sec group, we harvested tissue from one or more animals on the following time points: 1 hour, 8 hours, 1 day, 3 days, 7 days (3 animals), 10 days (3 animals), 14 days (3 animals), 21 days and 35 days. Additionally 2 animals were kept alive to days 58 and 65. In the 60 second burn group we sacrificed animals on the time points 1 hour, 8 hours, 1 day, 2 days, 4 days, 7 days, 21 days and 28 days (2 animals).

Tissue harvesting was performed on the carcass after confirmed euthanasia. Any attached frames were un-mounted before proceeding with harvesting. The whole wound area was removed below the panniculus carnosus muscle from the animal's back. The right burned area was consequently used for histological processing and was cut into four tissue compounds of equal size. Furthermore, the area was bisected to gain two specimens of the same interspace-burn-field pair for easier embedding (Figure 18). The skin samples were stretched out onto a corkboard using sterile injection needles and then stored in 4% formalin solution. The tissue samples were transferred to the Institute of Pathology, Technische Universität München, Munich, Germany where they were subsequently dehydrated and embedded in paraffin. Each tissue block was cut into 3-5µm thick section slides and stained with haemotoxylin and eosin (HE) with assistance by pathology staff.

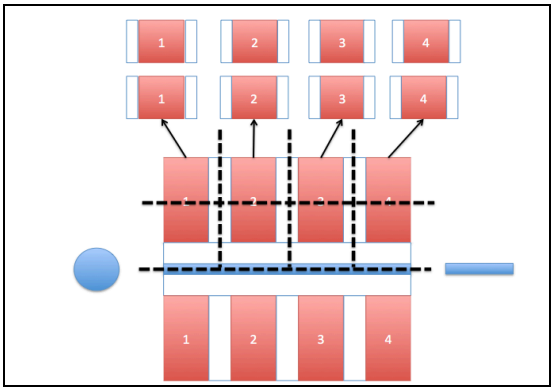

Figure 18: Schematic Illustration of Obtaining Histological Specimens
Cutting was performed along the dotted lines. Each burn field was dissected with its adjacent interspaces. The samples were cut in half for easier histological fixation and evaluation.

8.6.2 Histology Evaluation and Burn Depth Score

The HE-stained sections were evaluated for burn depth by PD Dr. med. Melissa Schlitter and Dr. med vet. Katja Steiger. Dr. Schlitter is a certified histopathologist and Dr. Steiger an animal pathologist. Both were blinded for burn time.

Histological definition of the burn depth was made according to Meyerholz (Meyerholz et al. 2009) and categorized into an ordinal-scaled burn depth score formerly used in burn research (Yuan et al. 2007, Tobalem et al. 2012, Tobalem et al. 2013)(Table 2). Briefly, collagen alterations, vascular patency, viability of skin appendages and cell nucleus changes were evaluated and the deepest afflicted skin layer determined. If both pathologists could not definitely state the burn depth in a section, the area was not used for further analysis.

Table 2: Burn Depth Score

Burn Depth Score	Damage Extending Through The
1	Epidermis
2	Superficial Dermis
3	Intermediate Dermis
4	Deep Dermis
5	Muscle

A single section was evaluated for three distinct burn depths: Burn depth of the burn field itself and two burn depths of the adjacent interspaces left and right. For each time point, burn depth scores of center areas (representing burn fields) and fringe areas (representing interspaces) were pooled separately. The medians of burn depth scores were calculated for interspaces and burn fields.

8.7 Evaluation of Macroscopic Interspace Necrosis

For evaluation of macroscopic interspace necrosis we used the data obtained by planimetric photo documentation from day 1 onward. Interspace necrosis was quantified using image analysis software (CapImage version 8.6.3, Zeintl Software, Heidelberg, Germany) with a defined 1:1.5 enlargement. In each animal, we analyzed the right burn side for interspace necrosis. We measured complete interspace extent, and necrotic areas were determined by gross surface tissue appearance in the interspaces. Black, brown, grey, or ashen tissue was regarded as non-vital eschar (Figure 19). The specified necrosis from all three interspaces at each analyzed time point was related to complete interspace dimensions and the result was read out in percent. In interspaces where gross appearance was ambiguous, we discussed the extent in our group until accomplishing consensus.

To determine group-specific surface interspace necrosis, we calculated the mean for each time point from all animals with the same burn time (10sec or 60sec). Results were given in percent interspace necrosis (% interspace necrosis).

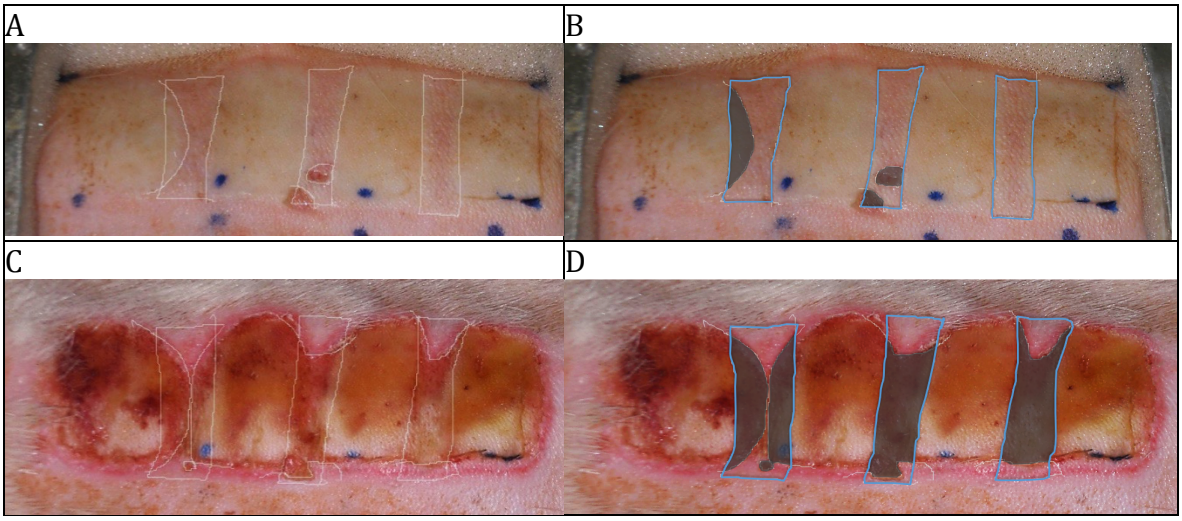

Figure 19: Interspace Necrosis Measurement
10sec specimen on day 1 with 14% interspace necrosis (A) and highlighted measurement areas (B). 10sec specimen on day 7 with 68% interspace necrosis (C) and highlighted measurement areas (D). On all images left side is cranial. Blue outline shows marked interspace area regardless of vitality, representing 100% interspace surface area (B and D). Discolorations in these areas were regarded as non-vital (highlighted with grey areas in B and D). Note vital hyperaemic margins in the interspaces in C and D.

8.8 LSCI Flowmetry Data Processing

The obtained Laser-Speckle-Contrast-Imaging data recordings were further processed using the manufacturer's digital software (moorFLPI Review V4.0; Moor Instruments Ltd., Devon, England). Flowmetry data up to 2 weeks was evaluated.

8.8.1 Digital Preparation of Flowmetry Images

Each flux image was prepared before data evaluation. For assessing flowmetry, the „micro"-perfusion recordings were used after averaging 60 frames. Blinding for flux values was done by using either the grey or color photo in single image display mode for setting the region of interest (ROIs) points (Figure 20 and Figure 21). The appropriate template with square-sized ROIs (0.4x0.4 software units) for either interspaces or respectively burn fields was loaded. The software extracted absolute flux parameters in arbitrary units from the ROI areas. The extracted flux values were copied into an Excel spreadsheet (Excel, Microsoft Office, Microsoft Corporation, Unterschleißheim, Germany). We proceeded with the placements and measuring for all time points. Placement of baseline ROIs was done according to pre-burn markings.

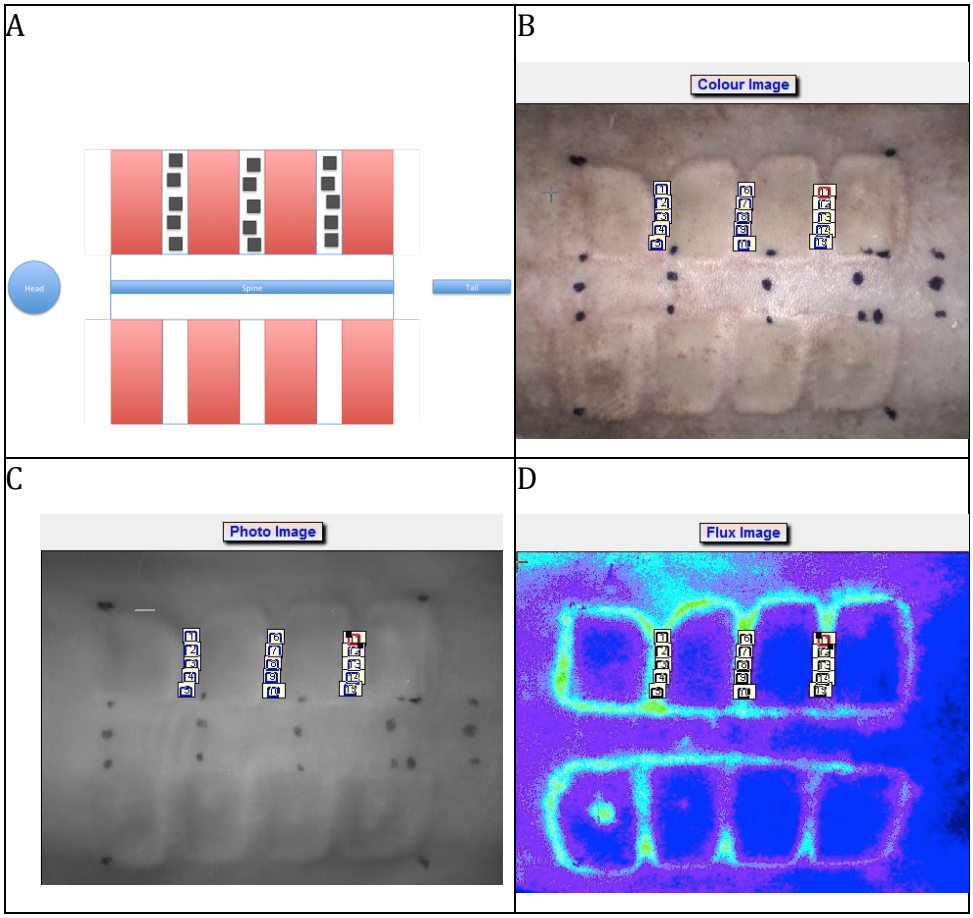

Figure 20: Placement of Interspace ROIs
Schematic Image (A). Software Color Image (B). Software Grey Photo Image (C). Software Flux Image (D). 15 ROI markers were placed in the interspaces as shown in B and C. Each interspace had five ROIs assigned. The black dots in the photo images were pre-burn positioning markers.

8.8.2 Obtaining Relative Interspace and Burn Field Flux Values

After preparing the image for measurement spot placing, we loaded a template of 15 Regions of Interest (ROIs). Starting with the post-burn image we placed five ROIs in the area where we could distinguish an interspace from the burn fields (Figure 20).
For burn field evaluation, we proceeded in the same manner as for the interspaces. We used 16 ROIs for burn field perfusion assessment, 4 ROIs for each burn field (Figure 21). We placed the ROIs approximately in the middle of the burn field stretching from lateral to medial.

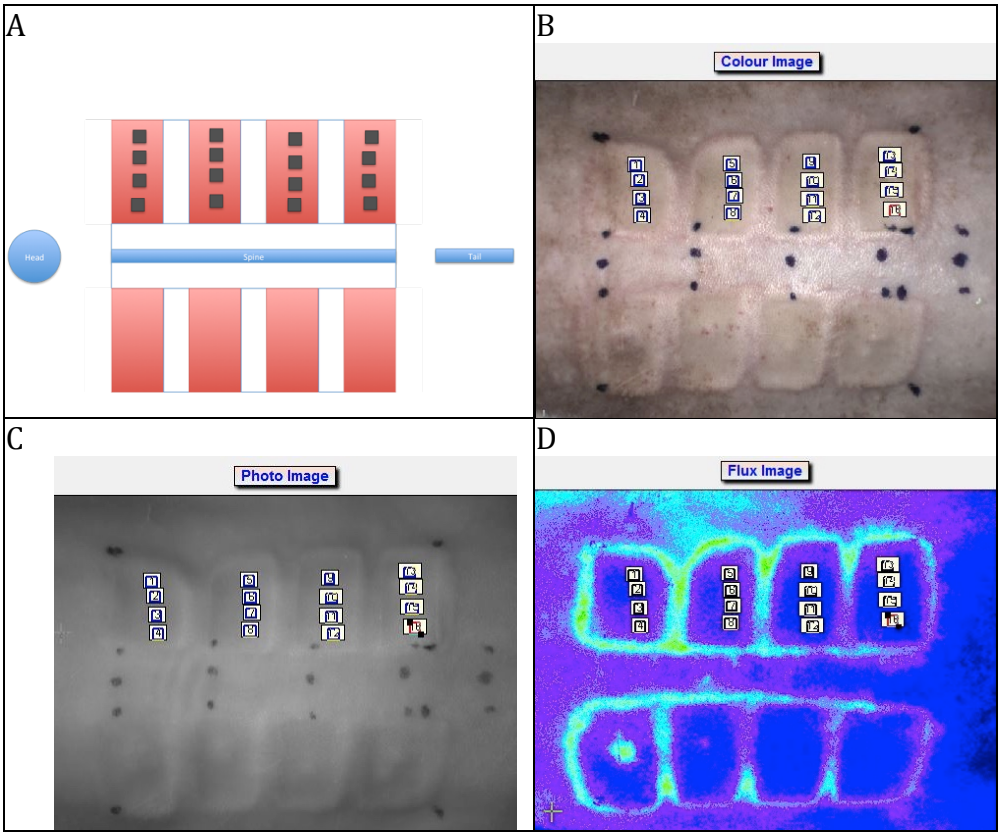

Figure 21: Placement of Burn Field ROIs
Schematic Image (A). Software Color Image (B). Software Grey Photo Image (C). Software Flux Image (D). 16 ROI markers were placed in the burn fields as shown in B and C. Each burn field had four ROIs assigned. The black dots in the photo images were template positioning markers.

Mean average flux values for each interspace and burn field were determined for each time point. The mean-averaged value was then set in relation to the corresponding baseline perfusion of the same interspace or burn field. This relation was read out in percent. In this manner we obtained data for each interspace or burn field at each time point in percent baseline perfusion (% baseline perfusion). To determine group-specific perfusion, we calculated the mean relative flux and its standard error of the

mean (SEM) of all interspaces or burn fields for each time point from all animals with the same burn time.

8.9 Statistical Analysis

Statistical analysis was performed with SPSS v23 (IBM, Ehningen, Germany). Perfusion and interspace necrosis data shown is expressed as arithmetic mean and the standard error of the mean (SEM). All graphs show SEM error bars unless stated otherwise. Differences were considered significant at $p<0.05$ and highly significant at $p<0.001$.

The development of the statistical model as well the model's computing was done with the assistance of Drs. Alexander Hapfelmeier and Bernhard Haller from the Institute of Medical Informatics, Statistics and Epidemiology of the Technische Universität München, Munich, Germany. We used a mixed linear regression model for testing variables with repeated measurement points in assessing perfusion parameters and gross interspace necrosis. The subjects were repeatedly measured in their burn fields and interspaces over time. We used a model with a compound symmetry correlation structure, testing for fixed effects in a two-way mixed-design analysis of variance, incorporating the main effects of "burn status" (i.e. burn field or interspace) or "burn time" (i.e. 10sec or 60sec) and "time" (analyzed time points). Where applicable, we also comprised the interaction term "burn time" by "time" or "burn status" by "time". In the LSCI data, due to right-skewed data as estimated by the residuals, we performed log10-logarithmic transformations to normalize data distribution. Baseline differences were adjusted by computing the baseline values as a covariate into the model. If the main effect showed a statistical significance at $p<0.05$, we extended the mixed linear model to test at each analyzed time point. Correction and adjustment for α-error in pairwise comparisons was performed with the Bonferroni post-hoc test.

Histological burn depth was assessed in an ordinal-scaled system and expressed as the median. Significance in burn depth was assessed using the Mann-Whitney-U-Test for nonparametric independent samples. Statistical significance was assumed with an exact 2-tailed p-value <0.05. Adequate post-hoc α-error correction in pairwise comparisons was performed with the Bonferroni method where applicable.

9 Results

9.1 Histological Burn Depth

9.1.1 Burn Depth Score

Burn depth was assessed using a burn depth score ranging from 0 (skin intact) to 5 (damage to the muscle) (Figure 22 and Table 2). Histological areas from the fringes of the sample represented the interspaces while the area from the center represented the burn fields (Figure 23). Examples of different burn depths as seen in HE-stained specimen can be found in Figure 24.

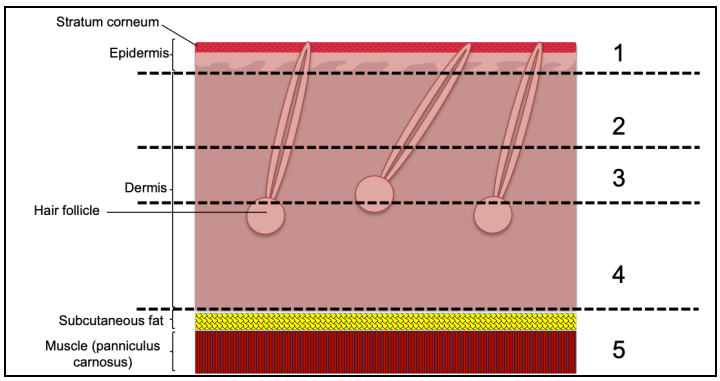

Figure 22: Schematic Burn Depth Score
If the damage extends to the epidermis, a score of 1 was given. Similarly damage extending through the superficial dermis, the intermediate dermis, the deep dermis or the muscle was respectively scored with 2, 3, 4 or 5.

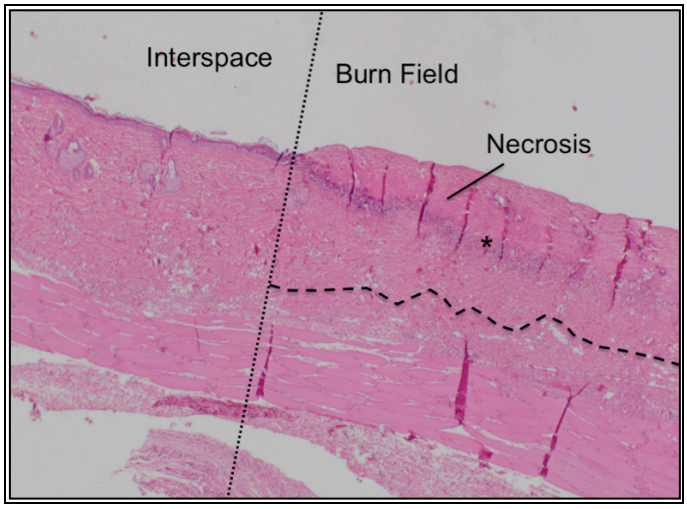

Figure 23: Histological Transition Zone between Burn Field and Interspace
Transition from interspace (left side) to burn field (right side). The burn damage extends to the intermediate dermis (burn depth score 3.0; marked with dotted black line) while the interspace skin is intact. Within the burn field, a necrotic area is girdled by inflammatory cells (*). In the interspace, all skin layers can be differentiated and the amount of inflammatory cells is not increased.

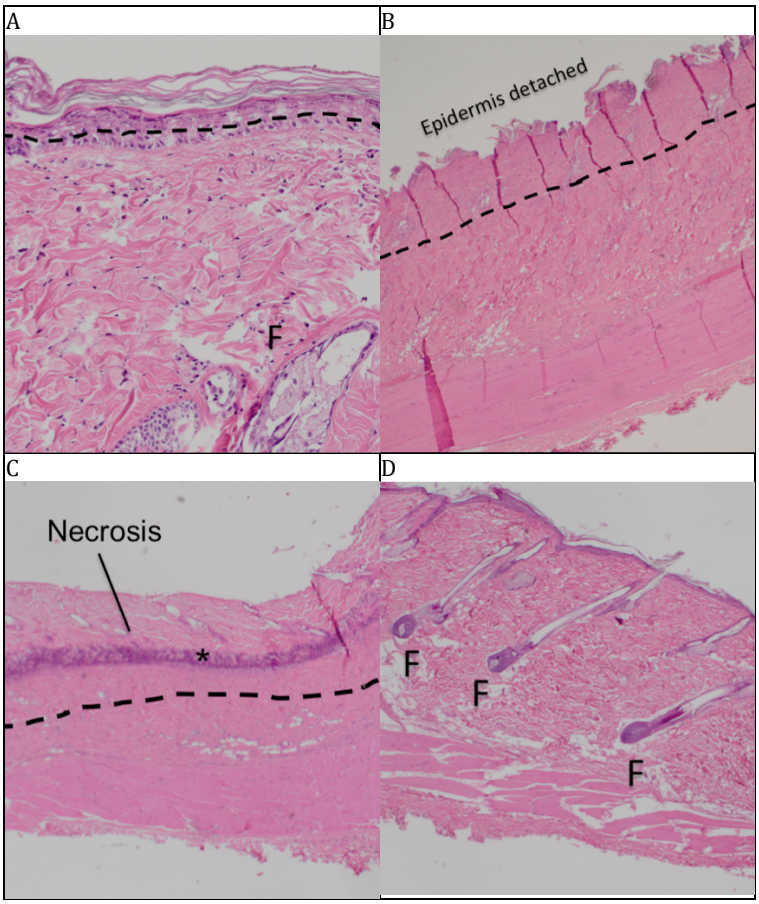

Figure 24: Burn Depths in Different Histological Samples
Histological burn depth restricted to the epidermis, burn depth score 1.0 (A). Above the black line, the epidermis is not intact and nuclei are not distinguishable.
Histological burn depth extending through the superficial dermis, burn depth score 2.0 (B). The black line marks the transition between injured and vital tissue. The epidermis is detached.
Histological burn depth extending through the intermediate dermis, burn depth score 3.0 (C). Necrosis is visible in the more superficial layers of the dermis and girdled by inflammatory cells (*). No vital follicles are distinguishable.
Vital skin, all layers are intact, burn depth score 0.0 (D). This burn field has healed after 65 days. Vital hair follicles are marked with F.

9.1.2 Maximum Burn Depth

Burn depth after 10sec burn showed maximum histological damage to the intermediate dermis throughout all time points; no burn depth score greater than 3.0 was found; neither in burn fields nor in interspaces. Maximum median burn depth in 10sec burn fields was seen on days 1, 3 and 7 with a burn score of 3.0 (Figure 25). In none of the obtained sections did the interspace damage exceed the burn field damage. After a 60sec burn, there was histological evidence of full-thickness injury in several sections. On days 4 and 7, the median burn field burn depth in the 60sec group was 5.0. Again, the interspace depth never exceeded the burn field depth. Burn field injury on day 7 was significantly deeper in the 60sec group than in the 10sec group (medians 5.0 and 3.0; p=0.012). The same pertained for interspaces on day 7:

The median interspace burn depth in the 60sec group was significantly deeper than in the 10sec interspaces (medians 5.0 and 1.5; p=0.006).

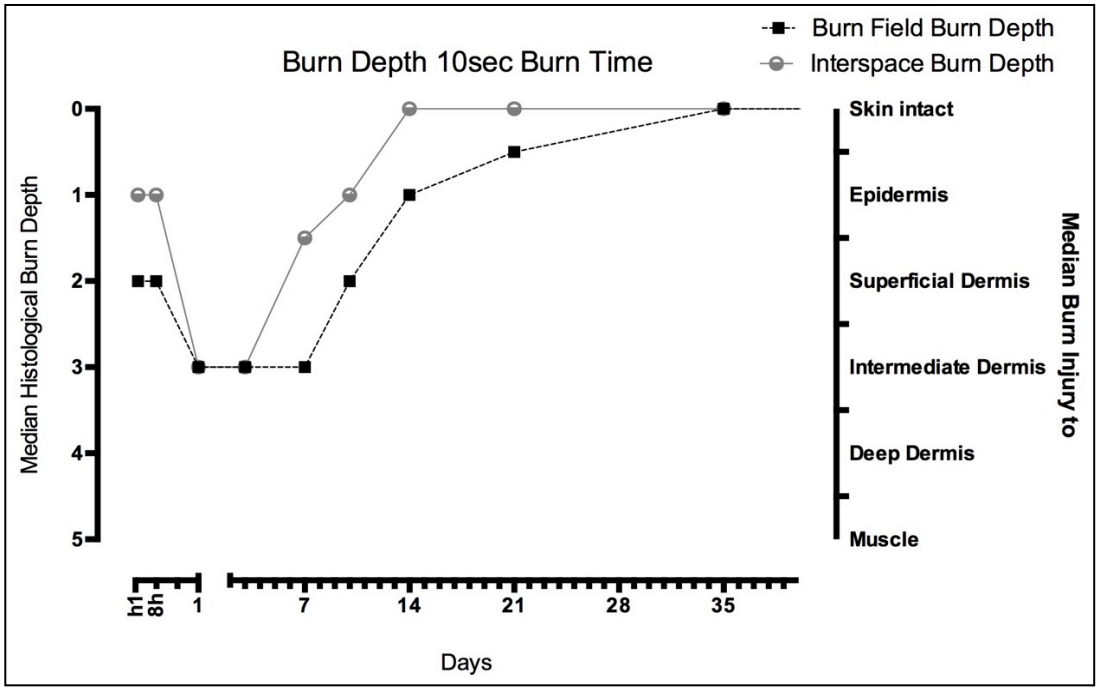

Figure 25: Median Histological Burn Depth after 10sec Burn
Depicted are medians of burn depth scores for interspace (grey line) and burn fields (black dotted line). The first day is expanded for visualization purpose. 10sec injury depth progressed between 8 hours and day 1, detectable in both interspaces and burn fields. No damage deeper than the intermediate dermis was found. Regeneration in interspaces was observed from day 7 onwards, while the burn fields showed regeneration after day 10. No histological damage can be spotted in the median burn depth score at day 14 for interspaces and day 35 for burn fields.

9.1.3 Progression and Regeneration of Burn Depth

The burn field injury depth in the 10sec group progressed from a median of 2.0 for 1 hour and 8 hours to a median of 3.0 on day 1. There was no further deepening of the burn field injury after day 1 in the 10sec group (Figure 25). At 1 and 8 hours after 10sec burn induction, the interspace depth was more superficial than the burn field depth (p=0.018 at h8) before interspace injury progressed to a median of 3.0 on days 1 and 3 (Figure 25). The 10sec burn injury in the interspaces had a regeneration trend towards more superficial damage from day 7 onwards (not significant; p=0.264 at d7) with a median interspace burn score of 1.5. After further declining to 1.0 on day 10, the median burn score for interspaces was 0.0 from day 14 onwards (Figure 25). In the majority of interspaces obtained after 2 weeks, no burn injury was histological evident. Also burn field injury depth following a 10sec burn was declining over time. After extending to the intermediate dermis on day 7, it showed a reduced

burn depth on day 10 (median 2.0), day 14 (median 1.0) and day 21 (median 0.5). In the obtained burn fields on days 35 and 65, there was no histological damage.

Burn wound deepening took longer following the 60sec burn: It took until day 4 to reach maximum median burn field damage to the muscle. While on day 2, none of the inspected 60sec interspace or burn fields had a burn depth score greater than 4.0 (damage to the deep dermis), most interspaces and burn fields were injured deeper on day 4 with medians of 5.0 for 60sec interspaces and burn fields. Decrescent burn depth was delayed in the 60sec group: On day 21 the median burn depth for the 60sec burn fields was 2.0 compared to 0.5 in the 10sec group (not significant; p=0.133) (Table 3). While 10sec interspaces had a median burn score of 0.0 after three weeks, the 60sec interspaces then still had deeper burn damage (median 2.0; p=0.002).

Table 3: Median Burn Scores in Interspaces and Burn Fields on Day 21

Day 21:	10sec	60sec	
Median Burn Score **Interspaces**	0.0	2.0	p=0.002
Median Burn Score Burn **Fields**	0.5	2.0	p=0.133

9.2 Macroscopic Interspace Necrosis

Macroscopic interspace necrosis was determined from day 1 onwards. 18 animals were included for interspace necrosis evaluation (Figure 26).

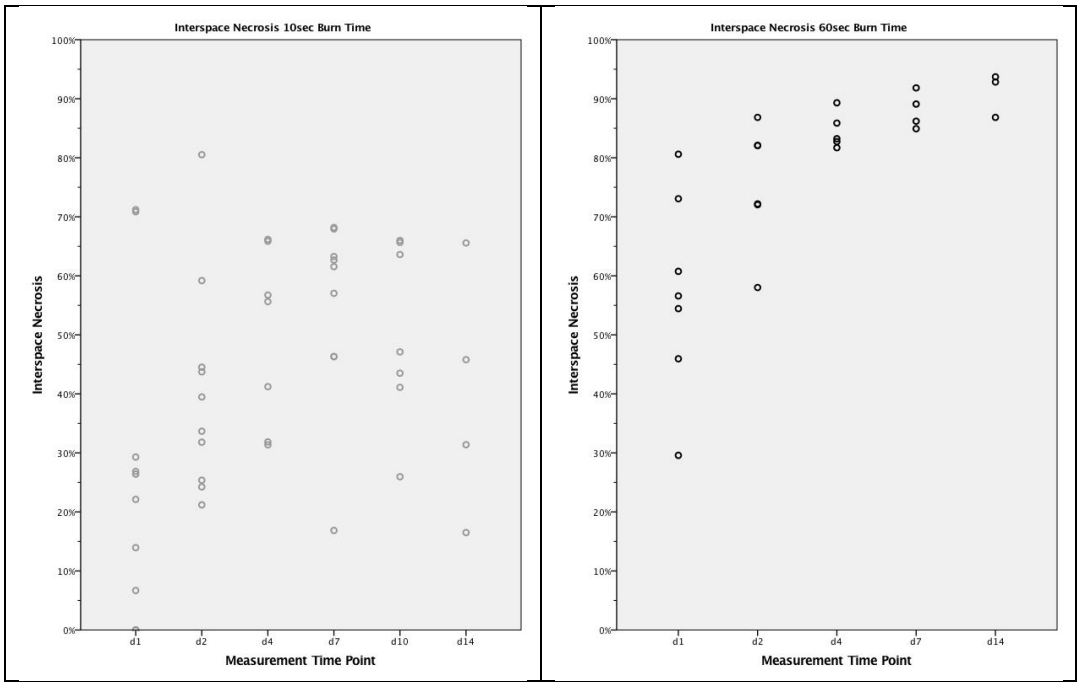

Figure 26: Scatter Plots of Interspace Necrosis after 10sec and 60sec Burn
Interspace necrosis after 10sec (left graph, grey dots) and 60sec (right graph, black dots) burn. Each dot represents one analyzed animal with its interspaces.

In the 10sec group, the mean gross macroscopic interspace necrosis progressed in the first seven days (Figure 27). On day 1, the mean interspace necrosis was 24% (SEM 8%). It significantly increased to a mean of 40% (SEM 6%) on day 2 (p=0.001). In all analyzed animals, interspace necrosis increased between days 1 and 2. All further increases did not show a significant change (d4 50%; SEM 6% and d7 54%; SEM 5%). The maximum observed interspace necrosis in a single animal was 81%, seen on day 2 (Figure 26). Interspace necrosis in the 10sec group decreased non-significantly on day 10 and 14 to a mean of 50% (SEM 6%) and 40% (SEM 10%) respectively.

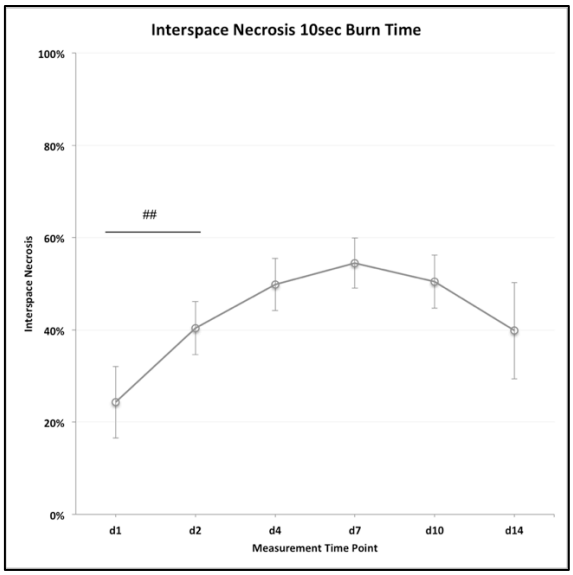

Figure 27: Interspace Necrosis after 10sec Burn
10sec mean interspace necrosis increased from day 1 to day 7. It decreased on days 10 and 14. Only the increase day 1 to day 2 showed a significant change (## p=0.001).

Macroscopic necrosis on day 1 of 57% (SEM 6%) was more marked in the 60sec group (p=0.009) (Figure 28). All evaluated 60sec animals had an increase in interspace necrosis between days 1 and 2, leading to a mean of 76% (SEM 4%). Further increases on day 4 (85%, SEM 1%), day 7 (88%, SEM 2%) and day 14 (91%, SEM 2%) did not show a significant change.

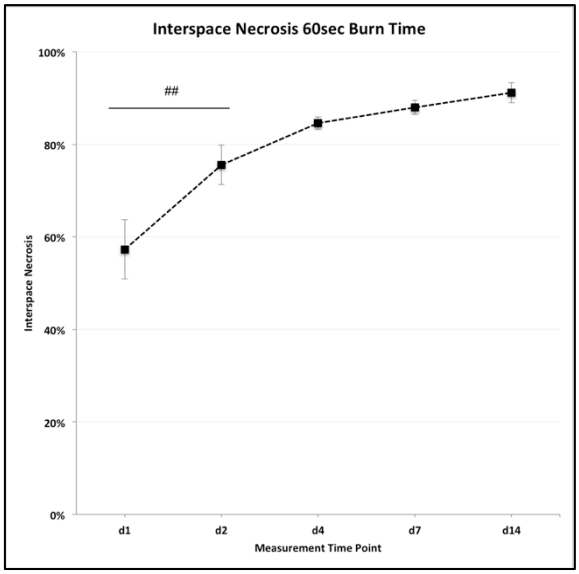

Figure 28: Interspace Necrosis after 60sec Burn
60sec mean interspace necrosis increased between each measurement. Only the increase from day 1 to day 2 was significant (## p=0.001).

The mean interspace necrosis in the 60sec group was significantly higher at all measurement time points (Figure 29 and Figure 30) (d1 p=0.009; d2 p=0.001; d4 p=0.001; d7 p=0.002; d14 p=0.009). Burn time did have a significant main effect onto interspace necrosis (p=0.002). The maximum mean interspace necrosis after a 10sec burn was 54% (day 7) while the minimum mean interspace necrosis after a 60sec burn was 57% (already on day 1). The major increment in interspace necrosis was seen between days 1 and 2, mirrored in the significant changes (p=0.001) in gross interspace necrosis between these days in both groups (Figure 27 and Figure 28). All changes between later time points were non-significant.

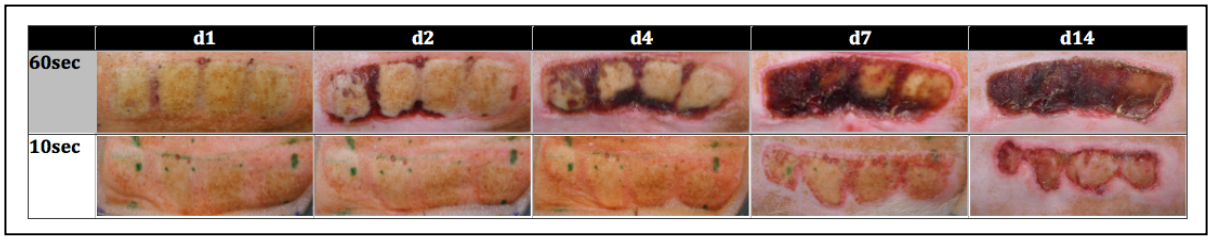

Figure 29: Macroscopic Wound Aspects after 60sec and 10sec Burn
Depicted are photographs of a 60sec and 10sec burn wound over a 14-day period. Following a 60sec burn, interspace necrosis is more pronounced with burn fields and interspaces conflating into one wound.

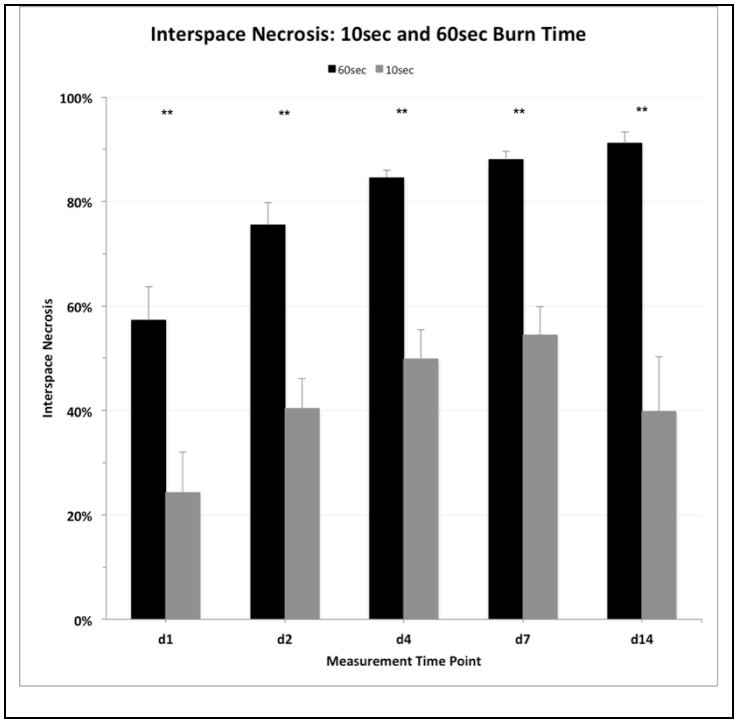

Figure 30: Interspace Necrosis after 10sec and 60sec Burn
Mean interspace necrosis after 60sec burn (black columns) and 10sec burn (grey columns). 10sec burn interspace necrosis was significantly lower throughout all time points (** $p<0.01$).

9.3 Microcirculatory Perfusion

9.3.1 Perfusion 10 Seconds Burn Time

In the 10sec group, perfusion data from 13 animals were analyzed (Figure 31).

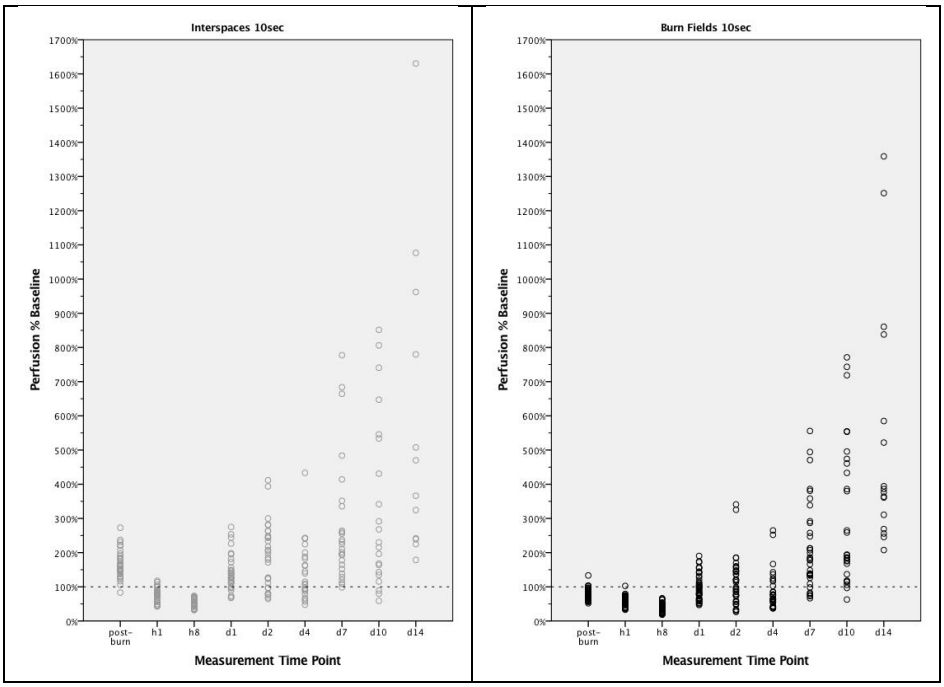

Figure 31: Scatter Plots of Interspace and Burn Field Perfusion after 10sec Burn
Each dot represents one analyzed interspace (left, grey) or burn field (right, black) after a 10sec burn. Note, all interspaces and burn fields are perfused below baseline levels at 8 hours after burn induction.

An example of the obtained LSCI images, sample perfusion and planimetric photography in one 10sec animal over 14 days is shown in Figure 32 and Figure 33.

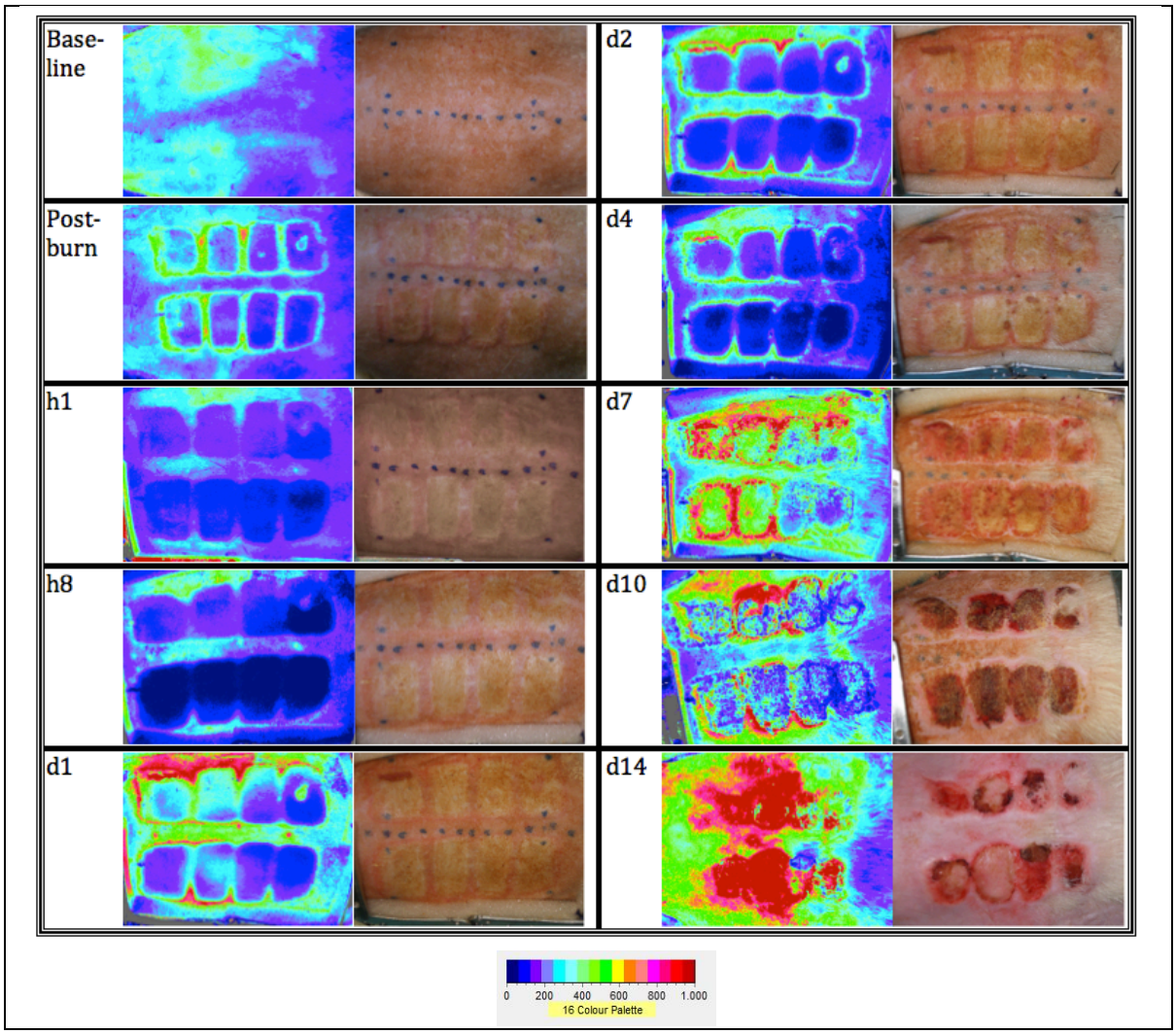

Figure 32: Sample Flowmetry and Gross Images after 10sec Burn
Gross macroscopic wound aspect and corresponding averaged flowmetry images for one animal from baseline to day 14. On all pictures left side is cranial. Animal from 10sec group. Note the changes in macroscopic appearance and in corresponding LSCI flowmetry. Refer to depicted color palette for perfusion reference. Also note how interspaces between single burn fields can still be distinguished.

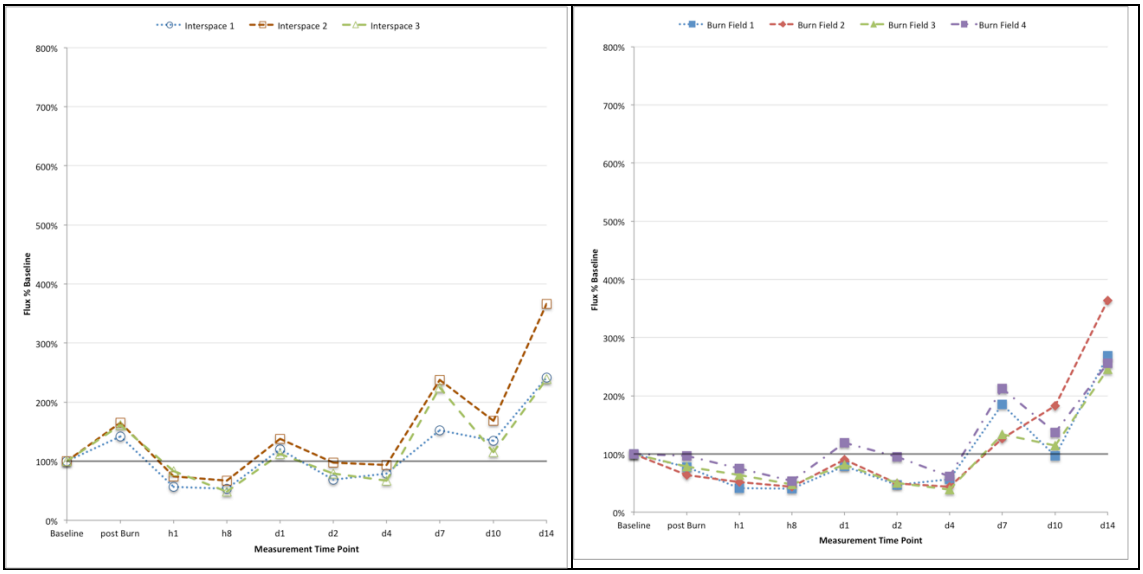

Figure 33: Sample Relative Perfusion after 10sec Burn
Relative perfusion from the animal in Figure 32 is shown for interspaces (left graph) and burn fields (right graph). Each dot represents interspace or burn field perfusion relative to baseline.

Throughout the experiment, the mean relative interspace perfusion was higher than the mean relative burn field perfusion (Figure 34) in the 10sec group with significant differences each time point between post-burn and day 7 ($p<0.001$ for post-burn, h1, h8, d1, d2, d4 and $p=0.006$ for d7). The interaction of burn status (interspace or burn field) and time did show a significant effect ($p=0.017$). Burn status alone also showed a significant main effect onto the perfusion ($p<0.001$).

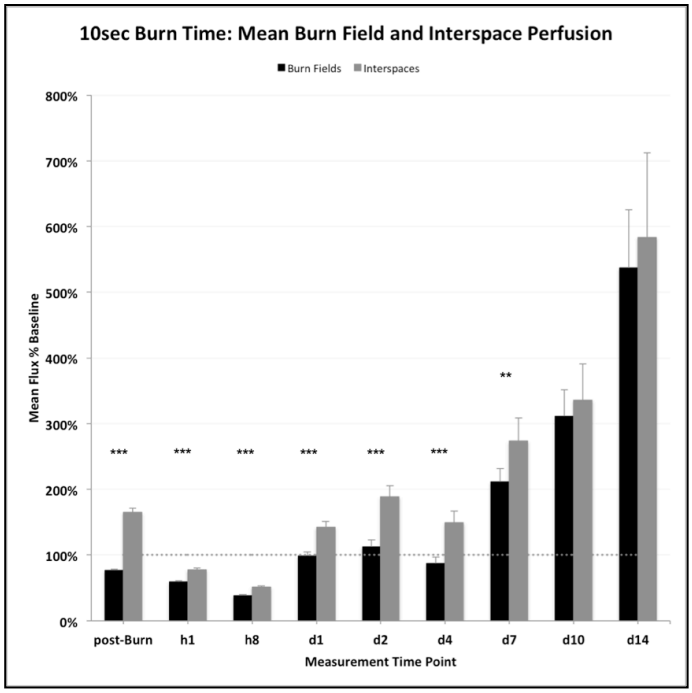

Figure 34: Burn Field & Interspace Perfusion after 10sec Burn
Mean relative interspace perfusion (grey columns) was higher than mean relative burn field perfusion (black columns) throughout all time points. Interspace perfusion was significantly higher from post-burn to day 7 (*** $p<0.001$ and ** $p=0.006$).

After burn induction, mean relative interspace perfusion even increased to levels above baseline (165%; SEM 6%; p<0.001) (Figure 35) while mean burn field flux decreased significantly (77%; SEM 2%; p=0.006) (Figure 36). The decrease in 10sec burn field flux continued from post-burn to 1 hour (59%; SEM 2%, p=0.016) and to 8 hours (38%, SEM 2%). Alike, also 10sec mean interspace perfusion decreased significantly (p<0.001) to levels below baseline on 1 hour (78%, SEM 3%, p=0.049 to baseline) and 8 hours (51%; SEM 2%; p<0.001 to baseline). All observed 10sec burn fields and interspaces were perfused below baseline at 8 hours (Figure 31) and had their minimum mean perfusion values then.

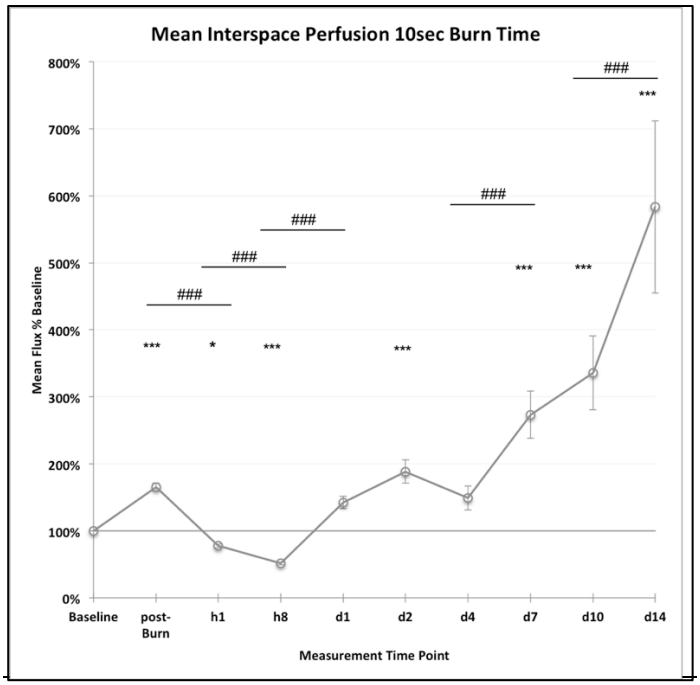

Figure 35: Interspace Perfusion after 10sec Burn
The mean relative interspace perfusion was significantly different from baseline throughout most time points except on days 1 and 4 (*** p<0.001; * p=0.049). After an increase in perfusion on post-burn, interspace perfusion decreased significantly on h1 and on h8. Afterwards, the 10sec interspace perfusion increased significantly between h8 and d1, between d4 and d7 as well as between d10 and d14 (### p<0.001).

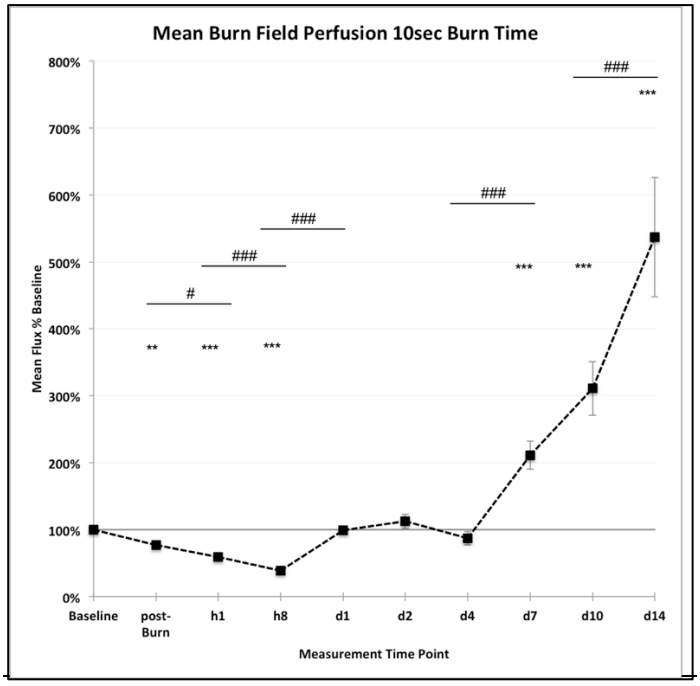

Figure 36: Burn Field Perfusion after 10sec Burn
The mean relative burn field perfusion was significantly different from baseline except on d1, d2 and d4 (*** p<0.001; ** p=0.006). Burn field perfusion decreased significantly between each time point until h8, before increasing again on d1. Later, the increase in perfusion was significantly different from d4 to d7 and d10 to d14 (### p<0.001; # p=0.016).

9.3.1.1 Interspaces & Burn Fields Reach Baseline One Day after 10sec Burn

10sec interspace and burn field perfusion, increased significantly from their minimum to day 1 (p<0.001 for both). All evaluated interspaces and burn fields were better perfused on day 1 than at 8 hours. The mean relative perfusion of 142% (SEM 9%; p=0.05) for interspaces and 99% (SEM 6%; p=1.00) for burn fields, did not differ significantly from baseline levels as presented in Figure 35 and Figure 36. On day 2, the perfusion further increased, not significantly, to 189% (SEM 17%) in interspaces and to 112% (SEM 11%) in burn fields. The interspace perfusion distinctively exceeded baseline levels at that time point (p<0.001). However on day 4, interspaces were perfused at a level of 149% (SEM 18%) while burn fields were perfused at 87% (SEM 10%). There was no statistical difference in perfusion levels between days 1, 2 and 4 for 10sec interspaces or burn fields but only interspace perfusion on day 2 was significantly above baseline. Following day 4, the perfusion steadily increased until 14 days after the burn. Interspaces and burn fields were better perfused than baseline (p<0.001) for all later time points. On day 7, the perfusion levels had increased significantly (p<0.001 for both) to mean relative interspace perfusion of 273% (SEM 35%) and burn field perfusion of 211% (SEM 21%). Only then - on day 7 - mean burn field perfusion was significantly higher than baseline. On day 10, interspace and burn

field perfusion levels were 336% (SEM 55%) and 311% (SEM 40%). With further increasing (both $p<0.001$), the perfusion 14 days after burn induction was 584% (SEM 129%) in interspaces and 537% (SEM 89%) in burn fields.

9.3.2 Perfusion 60 Seconds Burn Time

Perfusion data from 8 rats was evaluated for the 60sec burn group (Figure 37). An example of wound evolvement and corresponding LSCI data from a rat burned for 60sec is shown in Figure 38 and Figure 39.

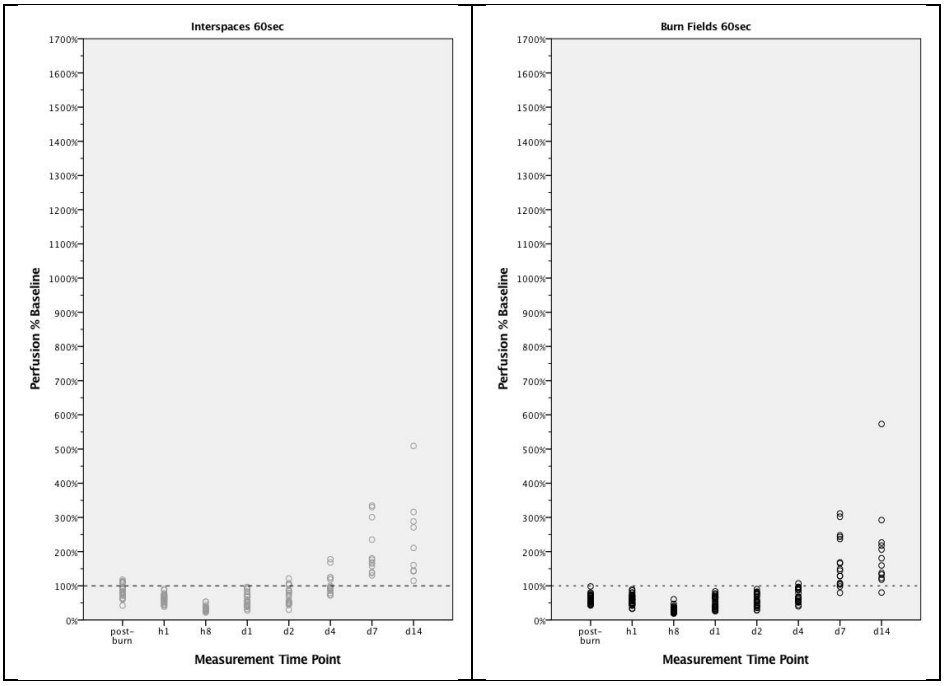

Figure 37: Scatter Plots of Interspace and Burn Field Perfusion after 60sec Burn
Each dot represents one analyzed interspace (left, grey) or burn field (right, black) after a 60sec burn.

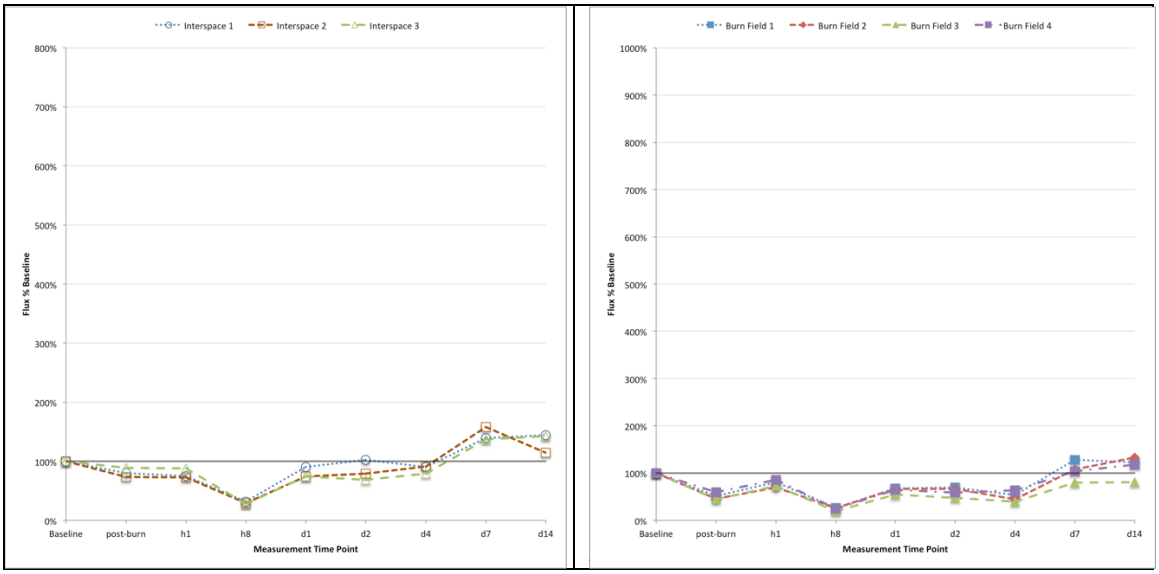

Figure 38: Sample Relative Perfusion after 60sec Burn
Shown are the results for relative interspace (left graph) and burn field (right graph) perfusion from the animal depicted in Figure 39. Color legend above graphs. Each dot represents the evaluated interspace or burn field perfusion relative to baseline. All baseline perfusion was set to 100%.

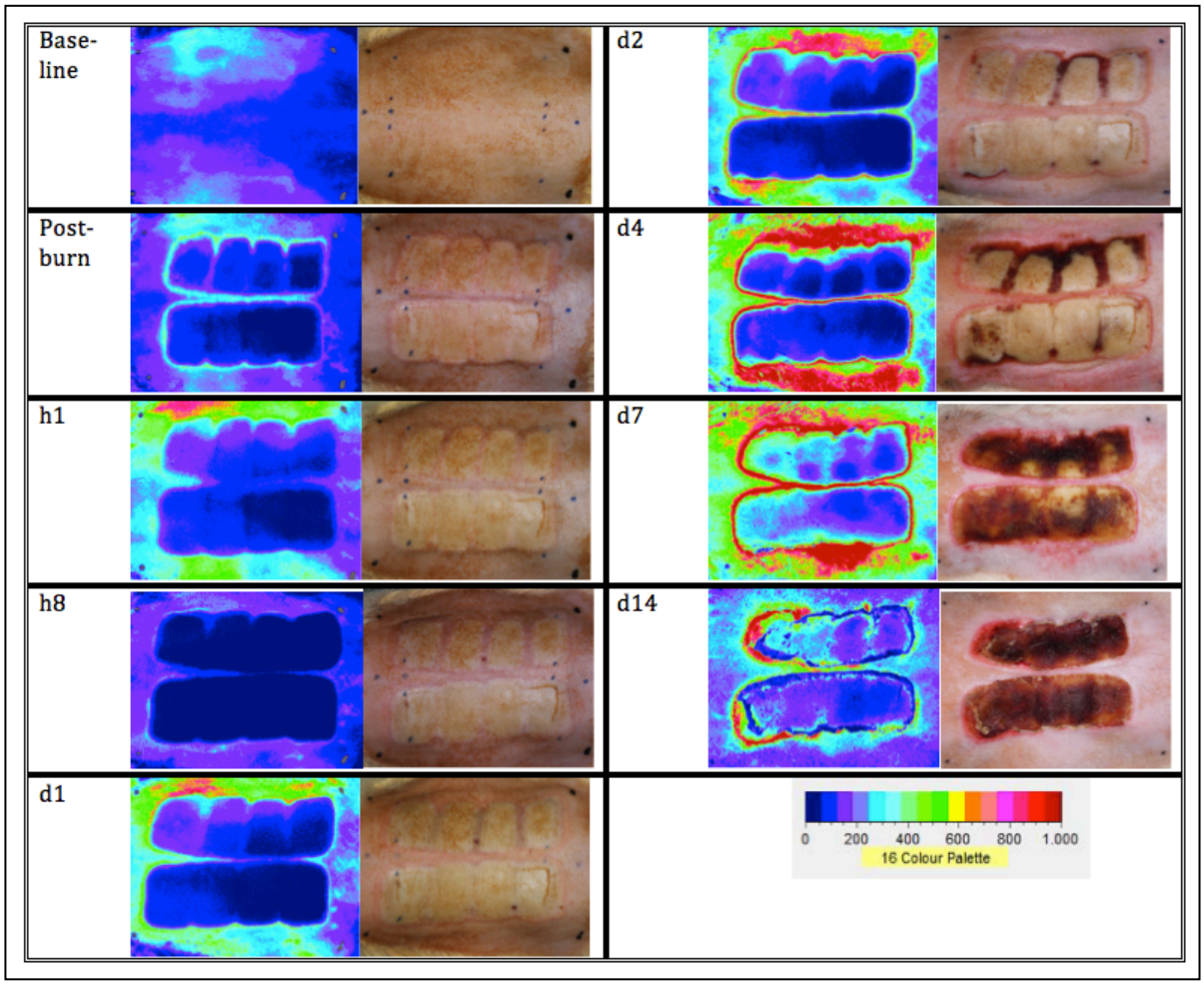

Figure 39: Sample Flowmetry and Gross Images after 60sec Burn
Gross macroscopic wound aspect and corresponding averaged flowmetry images for one animal from baseline to Day 14 following a 60sec burn. On all pictures left side is cranial. Note the changes in gross appearance and in corresponding LSCI flowmetry. Refer to depicted color palette for perfusion reference. Graphical representation of flowmetry can be found in Figure 38. Note how macroscopically no clear distinction between interspaces and burn fields can be made on later time points.

On all analyzed time points in the 60sec group, mean relative interspace perfusion was higher than burn field perfusion (Figure 40). The interaction of burn status and time did not show a significant difference (p=0.467) but burn status alone did have a significant main effect onto the perfusion (p<0.001) following a 60sec burn. Regarding single time points, the burn status had a significant effect onto the perfusion after a 60sec burn except at 1 hour and 14 days (Figure 40).

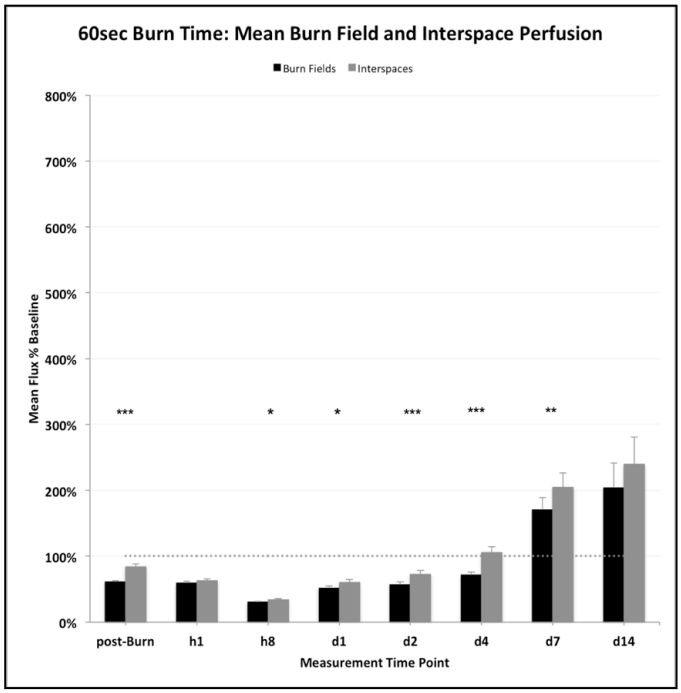

Figure 40: Burn Field & Interspace Perfusion after 60sec Burn.
The mean relative interspace perfusion (grey columns) was higher than mean relative burn field perfusion (black columns) throughout all time points. The perfusion between interspaces and burn fields was significantly different except at 1 hour and day 14 (*p<0.05, **p<0.01 and *** p<0.001).

9.3.2.1 Interspaces and Burn Fields Perfusion is Higher in the 10sec Group compared to the 60sec Group

We could observe a significant main effect (p<0.001) of burn time regarding interspace perfusion between the 10sec and the 60sec group. Throughout all time points the 10sec mean relative interspace perfusion was higher than in the 60sec group (Figure 41), with significant differences throughout post-burn to day 2. Comparing burn field perfusion between 10sec and 60sec, both the interaction of burn time and measurement time (p=0.001), as well as burn time alone (p=0.003) had a significant effect onto the perfusion. When comparing single time points, burn

field perfusions on post-burn (p=0.001), day 1 (p=0.001) and day 2 (p=0.045) showed a significant difference (Figure 42).

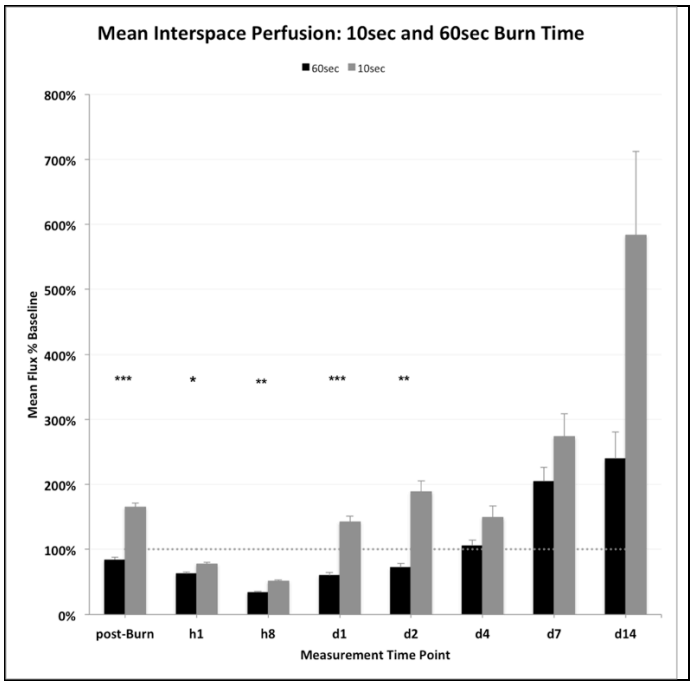

Figure 41: Interspace Perfusion after 10sec and 60sec Burn
Mean relative interspace perfusion after 60sec burn (black columns) and 10sec burn (grey columns). The 10sec interspace perfusion was higher throughout all time points with significant differences at post-burn, h1, h8, d1 and d2 (*** p<0.001; ** p<0.01; *p<0.05).

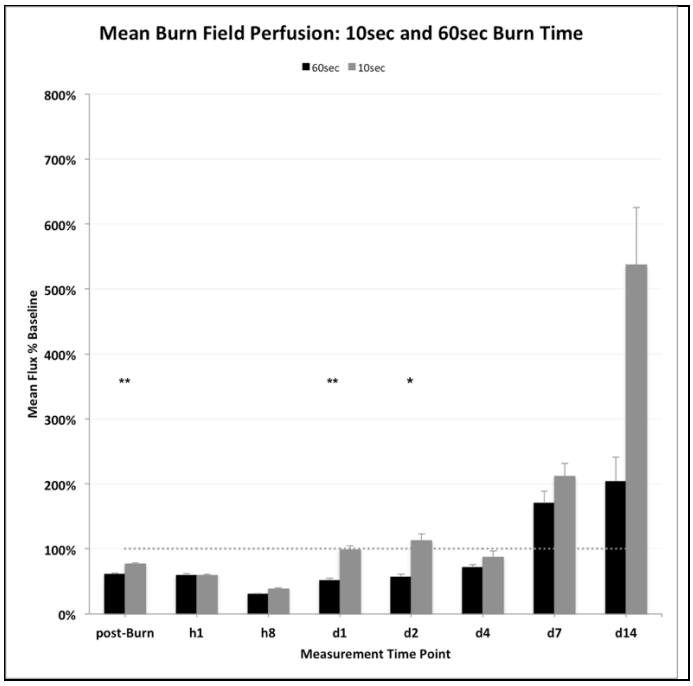

Figure 42: Burn Field Perfusion after 10sec and 60sec Burn
Relative burn field perfusion after 60sec burn (black columns) and 10sec burn (grey columns). On single time points, the burn field perfusion following a 10sec or 60sec burn was significantly different on post-burn, day 1 and day 2 (** p<0.01 and * p<0.05).

Unlike in the 10sec group, in the 60sec group, both - mean relative interspace and burn field perfusion - declined after the burn induction on the post-burn measurement (Figure 41). Perfusion in burn fields was lower than in interspaces ($p<0.001$). Mean interspace perfusion declined to 84% (SEM 4%, no significant difference to baseline) while burn field perfusion decreased significantly to 61% (SEM 2%; $p<0.001$) as shown in Figure 43 and Figure 44.

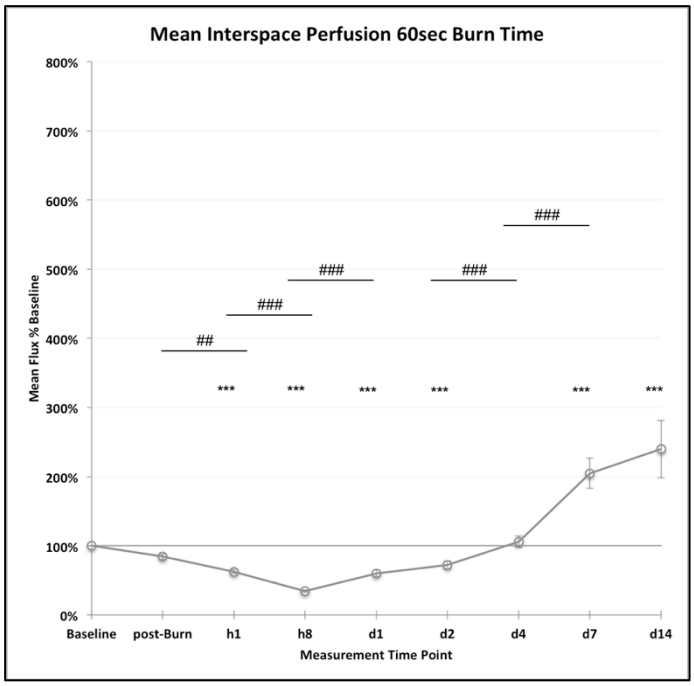

Figure 43: Interspace Perfusion after 60sec Burn
The mean relative interspace perfusion was significantly higher, respectively lower than baseline throughout the experiment except at post-burn and d4 (*** $p<0.001$). Significant changes in perfusion between two adjacent analyzed time points are depicted (## $p=0.003$ and ### $p<0.001$).

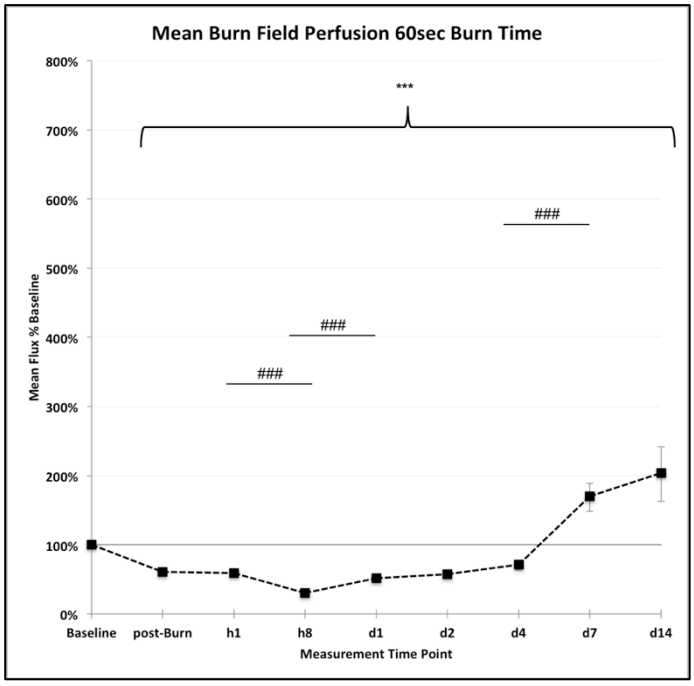

Figure 44: Burn Field Perfusion after 60sec Burn
The mean relative burn field perfusion was significantly different from baseline levels throughout all time points (*** p<0.001). Perfusion declined up to 8 hours before increasing afterwards. Significant changes are shown (### p<0.001).

Interspace perfusion reached significantly lower levels than baseline 1 hour after the 60sec burn (63%; SEM 3%; p<0.001) with a decreased perfusion compared to post-burn (p=0.003). There was no significant difference compared to burn field perfusion of 59% (SEM 3%) on that time point (Figure 40). Burn field perfusion had not changed significantly between post-burn and 1 hour (Figure 44). There was no difference in burn field perfusion at 1 hour between 10sec and 60sec burns (both means 59%; p=0.958) (Figure 42).

8 hours after 60sec burn induction both interspace and burn field perfusion had further declined (both p<0.001). Interspace and burn field perfusion in the 60sec group was at its minimum at 8 hours (interspace 34%; SEM 2%; and burn field 30%; SEM 2%) but interspaces were significantly higher perfused than burn fields (p=0.013) (Figure 40). Minimum mean interspace perfusion in the 60sec group was lower than in the 10sec group (p<0.001 on h8)(Figure 41).

After the nadir, the relative 60sec burn field and interspace perfusion increased significantly again on day 1 (both p<0.001). The mean interspace perfusion was 60% (SEM 5%). This was significantly better than the mean burn field perfusion of 52% (SEM 3%; p=0.022) (Figure 40). Still, on day 1 both mean perfusions were below baseline (p<0.001) and all measured interspaces and burn fields were perfused below 100% (Figure 37). At this time point in the 10sec group, more than 80 percent of the

interspaces had established greater than pre-burn levels (Figure 31) and mean interspace perfusion did not show any difference to baseline any more (Figure 35) 10sec interspace perfusion was significantly better than corresponding 60sec perfusion on day 1 ($p<0.001$)(Figure 41).

Between days 1 and 2, the 60sec interspace perfusion further increased (not significant) to a mean of 72% (SEM 6%). Again this was significantly higher than the corresponding burn field perfusion (57%; SEM 4%; $p<0.001$).

9.3.2.2 60sec Interspace Perfusion Recovers To Baseline Four Days After Burn

On day 4, the 60sec mean relative interspace perfusion reached pre-burn levels of 106% (SEM 8%; no significant difference to baseline). This perfusion was distinctively higher than on day 2 ($p<0.001$). 60sec burn field perfusion on day 4 (71%; SEM 4%) was still significantly lower ($p<0.001$) and below baseline ($p<0.001$). However, following the 60sec burn there was no non-significant drop in perfusion on day 4 as observed after the 10sec burn. Between days 4 and 7, 60sec interspace perfusion increased distinctively ($p<0.001$). This resulted in a mean perfusion of 205% (SEM 22%), substantially above baseline ($p<0.001$). With a significant increase ($p<0.001$), 60sec burn fields were also better perfused than baseline for the first time on day 7 (170%; SEM 19%; $p<0.001$). Day 7 was the last analyzed time point where burn fields were significantly lower perfused than interspaces in the 60sec group ($p=0.009$). The mean relative interspace and burn field perfusions 14 days after burn induction were 240% (SEM 41%) and 204% (SEM 38%), respectively. Both regions were better perfused than baseline ($p<0.001$). On days 4, 7 and 14, there was no distinct difference in interspace perfusion between the 10sec and the 60sec group, neither was there a significant difference on these days in burn field perfusion (Figure 41 and Figure 42).

9.4 Frame Quality

9.4.1 Frame Designs & Preliminary Frames

Most of the preliminary frames in the 12 initial animals were not durable enough. Only the aluminium frames seemed practical to allow adequate usability in larger groups and for the desired time period. The high flexibility of the proposed soft Varihesive® bandaging material of the first frame did not provide sufficient stability

on the rat's dorsum. Animals gnawed on the lateral sides of the frame (Figure 45). This was only observed on the lateral side with the cranial and caudal parts intact. We assessed this frame type as not suitable.

Figure 45: Lateral Sides of the Soft Frame
Soft frames two days after mounting. The animals with the soft frames gnawed at the lateral sides of the soft frame. Sutures and Varihesive® material were flawed. The cranial and caudal parts of the soft frame seemed intact.

After strengthening the lateral sides with thermoplastic material, rats were also able to gnaw on the enhanced frame. Rats disassembled the individual parts within 2 days after mounting. We decided to avoid materials that could be affected by gnawing for the following frame designs. However, the split design of the plastic appeared to allow frame fitting without restricting mobility.

We used aluminium for the next frame design. Due to the broad width and stiffness of the first created components of the aluminum frame, we struggled to mount all 8 individual parts of the broad frame onto the rat's dorsum (Figure 46).

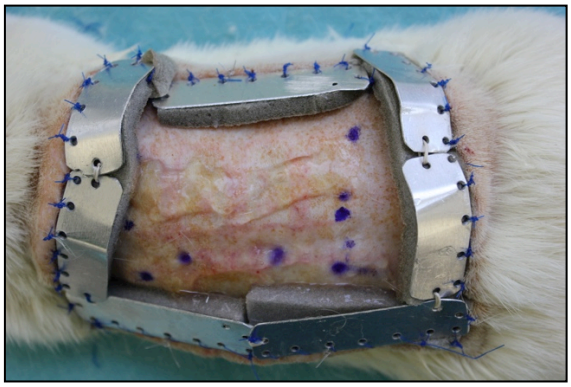

Figure 46: Mounted Single-Layered Aluminium Frame
This frame was too broad to be assembled in an easy fashion. Only 7 from 8 planned frame parts could be used in the shown specimen.

Over the first days, the rats did not attack the frame itself. Metal seemed a durable and lightweight material for frame construction. However, over the time course of 2-3 days, especially the lateral stitches were still gnawed at. With the aluminium design

showing improvement over the non-metal frames, we decided to further develop an alternative aluminium frame version.

9.4.1.1 Final Aluminium Frame

Further changes including re-sizing the frame, double-folding the components, solely suturing in single button technique and only applying the frame in combination with an Elizabethan collar then allowed a quick mounting and good fitting (Figure 47). On the preliminary rats with this frame, it showed a durability of more than 2-3 days. No friction of the rat's skin was observed. We decided to use this modified final 84x88mm aluminium frame in order to test for durability over the time course of ten days in our experiment animals.

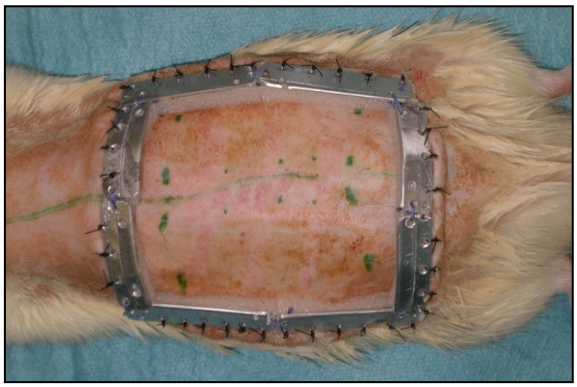

Figure 47: Mounted Frame with Eight Double-Layered Aluminium Components
The frame's dimension were 84mm laterally and 88mm cranially/caudally and consisted of 8 double-layered aluminum components.

9.4.1.2 Sufficient Frame Suture Protection Only with Elizabethan Collar

While testing the different frame designs on preliminary rats, we concluded that rats were only able to tackle the frame's sutures after removing the Elizabethan collar. Rats learned how to remove the E-collar, mostly with the help of cage components or content. When an E-collar was removed, we re-attached it after the next measurement since animals did not tolerate re-fixation without anesthesia. We could not see any difference between long (85mm outer radius) or short (75mm outer radius) E-collars, neither in durability nor in rat's behavior.

9.4.2 Mounted Frame Durability

All 12 rats on which a frame was mounted tolerated it for the first 8 hours. One frame (8%) was pulled on day 1. With adequate re-suturing (see 9.4.3), on day 2, ten out of twelve frames were still intact (83%). Eight animals tolerated the frame up until day

4 (67%), as shown in Figure 48. On day 7, four frames were still mounted (33%). At the end of frame observation period on day 10, two frames were still mounted and durable (17%).

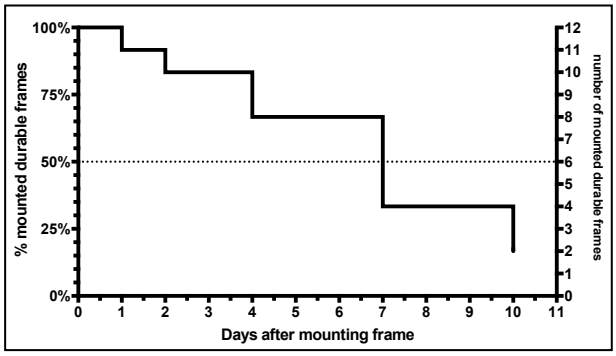

Figure 48: Frame Durability
Mounted frames over the experiment time course.
Frames were re-sutured as described when necessary.

9.4.3 Frame Quality

The frames were checked each time the animal was narcotized for measurements. The frame condition was used to assign a certain frame score according to Table 4. Examples of different frame conditions can be found in Figure 49.

Table 4: Frame Score

Frame Score	Corresponding frame condition
A	no sutures open, all sutures fixate the frame on animal
B	equal or less than five sutures are open
C	between 6 and 10 sutures are open AND no complete cranial/caudal/lateral long side is open
D	between 11 and 14 sutures are open AND no complete cranial/caudal/lateral long side is open
E	more than 15 sutures are open OR one complete cranial/caudal/lateral long side is open

If re-stitching was necessary, frame quality was documented according to its worst level from then on. No re-suturing was made if the frame was regarded as un-mounted equating a frame quality of E.

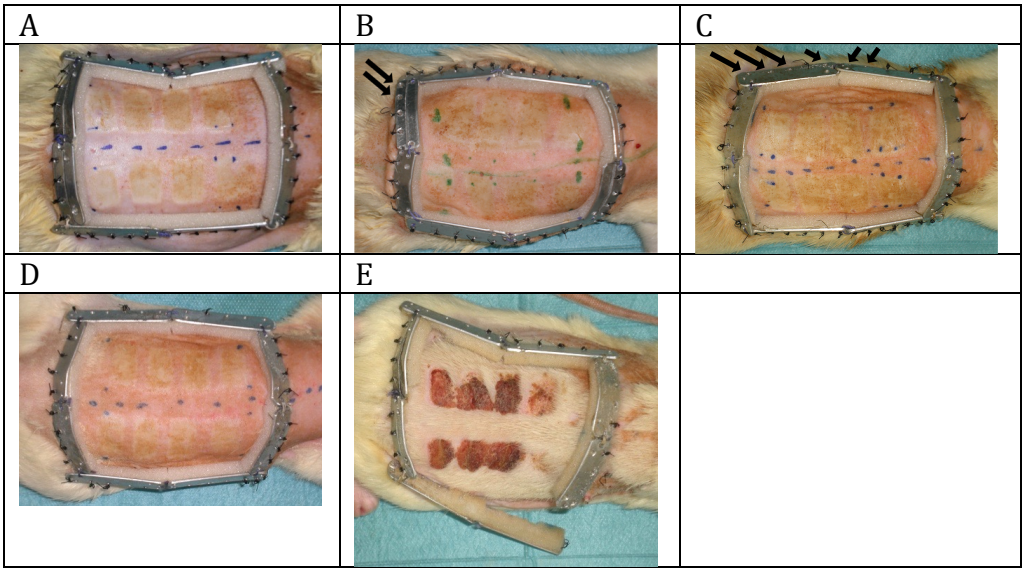

Figure 49: Frame Conditions and Corresponding Frame Scores
Animals in prone position, right side is cranial. Photographs stem from different animals and different time points. Frame scores according to Table 4.
Frame score A with no open sutures (A). Frame score B with 2 open sutures, marked with black arrows (B). Frame score C with 6 open sutures, all marked with black arrows, on left lateral components (C). Frame score D with 14 open sutures on the lateral sides (D). Note, that each frame side is at least still attached with one suture. Frame score E: Un-mounted frame with more than 15 open sutures and right lateral side components not attached anymore (E).

Figure 50 and Table 5 show the results for the "worst" frame qualities throughout the observation period. As shown, re-suturing is highly needed: While all frames were still mounted 8 hours after burn induction, nine frames were untouched (quality A) with the other three requiring re-fixation. After 7 days all but 2 frames had needed re-suturing until then. The two remaining frames on day 10 had a quality of B and were removed after completion of the measurements.

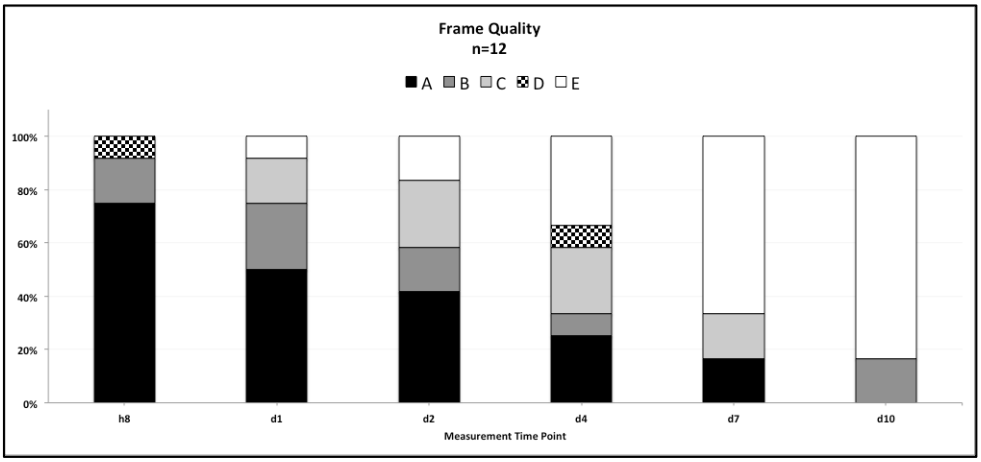

Figure 50: Frame Quality
Frame Qualities: A (no sutures open): Black; B: Dark Grey; C: Light Gray; D: Black-White-Checkered, E (frame un-mounted): White. Frame Quality assessed according to Table 4.

Table 5: Worst Frame Quality For Each Frame
12 Frames were mounted and assessed. Each row represents one specimen and its frame. Frame Quality E was assigned for un-mounted frames.

Worst Frame Quality over the Course of the Experiments						
Time Point	***h8***	***d1***	***d2***	***d4***	***d7***	***d10***
each row represents one specimen / one frame						
	A	C	C	C	C	E
	A	C	C	D	E	E
	B	B	B	E	E	E
	D	E	E	E	E	E
	A	A	A	A	A	B
	B	B	B	B	E	E
	A	A	A	E	E	E
	A	A	A	A	A	B
	A	B	E	E	E	E
	A	A	C	C	E	E
	A	A	A	C	C	E
	A	A	A	A	E	E

10 Discussion

The proposed 10sec burn comb rat model created a burn wound developing into a non-full-thickness injury. After burn wound progression, the untreated wound extended to the intermediate dermis. The model allowed LSCI measurements over two weeks, macroscopic wound evaluation and histopathological assessment. BWP was observed in histopathology and surface interspace necrosis. This non-full-thickness burn comb model showed significant differences in all three parameters when compared to the 60sec full-thickness model.

Another goal was to develop a dressing for local application of lotions or hydrogels without impairing the rat and wound assessment. The proposed frame proved to be easy to mount and allowed the desired measurements. However, for experiments over a longer period, close monitoring, repeated re-suturing and using Elizabethan collars seemed inevitable. While the frame seems feasible for the time frame where BWP is observed, an extended use for more than four days does not look practical. Further adjustments to this frame model appear necessary.

10.1 Burn Depth

10.1.1 10sec Burn Does Not Lead to Full-Thickness Injury

One purpose of this study was to establish a burn comb model with a non-full-thickness-injury. Histological analysis showed no deeper vertical damage than to the intermediate dermis following a 10sec burn. Compared to a 60sec burn, the 10sec burn led to a decreased vertical extent of the burn injury even after progression and no single specimen showed deeper damage than to the intermediate dermis.

The obtained burn depth results are according to other studies inducting the injury with a burn comb. In those experiments, an exposure of 20 seconds and above generally led to a full-thickness burn (Table 6). Only one group assessed an exposure of greater than 20 seconds, i.e. 30 seconds, as reaching only the intermediate dermis (Prindeze et al. 2016) but did not offer insights in rats' or stamp weights which could alter application time for more or less severe burns.

Table 6: Burn Comb Studies with Different Application Times and Resulting Burn Depths
All listed studies used a burn comb stamp rat model to induce a burn injury. Several studies did not provide information about stamp weight and application pressure (marked with n.a.). Most studies heated the burn comb stamp in 100° C boiling water until equilibrium was reached.

Study	Application Time (seconds)	Heating Temperature	Rat Weight (g)	Application Pressure	Stamp Weight (g)	Burn Depth
Ponticorvo et al. (2017)	4	100° C	300-450	without pressure	313	superficial partial-thickness
Ponticorvo et al. (2017)	8	100° C	300-450	without pressure	313	deep partial-thickness
Crouzet et al. (2015)	2-10	100° C (boiling water)	300-400	without pressure	313	ranging from superficial partial to deep partial - thickness
Nguyen et al. (2013)	2-15	100° C (boiling water)	350-600	without pressure	313	superficial to full-thickness
Prindeze et al. (2016)	15	100° C	n.a.	n.a.	n.a.	superficial
Tan et al. (2013)	20	100° C (boiling water)	300-350	without pressure	150	full-thickness
Eski et al. (2012)	20	100° C (boiling water)	300-350	without pressure	n.a.	full-thickness
Battal et al. (1996)	20	100° C (boiling water)	average 450g	without pressure	140	full-thickness
Battal et al. (1997)	20	100° C (boiling water)	average 450g	without pressure	140	full-thickness
Isik et al. (1998)	20	100° C (boiling water)	350-400	without pressure	n.a.	full-thickness
Uygur et al. (2009)	20	100° C (boiling water)	350-400	n.a.	n.a.	full-thickness
Regas and Ehrlich (1992)	20	100° C (boiling water)	300-500	without pressure	n.a.	full-thickness
Guo et al. (2015)	20	100° C (boiling water)	250-300	without pressure	n.a.	full-thickness
Firat et al. (2013)	20	100° C (boiling water)	300-350	without pressure	n.a.	full-thickness
Hayati et al. (2018)	20	boiling water (5 minutes stamp heating)	300-350	without pressure	n.a.	full-thickness
Prindeze et al. (2016)	30	100° C	n.a.	n.a.	n.a.	intermediate
Singer et al. (2008)	30	100° C (boiling water)	300-325	without pressure	n.a.	full-thickness
Singer et al. (2007)	30	100° C (boiling water)	300-325	without pressure	n.a.	full-thickness
Singer et al. (2011)	30	100° C (boiling water)	300-350	without pressure	n.a.	full-thickness
Rizzo et al. (2013)	30	100° C (boiling water)	300-500	without pressure	n.a.	only given in µm
Reddy et al. (2015)	30	100° C (boiling water)	240-300	without pressure	150	full-thickness
Choi et al. (1995)	30	100° C (boiling water)	325-375	without pressure	n.a.	full-thickness
Choi and Ehrlich (1993)	30	100° C (boiling water)	300-325	without pressure	n.a.	full-thickness
Wang et al. (2015)	30	100° C (boiling water)	average 420	minimal pressure	n.a.	full-thickness
Prindeze et al. (2016)	45	100°C	n.a.	n.a.	n.a.	deep partial-thickness
Tobalem et al. (2013)	60	100° C (boiling water)	432-478	without pressure	136	full-thickness
Tobalem et al. (2012)	60	100° C (boiling water)	mean 456	without pressure	136	full-thickness
Tobalem et al. (2013)	60	100° C (boiling water)	461-481	without pressure	136	full-thickness
Tobalem et al. (2019)	60	98° C (boiling water)	450-500	without pressure	136	full-thickness

Shorter than 20sec exposure times did not lead to a full-thickness injuries in burn comb models (Nguyen et al. 2013, Crouzet et al. 2015, Prindeze et al. 2016). However, none of these studies assessed the development of histopathological necrosis of the thermal injury by several biopsies in short intervals throughout the first week:

Ponticorvo and his group induced superficial and deep partial-thickness burns in rats weighing 300-450g through application of the heated burn comb for 4 seconds, respectively 8 seconds (Ponticorvo et al. 2017). The rats were lighter and the burn comb heavier than in this study accounting for a deeper depth despite shorter burn time. There was no histological observation of BWP in this study, neither was histological evaluation of interspaces since only biopsies from burn fields were taken one hour apart from the induction and on days 7, 14 and 28. Our serial biopsies offer insight into the time period where burn wounds progress; unveiling differences in intermediate and full-thickness burns regarding BWP intervals. The Ponticorvo group also applied the 313g burn comb onto rats' dorsa to create graded burn depths by exposure between 2 to 15 seconds (Nguyen et al. 2013). Depths ranged from superficial partial-thickness over deep partial-thickness to full-thickness burns as examined by viable adnexal structures. The authors graded the burn injury 3 hours after burn induction (Nguyen et al. 2013). In a different study, the same group also used LSCI to distinguish between superficial-partial and deep partial-thickness burns (Crouzet et al. 2015). They used rats weighing 300-400g and applied the same burn comb between 2-10 seconds. The investigators took biopsies from the burn sites 3 hours after burn induction. With a 10 second exposure, they created a deep partial-thickness burn (Crouzet et al. 2015) (Table 6). This again shows that a 10 seconds contact time with a heated burn comb does not lead to a full-thickness burn within the first hours. A limitation in these studies is the short follow-up of 3 hours. The authors themselves state that BWP dynamically alters burn depth within 48 hours (Crouzet et al. 2015).

No 10sec burn comb injury and its BWP has been described in rats with the same size and weight as done in this study. We believe our study demonstrates how the burn comb can be used to induce an injury progressing only to the intermediate dermis. This could be the result of a less intense thermal energy or a lower tendency of shallow burns to progress vertically. Another possible explanation could be that more superficial burns do not trigger the same systemic reactions to further aggravate BWP. Since most burn injuries in a clinical setting are more superficial than full-

thickness (Waitzman and Neligan 1993, Evers et al. 2010, Taira et al. 2010), further burn research focusing on less severe burns is necessary.

A more technical approach to induce burns in varying depths was described in 2016 (Sakamoto et al. 2016). One of the few groups using an automated device, Sakamoto et al. developed a tool to control temperature, time and pressure of the applied stamp. While they did not apply a burn comb with separated notches but instead used a circular stamp of 2cm in diameter, they were able to control the surface temperature of the stamp with an error range of 2°C and the contact time within a range of 0.05 seconds. In rats weighting 200g, a 10 seconds exposure to an 80°C heated stamp induced a histological full-thickness burn on day 1 (Sakamoto et al. 2016). This can be explained through the distinct lighter weight and thinner skin of the rats (Tobalem et al. 2019). In contrast, Tobalem et al. demonstrated that the stamp cools off over the application when not paired with constant heating: Over the 60sec application period, the stamp cooled from 87°C to 60°C (Tobalem et al. 2013). The same group repeatedly showed this in a later study (Tobalem et al. 2019). Sakamoto's burn device with a calibrated temperature has to be considered as a higher energy source over the whole application time, necessarily leading to more severe damage compared to the burn comb. The automatic device opens up new possibilities in reproducible burn depths and extents but might be difficult to use since studies often require a cost-efficient approach and patented devices might be hard to obtain, especially in pairing the device with a burn comb. However, in follow-up studies we plan to measure stamp temperature over the application time.

For better comparison, further reports using the burn comb model should include details regarding animal and stamp weight, application pressure, exposure time but also publish stamp temperature levels before and after burn induction.

10.1.2 Vertical Burn Wound Progression in Interspaces and Burn Fields

Histopathological vertical interspace necrosis was evident as early as 1 hour after burn induction in all examined 10sec interspaces. This is earlier than reported by Singer and his coworkers: They reported no evidence of necrosis following a full-thickness burn 30 minutes after burn induction, some cellular changes after 24 hours and necrosis after 48 hours (Singer et al. 2008). However, Tobalem's group could observe damage to the superficial layers as early as one hour before its progression on later time points in a 60sec burn comb model (Tobalem et al. 2019). Also the data

from Nguyen and Crouzet in their model as outlined earlier, underline that even after a short interval of three hours, histological evidence of tissue changes and impairments can be found (Nguyen et al. 2013, Crouzet et al. 2015). We believe BWP in intermediate burns can be observed as early as one hour after burn induction in interspaces and burn fields, when taking histologic samples that early.

This study shows that vertical BWP reaches its final extent within one day in intermediate burns. No further deepening was observed on later time points. The BWP interval in the 10sec model is consistent, but on the short end, with the commonly assumed BWP time frame of up to 72 hours (Hinshaw 1968, Singh et al. 2007, Singer and Dagum 2008, Singer et al. 2008). The 24 hours time frame is shorter than the analyzed BWP by Xiao and colleagues who used a brass rod to induce a partial-thickness burn in rats. They observed a deeper injury extent on 48 and 72 hours compared to 6 and 24 hours in Masson staining (Xiao et al. 2014). However, we could also observe increasing burn depth in the 60sec group on day 4. These results of vertical necrotic extension in untreated full-thickness burns following a 60 seconds exposure was accordingly to earlier publications by Tobalem et al. (Tobalem et al. 2012, Tobalem et al. 2013, Tobalem et al. 2013). The authors assessed vertical BWP through histology but did not report any differences between BWP in burn fields or interspaces instead the histology was done en-bloc of the whole burn area. In their latest study, Tobalem and colleagues assessed the correlation between horizontal and vertical BWP after a 60sec burn (Tobalem et al. 2019): The group reported damage to the superficial dermis as early as one hour and a significant vertical increase on day 1 (deep dermis) and days 4 and 7 (full-thickness) respectively (Tobalem et al. 2019). This is according to the shown results: After our 60sec burn, the injury extended to the deep dermis on day 2 and reached final full-thickness extent on day 4; both in interspaces and burn fields.

The results suggest that less severe burns do not progress vertically as long as deeper burns and tend to regenerate earlier: The tissue after a 10sec burn comb injury showed regenerative potential one week after the burn induction. Especially in the interspaces, evident damage decreased starting from day 7. Re-epithelization was noticeable within three weeks after the 10sec burn. After the 60sec burn, microscopic damages was still visible after day 21. Consistent with our results, Ponticorvo et al. could see fast re-epithelization after a 4 second, superficial partial-thickness burn (Ponticorvo et al. 2017). They showed re-epithelization by hyperplastic epithelium

from day 7 onwards and baseline thickness epithelium between days 13 and 28 while a deeper 8 seconds burn then still had hyperplastic epithelium. Ponticorvo stated that re-epithelization originated from undamaged hair follicles in superficial partial-thickness burns while healing in deeper burns could be observed stemming from the bulge of damaged hair follicles (Ponticorvo et al. 2017), offering a possible explanation for faster re-epithelization following a scarcer energy exposure. This lets us believe that in our intermediate burn, skin appendages are still intact while after the 60sec burn they are damaged. However, histopathological workup did not show clear vital hair follicles in most of the intermediate burns. Another explanation for less BWP and fast regeneration could be attenuation through earlier re-perfusion (Schmauss et al. 2014). After a 10sec burn, interspace and burn field perfusion levels were earlier increased compared to prolonged exposure. Since sustained limited perfusion attributes to ischemia and tissue damage, an earlier restored perfusion reduces histological necrosis and promote faster healing (Hettiaratchy and Dziewulski 2004). The observed longer perfusion impairment after the 60sec burn might explain longer and deeper BWP and delayed regeneration. However, the post-burn increased interspace perfusion in the 10sec group could not avoid tissue damage and BWP. Arguably, the increased perfusion following the burn was either not sufficient or not maintained long enough to avert BWP since interspace perfusion increased post-burn, yet still dropped below pre-burn levels within few hours.

Our study showed vertical progression to full-thickness in burn fields and interspaces after a 60sec burn. Burn depth did reach the same dermal layers irrespective of burn status (interspace or burn field). The same applied to the 10sec burn where vertical BWP could be seen in interspaces and burn fields but only extending to the intermediate dermal layer and reaching its final extent within 24 hours. We showed burn depth does not compulsory differ after BWP in interspaces and burn fields, defining morbidity in these wounds, regardless of direct or indirect damage.

However, in our intermediate burn, BWP only took one day to reach its final vertical extent, which is shorter than the formerly described time frame of 48-72 hours. The final vertical extent in the full-thickness group was only reached within 4 days after burn induction. We therefore argue, that the time frame where burn wounds progress also depend on the originally inflicted damage.

10.2 Macroscopic Interspace Necrosis

Horizontal BWP leads to increased surface extent of the burn wound (Lanier et al. 2011, Macri et al. 2013). This was observed in this study through macroscopic decay in the originally unburned interspaces.

10.2.1 Horizontal Burn Wound Progression is Most Prominent Until Day 2

Interspace necrosis, and hence horizontal BWP was significantly less severe following the 10sec burn. Interspace necrosis was evident from day 1 onward in both groups. Only the increase between days 1 and 2 showed a significant increment, both following a full-thickness and an intermediate burn, which places the horizontal progress within the BWP period of 48-72 hours.

Only in the 10sec group a trend towards less macroscopic interspace damage was observed on days 10 and 14. This could be attributed to regeneration and earlier re-establishing of adequate perfusion as sufficient resuscitation in the zone of stasis can reduce horizontal BWP (Jackson 1953, Hettiaratchy and Dziewulski 2004). As described above, also in histopathology we could see regeneration from day 7 onwards. However since the decrease in interspace necrosis following the 10sec burn was not significant and macroscopic evaluation remains highly subjective, the early decrease in necrosis extent needs to be reproduced in further studies before making assumptions.

10.2.2 Surface Burn Wound Progression in Other Burn Comb Models

Other studies have assessed interspace necrosis after a burn injury and subsequent BWP. Unfortunately, the assessment methods of necrosis are manifold and often only graphic representation is given instead of numerical data (Table 7).

Table 7: Burn Comb Studies Assessing Progression of Surface Interspace Necrosis in Rats
All listed studies used a burn comb stamp rat model to induce a burn injury. Several studies did not provide information about all listed parameters (marked with n.a.). Data provided is shown without confidence intervals. Different methods for assessing interspace necrosis and horizontal burn wound progression were used. Refer to text or notes for details.

Study	Burn Time	Burn Depth	Interspace Necrosis Day 1	Interspace Necrosis Day 7	Note
This Study	**60sec**	**Full-Thickness**	**57%**	**88%**	
Tobalem et al. (2013)	60sec	Full-Thickness	<10%$	94%	$Only graphic data is provided
Tobalem et al. (2013)	60sec	Full-Thickness	<20%$	81%	Control animals received local cooling. $Only graphic data is provided.
Tobalem et al. (2012)	60sec	Full-Thickness	<20%$	78%	Control animals received local cooling. $Only graphic data is provided.
Tobalem et al. (2019)	60sec	Full-Thickness	4%	94%	
Reddy et al. (2015)	30sec	Full-Thickness	n.a.	100%	Control animals were injected i.p. or i.v. with DSMO vehicle. Percentage of interspaces turning necrotic.
Singer et al. (2013)	30sec	Full-Thickness	n.a.	100%	Control animals were injected with saline. Percentage of interspaces turning necrotic.
Singer et al. (2011)	30sec	Full-Thickness	n.a.	82%	Control animal received unnamed vehicle intravenously. Percentage of interspaces turning necrotic.
Taira et al. (2009)	30sec	Full-Thickness	21%	90%	Control animals received saline. Percentage of interspaces turning necrotic.
Singer et al. (2007)	30sec	Full-Thickness	30%	95%	Control animals received vehicle. Percentage of interspaces turning necrotic.
Choi et al. (1995)	30sec	Full-Thickness	89%	100%	Percentage of interspaces turning necrotic.
Choi and Ehrlich (1993)	30sec	Full-Thickness	100%	n.a.	Percentage of interspaces turning necrotic.
Uraloglu et al. (2018)	20sec	n.a.	n.a.	45%◆	◆Sample images show marked necrosis. Control animals received saline.
Deniz et al. (2013)	20sec	n.a.	n.a.	96% (measured on day 10)	
Uygur et al. (2009)	20sec	Full-Thickness	≈18%	≈ 99%	Interspace viability was assessed with scintigraphic imaging.
Isik et al. (1998)	20sec	Full-Thickness	≈18%	≈ 68%	Control animals received saline. Interspace viability was assessed with autoradiography.
Battal et al. (1997)	20sec	Full-Thickness	n.a.	99%	
Battal et al. (1996)	20sec	Full-Thickness	n.a.	99%	
Jin et al. (2018)	10sec	n.a.	≈30%$	n.a.	$Only graphic data is provided. Animals received saline.
This Study	**10sec**	**Intermediate**	**24%**	**54%**	

Tobalem et al., who also used the same comb model with a 60sec full-thickness burn, evaluated interspace necrosis on days 1, 4 and 7. In all three published studies interspace necrosis increased between days 1 and 4 (Tobalem et al. 2012, Tobalem et al. 2013, Tobalem et al. 2013) while no data is provided how interspace necrosis changed between days 1 and 2. Graphical representation shows less than 10% interspace necrosis on day 1, which increased to around 80% on day 4. In the untreated 60sec group, Tobalem et al. demonstrated 94% interspace necrosis on day 7 (Tobalem et al. 2013). The other control groups received local cooling, and had interspace necrosis of 81% (Tobalem et al. 2013), respectively 78% (Tobalem et al. 2012) on day 7. Our observed interspace necrosis of 88% in the 60sec group on day 7 seems consistent. This appears reasonable since we used the same burn comb model with the 60sec exposure time and rats with similar weight. However, in their most recent study, the interspace necrosis on day 1 was less than earlier described but progressed to similar extent on day 7 following a 60sec burn (Tobalem et al. 2019). Interestingly, the main increase in interspace necrosis was described between days 1 and 4 with no performed measurement on day 2. This could be in unison with the presented data since we were able to observe the main increase between days 1 and 2 but in both groups we could not observe any significant increase in horizontal BWP following day 2. As Tobalem stated, the differences in horizontal necrosis could stem from different animal weights or ambient air (Tobalem et al. 2019). However, the main increase within 2 days seems reasonable when considering the assumed time frame of 48-72 hours for BWP. However, even though the increases in horizontal BWP are not significant anymore, we cannot rule out that horizontal BWP also further progresses for more than 2 days.

Singer and his group used a 30sec rat burn comb model where a full-thickness injury was achieved. In several studies of this group, the number of interspaces turning necrotic was assessed (Singer et al. 2007, Taira et al. 2009, Singer et al. 2011, Singer et al. 2013, Reddy et al. 2015). Control animals received saline or vehicle administration. Where reported, 21% (Taira et al. 2009) to 30% (Singer et al. 2007) of interspaces turned necrotic on day 1. Percentage of necrotic interspaces on day 7 was between 82% (Singer et al. 2011) and 100% (Singer et al. 2007, Taira et al. 2009, Singer et al. 2013, Reddy et al. 2015). In one of these studies the authors did not observe an increase in number of necrotic interspaces after four days following injury induction (Singer et al. 2013). We could observe the major increase in horizontal

BWP between days 1 and 2 following both intermediate and full-thickness groups. While Singer's evaluation in the first days is less than what we observed, the full-thickness necrosis on day 7 seems similar.

Choi et al. measured the quantity of necrotic interspaces following a 30sec brass burn comb full-thickness rat model. A high percentage of interspaces turned necrotic within 24 hours (89%) and on day 7 in the untreated control group all interspaces turned necrotic, conflating with the burn fields (Choi et al. 1995). In an earlier work of the same group they reported signs of necrosis in all untreated interspaces 24 hours after the burn injury (Choi and Ehrlich 1993). This is the only group which reported high interspace necrosis so early (Table 7).

In a study assessing heparin on BWP after a 20sec burn, the authors reported the mean surviving interspace area with 55% 7 days after burn induction (Uraloglu et al. 2018). Translucent graph paper was used for measuring surviving interspace areas. The sample images of the control group, receiving saline, on day 7 however show marked interspace necrosis where burn fields and interspaces cannot be separated anymore. Interspace necrosis higher than 55% in the untreated group on day 7 would be plausible according to the published images (Uraloglu et al. 2018). Furthermore, the group did not offer any insights in vertical burn depth.

A high percentage of interspace necrosis of 96%, as assessed with using millimetric graphic paper, was observed by Deniz et al. on day 10 in a 20sec burn comb study on 350-450g rats. No data was given for earlier time points (Deniz et al. 2013).

Uygur et al. used a brass burn comb model for 20sec to induce a full-thickness burn in 350-400g rats. They assessed viability of interspaces by using scintigraphy. In their untreated group, interspace viability was 82% on day 1 and 19% on day 7 (Uygur et al. 2009). While on day 1 necrosis is less compared to our results, the interspace necrosis on day 7 is similar to our data. Isik et al. assessed interspace survival using nuclear imaging and autoradiography following a 20sec full-thickness burn in rats and saline injection in their control group (Isik et al. 1998). Interspace necrosis was reported with about 18% on day 1 and 68% on day 7. Unfortunately, no interspace viability data was complied on interjacent days in the studies by Uygur and Isik (Isik et al. 1998, Uygur et al. 2009).

After a 20sec full-thickness burn in rats, Battal et al. observed an interspace necrosis of 99% in untreated animals one week after burn induction (Battal et al. 1997). No

information regarding earlier interspace necrosis is provided. The group also demonstrated the same necrosis rate on day 7 in another study (Battal et al. 1996).

Jin et al. measured interspace necrosis following a burn comb injury after 10sec exposure in rats weighing 180-220g but did not report results of burn depth (Jin et al. 2018). They followed-up rats 1 hour, 24 hours and 96 hours after injury and observed interspace necrosis around 30% on day 1 and around 60% on day 4 in their control group where animals received a saline injection after burn induction.

Differences in interspace necrosis and horizontal BWP in various burn comb models can be explained through different assessment methods of necrosis. Different techniques lead to different definitions of "necrotic tissue". Since macroscopic evaluation of necrosis and tissue decay in clinical burn wounds is mostly made through inspection (see 6.3.3), we deem this technique as the most reasonable. However, one shortcoming is the high inter-observer variability and the low rates of correct assessment of tissue viability (Heimbach et al. 1984, Jaskille et al. 2009). This could explain the high variability in interspace necrosis in different studies. We present a thorough approach to interspace necrosis due to close monitoring over the time course. Interestingly there has not been a burn comb study with an intermediate burn assessing horizontal interspace necrosis and its burn wound progression (Table 7). We argue that the obtained results for interspace necrosis are plausible even if the rate of interspace necrosis is by trend high on day 1 and low on day 7 compared to earlier studies. A longer burn time leads to a more pronounced interspace necrosis than a shorter and more superficial burn. For better comparison of horizontal BWP further studies should report burn time, depth and repeatedly measure interspace necrosis, especially for the time span where BWP is suspected to happen. Data from this study might hint that more superficial burns progress shorter than 48 hours as originally assumed and deeper burns might progress longer than 72 hours. Differences in observed interspace necrosis could also be explained through different viability assumptions of altered interspaces or due to different energy exposure following alternating application times. However the general trend of high interspace necrosis and hence elevated surface wound progression seems consistent over different burn comb models.

10.3 Perfusion Parameters

We were able to measure burn field and interspace LSCI perfusion over a period of 14 days following 10sec and a 60sec burns in the presented burn comb rat model.

In the intermediate burn group, burn field perfusion decreased within the first 8 hours and baseline levels were re-established within one day. The respective interspace perfusion also dropped in the first 8 hours but with significantly prior increased perfusion compared to baseline. Pre-baseline levels in the interspace were re-established within one day and exceeded them on day 2. Noteworthy, on all time points, interspace perfusion was higher than burn field perfusion with significant better perfusion from post-burn throughout day 7. But maximum histological burn depths were the same for interspaces and burn fields following a 10sec and 60sec burn. Apparently the higher LSCI perfusion on the early time points and early re-establishing baseline perfusion could not negate vertical progression in the intermediate burn group.

In full-thickness burn wounds, interspace and perfusion dropped within the first eight hours. Interspace pre-burn levels were established only within four days while in burn fields these levels were just reached and exceed one week after the burn. Reaching baseline perfusion levels only on day 4 could however explain why final vertical injury extent was reached on day 4 in 60sec interspaces.

10.3.1 Laser-Speckle-Contrast-Imaging in Burn Research

The benefits of LSCI (see 6.8) have made clinical researchers use it since its introduction. Already the first publication on digital supported laser-speckle-contrast analysis introduced the application in burn research (Briers and Webster 1996) and it has been established in human patients since 2005 (Stewart et al. 2005). More recently, Lindahl et al. assessed pediatric scalds with LSCI and showed that the technique can be easily applied and perfusion is related to 2-week-burn-injury outcome (Lindahl et al. 2013). Mirdell could show characteristic patterns in LSCI perfusion regarding the wound healing time in pediatric scalds (Mirdell et al. 2016). The same group also developed LSCI cut-off values for predicting healing outcomes in pediatric scalds: With combining two LSCI measurements, one within 24 hours and one between 72-96 hours after the burn, they exceeded their clinical-judgment accuracy of 67% with sensitivity and specificity up to 100% (Mirdell et al. 2017).

LSCI hast been also used in non-clinical experiments regarding perfusion, microcirculation as well as pre-clinical skin and burn research (Senarathna et al. 2013, Zötterman et al. 2017): While it had been applied to elaborate microcirculation in the retina (Briers and Fercher 1982, Senarathna et al. 2013) and brain tissue (Dunn et al. 2001, Ponticorvo and Dunn 2010), it has been used to test a burn device in rats (Sakamoto et al. 2016), combined with vessel network imaging in rodent burn injuries (Qin et al. 2012) or to monitor tissue perfusion in burn models (Crouzet et al. 2015, Ponticorvo et al. 2017). However, to the best of our knowledge, no measurement with the LSCI method has been done to assess BWP in intermediate burns in a short-clocked manner over the time course of 2 weeks in interspaces and burn fields. This study showed that LSCI measurement could be performed repeatedly in an easy fashion. The short measurement time and quick image acquisition could make it possible to measure perfusion parameters without the need for repeated animal anesthesia and narcosis, but further research is needed.

10.3.2 LSCI Perfusion In Burn Fields and Interspaces

In previous animals studies, measuring flux in burns with the LSCI technology have focused on the directly burned areas (Crouzet et al. 2015, Sakamoto et al. 2016, Ponticorvo et al. 2017), not assessing the area at risk. This astonishes since according to Jackson (Jackson 1953), the area directly burned cannot be salvaged and therapies to ameliorate BWP should target the zone of stasis. Burn field perfusion in the 10sec and 60sec group did not show a significant difference in relative LSCI flux at one hour and eight hours; this underlines the immediate direct damage to the burn fields. To our knowledge there has not been a previous study where LSCI perfusion was measured in the area at risk in a rat model. In studies regarding LSCI burn field perfusion; often only graphical representation is provided, making it more difficult to compare results (Table 8).

Table 8: LSCI Burn Field Perfusion in Other Rat Burn Comb Models.
LSCI Perfusion was measured in the burned areas („burn fields"). The listed experiments applied a burn comb rat model and repeatedly measured burn field perfusion. Not all studies offered relative data for all time points. Not all time points of the studies are listed. Where no absolute or relative data was published, relative data was estimated from the published graphs.

Study	Burn Time Depth	Rat Weight	LSCI Perfusion (Burn Fields)						
			Post-Burn	h1	h2	h3	h8	d1	d7
This study	10sec Intermediate Thickness	435-535g	77%	59%	n.a.	n.a.	38%	99%	211%
This study	60sec Full-Thickness	435-535g	61%	59%	n.a.	n.a.	30%	52%	170%
Crouzet et al. (2015)	2-10sec Superficial Partial-Thickness	300-400g	105%	90%	75%	72%	n.a.	n.a.	n.a.
		Note:	Perfusion percentage is estimated from the published graphs. Post-burn perfusion higher than baseline						
Crouzet et al. (2015)	2-10sec Deep Partial-Thickness	300-400g	75%	70%	65%	56%	n.a.	n.a.	n.a.
		Note:	Perfusion percentage is estimated from the published graphs.						
Ponticorvo et al. (2017)	4sec Superficial Partial-Thickness	300-450g	n.a.	60%	n.a.	n.a.	n.a.	n.a.	220%
Ponticorvo et al. (2017)	8sec Deep Partial-Thickness	300-450	n.a.	64%	n.a.	n.a.	n.a.	n.a.	166%
		Note:	Relative Perfusion in deep partial-thickness burns one hour after burn induction is non-significantly higher than in superficial partial-thickness burns.						

Crouzet and his group measured burn field LSCI perfusion following superficial and deep partial-thickness burns in rats over a time course of three hours (Crouzet et al. 2015). In their deep partial-thickness wounds, LSCI perfusion roughly halved within the first 3 hours but was higher than in our study population (Table 8). Interestingly they were able to observe a slight increase in burn field perfusion in their superficial partial-thickness wounds between 10-20 minutes after burn induction (Crouzet et al. 2015). In the same study, the provided sample speckle flow index maps, calculated

from LSCI, hint to an increased interspace perfusion following superficial- and deep partial thickness burns but no further data is provided (Crouzet et al. 2015) as no LSCI measurement was performed in interspaces.

Ponticorvo and his group observed a decrease to 60%, respectively 64%, burn field perfusion one hour after inducing a superficial partial- or deep partial-thickness burn in a similar model (Ponticorvo et al. 2017). The amount of decrease is similar to our 10sec results. In burn fields, they were able to show perfusion above baseline one week after the burn. Interestingly, differing from our results, superficial burn fields were relatively worse perfused than deep burn fields on some time points in their study. They did not offer an explanation for this observed phenomenon, maybe due to the non-significant nature of the results. Our reported 10sec LSCI perfusion levels one week after the burn however are in unison with the data published by Ponticorvo et al. (Ponticorvo et al. 2017). The group also observed a high laser speckle imaging perfusion up to a period of 4 weeks and attributed longer pre-baseline levels as a marker for wound healing (Ponticorvo et al. 2017). In both groups, we observed higher than baseline levels two weeks after burn induction in both areas. However they only measured post-burn and then weekly, neglecting the BWP time span within the first couple days.

LSCI burn field perfusion in this study is therefore in concordance to other studies using the same technique, especially around h1 and d7. This study provides continuous LSCI data within the first week after burn induction. Directly burned areas are strongly impaired following a burn irrespective of burn duration. The observed hyperperfusion in interspaces following an intermediate burn, but not in the deep burn could be explained through reactive hyperemia to recruit inflammatory cells into the damaged wound areas via vasodilatory peptides. Hyperemic areas could be macroscopically observed with reddish seams around the interspaces and are presumed in the Jackson burn model (Jackson 1953). Another possible explanation could be an already dysfunctional vasoregulation in the zone of stasis. This would explain the sharp decline in interspace perfusion in the hours following the hyperperfusion immediately after burn induction. In deeper burns this vasoregulation might already be impaired and no immediate increase in the perfusion can be seen (Singh et al. 2007, Shupp et al. 2010). Molecular and biochemistry research is warranted in more superficial burns and especially in the earlier time frame to better understand immediate changes.

In the 10sec group, baseline levels are accomplished within 24 hours after burn induction. Histologically, there is no further BWP after that time point. We argue that the re-establishment of perfusion levels hinders further progression. This is in unison with the original proposition by Jackson (Jackson 1953, Hettiaratchy and Dziewulski 2004). However, this does not explain why one could still observe progression of surface interspace necrosis at least until day 2. Baseline perfusion in 60sec interspaces was re-established on day 4, again on the time point where maximum vertical interspace necrosis was reached. Again this lets us believe, that perfusion hinders further progression. We emphasize the need to measure both directly burned and unburned areas especially within the first week in order to better construe the mechanisms of interspace perfusion.

10.3.3 Perfusion Drop on Day 4 in Intermediate Burns

We could see a non-significant decrease in interspace and burn field perfusion in the intermediate burns on day 4 compared to day 2 but not in the deeper burns. We do not have an explanation for the reason of the anew drop and no data has been published applying the LSCI method for that time frame. A similar observation was made by Hayati et al. in a 20sec full-thickness burn comb model assessed with Laser Doppler technique where they treated rats with topical carbomer hydrogel or saline. In their study population they observed a trend towards slightly less perfusion - but also not significantly different - in the zone of stasis between days 3 and 7 (Hayati et al. 2018).

10.3.4 Full-Thickness Burns and Laser Doppler Perfusion in Rats

Since LSCI is a relative young modality, most of the earlier studies have assessed perfusion in animal burn models with Laser Doppler. Stewart and colleagues assessed LSCI and LDI perfusion and showed similar results between the two measurement techniques in humans (Stewart et al. 2005). We are the only group that observed an early establishment of interspace baseline perfusion levels, on day 1 in the 10sec group and on day 4 in the 60sec group. Establishment of pre-burn perfusion levels neither in interspaces nor in burn fields was observed in earlier studies using the LDI technique (Table 9). The only exception to this observation is the study by Hayati (Hayati et al. 2018). While they did not offer relative values compared to baseline after their burn comb injury, in their saline treated control group a sharp increase in

burn field perfusion was shown following day 5. The authors did not offer an explanation for this change.

Tobalem et al. conducted a study where they compared warm and cold water versus no treatment following the same 60-second rat burn model used in this study (Tobalem et al. 2013). Only interspace perfusion was assessed using a LDI device. Baseline perfusion of 100% decreased to 63% interspace perfusion 1 hour after burn induction. This is similar to our perfusion values with the LSCI device. LDI interspace perfusion steadily increased on days 4 and 7, with levels of 80% on day 4, which is close to our full-thickness LSCI perfusion (60sec interspace LSCI perfusion 106%). However, with a perfusion of about 85-90%, baseline values were not re-established on day 7 (Tobalem et al. 2013). In a similar study assessing the effect of EPO in full-thickness burn wounds, the group treated the control animals with cooling (Tobalem et al. 2012, Tobalem et al. 2013). LDI interspace perfusion was 67% on day 1 and reached slightly less than pre-burn levels on day 7. No measurements beyond day 7 were made in these studies (Tobalem et al. 2012, Tobalem et al. 2013, Tobalem et al. 2013). The reported interspace perfusion levels by Tobalem et al. were higher than in other groups. Similar values for non-treated rats were recently published by the same group following a 60sec burn (Tobalem et al. 2019): Interspace perfusion decreased to 63% one hour after burn induction. Over the following period the interspace Laser Doppler perfusion increased but never reached baseline levels within one week (86% on day 7).

Table 9: Burn Comb Rat Models with Laser Doppler Perfusion Assessment.
Laser Doppler Perfusion was measured in the directly burned areas („burn fields") or indirectly damaged areas („interspaces"). The experiments applied a burn comb rat model and repeatedly measured perfusion. Not all studies offered relative data for all time points and not all time points are listed. Where no absolute or relative data was published, relative data was estimated from the published graphs as noted.

Study	Burn Time Depth	Rat Weight (g)	Treatment of Control Group	Area measured	Laser Doppler Perfusion					
					Post-Burn	h1	h8	d1	d4	d7
Tobalem et al. (2013)	60sec Full-Thickness	432-478	Local Cooling	Interspaces	n.a.	55%	n.a.	67%	80%	90%
					Perfusion percentage is estimated from published graphs, except for day 1.					
Tobalem et al. (2012)	60sec Full-Thickness	456	Local Cooling	Interspaces	n.a.	n.a.	n.a.	67%	91%	94%
Tobalem et al. (2013)	60sec Full-Thickness	461-481	none	Interspaces	n.a.	63%	n.a.	n.a.	80%	85%
					Perfusion percentage for day 7 is estimated from published graphs.					
Tobalem et al. (2019)	60sec Full-Thickness	450-500	none	Interspaces	n.a.	63%	n.a.	70%	80%	86%
					Perfusion percentage for day 1 is estimated from published graphs.					
Battal et al. (1997)	20sec Full-Thickness	450	Saline	Interspaces	22%	4%	22%	22%	n.a.	n.a.
				Burn Fields	15%	13%	n.a.	n.a.	n.a.	n.a.
					Perfusion percentage is estimated from published graphs.					
Battal et al. (1996)	20sec Full-Thickness	450	Saline	Interspaces	21%	7%	17%	17%	n.a.	n.a.
				Burn Fields	8%	15%	8%	8%	n.a.	n.a.
					Perfusion percentage is estimated from published graphs.					
Isik et al. (1998)	20sec Full-Thickness	350-400	Saline	Interspaces	70%	n.a.	n.a.	n.a.	n.a.	11%
				Burn Fields	2%	n.a.	n.a.	2%	n.a.	2%
					Perfusion percentage is estimated from published graphs. Interspace perfusion was calculated from absolute values.					
Choi and Ehrlich (1993)	30sec Full-Thickness	300-325	none	Interspaces	n.a.	n.a.	21%	35%	n.a.	n.a.
				Burn Fields		6-13%	6-13%	6-13%	n.a.	n.a.
Choi et al. (1995)	30sec Full-Thickness	325-375	none	Interspaces	n.a.	45%	n.a.	32%	n.a.	n.a.
				Burn Fields	n.a.	18%	n.a.	6%	n.a.	n.a.
					Perfusion percentage is estimated from published graphs. Interspace perfusion on day 1 is given.					
Uygur et al. (2009)	20sec Full-Thickness	350-400	saline	Interspaces	66%	n.a.	n.a.	57%	n.a.	n.a.
					Perfusion percentage is calculated from absolute values.					
Regas and Ehrlich (1992)	20sec Full-Thickness	300-500	none	Interspaces	n.a.	58%	n.a.	29%	n.a.	n.a.
				Burn Fields	n.a.	14%	n.a.	15%	n.a.	n.a.
					Perfusion percentage is calculated from absolute values.					
Prindeze et al. (2016)	15sec Superficial	n.a.	none	Interspaces	23%	n.a.	23%	53%	n.a.	n.a.
				Burn Fields	19%	n.a.	16%	21%	n.a.	n.a.
	30sec Intermediate	n.a.	none	Interspaces	40%	n.a.	30%	45%	n.a.	n.a.
				Burn Fields	38%	n.a.	30%	33%	n.a.	n.a.
	45sec Deep Partial-Thickness	n.a.	none	Interspaces	18%	n.a.	7%	11%	n.a.	n.a.
				Burn Fields	15%	n.a.	4%	10%	n.a.	n.a.
					Perfusion percentage is estimated from published graphs.					

Isik and his group evaluated the Laser Doppler perfusion after a 20sec burn comb injury in rats (Isik et al. 1998). Burn field perfusion dropped sharply without any increase over the one-week period. Interspace perfusion decreased to an average of 70% within 15 minutes and to 60% within 2 hours. These values resemble our data of the full-thickness burn fields within the first hours. However, Isik et al. reported day 7 perfusion in the burn fields without any treatment at 11%. At this time point the measured perfusion in our study was well above baseline, also in deeper burns, for both interspaces and burn fields.

Choi and Ehrlich used LDI for perfusion evaluation following a 30sec full-thickness burn in a rat burn comb model (Choi and Ehrlich 1993, Choi et al. 1995). While they measured LDI perfusion from baseline until day 1 repeatedly, they did not offer absolute data for the time course. From the published data, interspace perfusion in Laser-Doppler imaging decreased to 21% eight hours after the burn (Choi et al. 1995) and to 32-35% on day 1 (Choi and Ehrlich 1993, Choi et al. 1995).

Uygur provided interspace LDI flowmetry for a saline treated control group following a 20sec full-thickness comb burn in rats (Uygur et al. 2009). Interspace perfusion decreased to 66% post-burn and to 57% on day 1 as calculated from the published absolute values. This perfusion is close to the perfusion we measured with the LSCI device in the 60sec interspaces on the same time points.

When converting the LDI flux units into relative parameters from the original burn comb study by Regas and Ehrlich, where they induced full-thickness burns, interspace LDI perfusion decreased to 58% one hour after the burn before further decreasing to a minimum of 29% on day 1. Burn field perfusion had a stronger decline with 14%, 11%, 10% and 15% for one, two, four hours and day 1, respectively (Regas and Ehrlich 1992).

Three studies have assessed Laser Doppler perfusion in non-full-thickness burns (Xiao et al. 2013, Xiao et al. 2014, Prindeze et al. 2016):

Prindeze et al. measured Doppler perfusion in burned and interspace areas in a rat burn comb model following superficial, intermediate and deep partial-thickness burns. The authors provided only graphical representation of the LDI data. Follow-up was short (36 hours). The worst perfusion was observed in the deep partial-thickness burn where burn field perfusion decreased right after the burn (approx. 15%) to a minimum of approx. 3% at 12 hours. Interspace perfusion was significantly higher with perfusion decreasing from approx. 18% (post-burn) to 6% (12 hours).

Approximations of the other burn times can be found in Table 9. Noteworthy, relative perfusion data in the superficial burn showed worse perfusion than the intermediate burn. However, when taking into account the lower baseline for the intermediate burn group, absolute perfusion in burn fields was similar in all three burn depths and absolute interspace perfusion the highest in the most superficial burns (Prindeze et al. 2016).

Xiao et al. induced a 6sec II° burn in 200-220g rats to examine apoptosis and measure LDI flux in the burn wounds (Xiao et al. 2013, Xiao et al. 2014). Xiao also only offered graphical perfusion. Perfusion slightly differed in the two studies with one control group being injected intraperitoneally with a vehicle solution (Xiao et al. 2013) while in the other study no sham treatment was performed (Xiao et al. 2014). In the first study burn wound perfusion was estimated at 42% 8 hours after burn induction and approximately 40% on day 1. Perfusion then rose to approx. 58% and 67% on days 2 and 3 (Xiao et al. 2013). In the second study, Doppler values decreased over 12 hours to approx. 25% with a slight increase to approx. 33%, 50% and 55% on days 1, 2 and 3 (Xiao et al. 2014). The group explicitly states baseline levels were not reached in the II° burn. Since the group did use a brass rod with constant temperature and no burn comb, no area at risk was created.

Concluding, other study groups assessing LDI perfusion in non-full-thickness and full-thickness rat burns could not observe an increase to baseline levels following the injuries but could often notice an increase in perfusion following a nadir within the first couple of days. Contrasting to the outlined evidence, we could see reperfusion at baseline levels in the 60sec group and even earlier in the 10sec group. This might be attributed to the different perfusion measurement techniques with LSCI and LDI but again further testing using LSCI in burn comb models is warranted.

10.3.5 Laser Doppler Perfusion in Burn Models with Animals other than Rats

Laser Doppler perfusion assessment was also performed in models applying animals other than rats. Mileski and his group measured the Laser-Doppler perfusion in a rabbit full-thickness burn comb model. They assessed relative blood flow in both burn contact sites and in the interspaces on the time points 1 hour, 2 hours, 3 hours, 4 hours, day 1, day 2 and day 3. In the full-thickness burn sites perfusion decreased to *"less than 20% of baseline perfusion"* (Mileski et al. 1992) and graphs depict perfusion at approximately 5%. There was no rise in perfusion within 3 days in the burn fields.

The decline in burn field perfusion was plainly sharper than other studies demonstrated. In contrast, interspace perfusion decreased less within the first hours to approx. 30% 4 hours after burn induction according to the given graphs. Mileski's interspace results lie in unison with our data since minimum interspace perfusion after a full-thickness burn was about 30% of baseline perfusion. Just like in our study, Mileski and his team measured an increase in rabbit skin perfusion in the interspaces on day 1 and day 2 (Mileski et al. 1992).

Fourman and his group analyzed interspaces perfusion after a full-thickness burn in a porcine comb model (Fourman et al. 2014) with Laser-Doppler and ICG angiography. They were able to show a decrease in interspace LDI perfusion after 1 and 4 hours following the burn. LDI perfusion increased to values between 75% and above baseline days 1 and 2 after the burn. LSCI interspace perfusion in our full-thickness group did not reach baseline levels that early and neither did LDI perfusion in other rat studies. Interestingly with the ICG angiography method, Fourman et al. saw an increase of perfusion within the first four hours but a decrease on day 1 and 2, which acts in a converse manner compared to LDI. The authors explained this by different penetration depths of the two techniques (Fourman et al. 2014). Not only does this show that perfusion evaluation depends on the used method, but also some perfusion seems increased within the interspace after one hour. While we did not observe this behavior in the interspaces neighboring the 60sec burns, we could observe an increase in LSCI perfusion in the 10sec interspaces. Fourman and his group explained the increase in ICG angiography perfusion through dye extravasation and edema through plugging (Fourman et al. 2014) - something LSCI avoids by eluding dye. Arguably, the two methods of ICG angiography and LSCI measure the vascular response pattern in the same tissue layer which would explain similar measurement patterns. But no final statement can be derived before further studies are targeting early perfusion changes.

Stewart and colleagues who established LSCI as coherent with LDI (Stewart et al. 2005), reported measurement impairments in a porcine wound healing model due to wound eschar (Stewart et al. 2006). While we could not observe clear impairments from the eschar and also other groups did not attribute lower perfusion to wound eschar (Nguyen et al. 2013, Crouzet et al. 2015, Sakamoto et al. 2016, Ponticorvo et al. 2017) we cannot rule out changes in obtained perfusion. We hypothesize that similar problems could also emerge in established LDI models and possibly more commonly

in larger animals. Further research in rodent and other animal models is needed to address possible measurements impairment due to eschar especially when using the LSCI technique where tissue penetration is assumed to be 1mm.

10.4 Frame Evaluation

We developed an 8-component aluminium frame with a dimension of 84x88mm weighting 5g and it was aimed at reducing wound manipulation and as an adequate dressing to apply topical agents onto the burn wound and adjacent interspaces. The frame was easily mounted in less than 15 minutes in single suture technique, using the debossed holes and Vicryl® suture material. The used final frame had sufficient flexibility due to its construction out of 8 interconnected movable components. The foam allowed sealing and padding without irritating the rat's skin or wound area. No reduced motion was observed in the rats with mounted frame.

10.4.1 Frame with E-Collar Allows Sufficient Durability Only Over the First Days

Without the Elizabethan collar, rats manipulated the sutures shortly after antagonizing the anesthesia, as seen in our preliminary animals. One possible reason for that may also be the adverse effect of the applied analgesia of Buprenorphine that may lead to uncontrolled devouring. This Pica behavior is a side effect of Buprenorphine in rats. After opioids, rats tend to ingest toxic material and manipulate on wound areas (Clark et al. 1997, Thallmair 2015). After observing the manipulation attempts in the preliminary animals, frame mounting was only performed in combination with the Elizabethan collar. While some rats seemed to be more distracted by the E-collar than the frame, others did not show any impulse to discard the collar or frame early in the experiment. While no adequate durability could be achieved without the use of an E-collar, still some animals learned how to remove the E-collar quickly and were able to tackle the sutures and frame. This is mirrored in the high variability in frame durability and incoherent need for re-suturing in different rats. Beyond the attempts of removing sutures, none of the rats showed any signs of distress, weight-loss or general apathy. As a consequence of our observations concerning frame durability, it can only be recommended when simultaneously applying an E-collar, which is far from ideal and needs future refinements, being a major limitation of the shown design. However, with adequate clinical control, sensitive size adjustment and supervised hygiene intervals, the E-

collar seems a tolerable method for wound protection in combination with the aluminium frame.

In 10 out of 12 specimen the frame was durable in the critical period for BWP with re-suturing when necessary. 6 out of 12 rats did not need re-suturing of their frame up until day 1. Since the frame was developed for facilitating topical agents like lotions, gels or hydrogels hindering burn progression, the frame seemed sufficient to allow application in the relevant time frame throughout the first days. However, the frame was surely limited when applied longer than 4 days. The frame durability might not be sufficient to investigate topical agents over extended periods. We aimed for a longer mounting of the frame but were not able to assess a possibility to do so without risking animal welfare. With these considerations, we believe the shown frame is a flexible tool for researching topical agents acting upon wounds over the relevant time span of 2-3 days but further advancements should be made.

10.4.2 Formerly Used Wound Protection Devices Not Suitable for Topical Agents

The presented wound protection frame dressing had to be combined with an E-collar and made it necessary to re-suture any opened stitches. However, none in the literature formerly described wound dressings seemed more suitable for the administration of topical agents. The different used wound protective dressing and devices are presented in chapter 6.6.2.

The Orthoplast saddle of Fox and Frazier only allows for the protection of a 3x5cm dressing (Fox and Frazier 1980), which is too small to cover the wound created by the burn comb. Additionally, they did not state the durability of their saddle and it is unclear in how many rats the small saddle was used. Due to its covering design, it did not allow continuous wound assessment without opening the saddle. Repeated topical application over BWP relevant time frame seemed impractical with this dressing.

With the tube dressing from Ueda et al. no topical application of hydrogels would be possible (Ueda et al. 1981). The authors stated that they used the dressing in over 200 rats but failed to report the animals' size or weight. The vinyl chloride tubes as shown in the in the original publication (Ueda et al. 1981) could possibly hinder rat mobility and respiratory functions especially in larger rats. Moreover it is unclear if the experiment rats were able to manipulate the vinyl chloride tube.

While the wound vest used by Pynn or Fujimori showed promising results, it did not cover the wound area itself (Pynn et al. 1983, Fujimori et al. 1990). This makes a second device necessary to allow topical application. Furthermore, both vests have only been used in smaller rats up to 350g. A similar vest used in 42 rats weighing between 400 and 500g - around the same size as used in this study - did not hinder 8 rats to manipulate on the wound area and required the researchers to exclude the rats from their study (Griffiths and Humphries 1981). Furthermore, the original X-ray vest by Pynn (Pynn et al. 1983) made it possible to have a foreleg slide out of the vest as the authors have stated, further limiting the broad use of this wound protection type.

Komorowska-Timek et al. showed that simple shortening of the teeth seemed sufficient to avoid auto-cannibalization in their flap model (Komorowska-Timek et al. 1999). While cutting the teeth would have been possible in our study every 3-4 days since the animals were anaesthetized for measurements throughout the first 2 weeks, we still had to use the metal frame to allow topical application. Furthermore, we did not have the permission to shorten teeth from an animal welfare perspective, but also did not observe the severe distress in our rats with the Elizabethan collar in the same amount as reported by the authors. They fastened the used collar with staples, which possibly compromises blood flow. Our collar did not impair movement, reduce food intake or evoke bloody discharge from the eyes as described (Komorowska-Timek et al. 1999). In the study by Komorowska-Timek et al., two animals with collars even died from no apparent cause. Thus, we hypothesize that the collar and the staples were mounted too tightly. While we paid close attention to congestion symptoms after our rats woke up with the collars, we never closed the collar with the brass fastener so tight, that the animals seemed distressed. Nonetheless, shortening of the teeth seems a good opportunity to avoid self-mutilation in future studies, especially when used in a combination with other methods (Ozkan and Ozgentas 2006).

Due to the severe restrictive nature of the proposed protection by Macionis (Macionis 2000), we decided not to use the suggested technique.

While the dressing by Martineau and Chua Chiaco seemed to be cheap, light and easy (Martineau and Chua Chiaco 2000), we could not use it in our research approach. The transparent shield did not seal the wound area in order to allow for topical application and the described hole in the polycarbonate dome would be required to be large enough to expose the whole wound area for unimpaired perfusion

measurements. Otherwise, this protection device seems to be useful and durable with the limitation of not sealing the wound area onto the rat's dorsum.

The armor dressing shown by Pfurtscheller et al. was a skilled approach for wound protection (Pfurtscheller et al. 2013). The authors reported a thermoplastic dressing but also stated that combining it with aluminium material seemed more suitable from a wound protection perspective. The laid-out results were excellent for wound protection in rats and the authors correctly recognized the need for further development of wound protective devices in rats concerning flap and burn research. Our observations with thermoplastic material in the preliminary frames let us use aluminium components for our frame. When we tried wire sutures in order to fixate the frame onto the animals as Pfurtscheller did, we had problems to mount the frame in a time-effective manner and to avoid sharp edges. Pfurtscheller and his group themselves argued that the sutures had to be checked regularly. An advancement from the wire sutures could be the use of stapling devices used in clinical surgery settings as well. While stapling of the E-collar should be avoided due to the mentioned possibility of compromising blood flow, the proposed frame dressing might be easily fixed by stapling. Unfortunately, we did not have the permission to use such an automated stapling device and its possible application has to be evaluated in further research projects.

10.4.3 Local Application Without Wound Protection

Endorsing further research with using topical agents in a wound model, authors should be compelled to report how these agents are applied. Interestingly some groups did not report any limitations of using topical agents in rats: Fu repeatedly used topical hydrogel, covered with Vaseline and gauze (Fu et al. 2017) but did not report any problems with local application or the wound dressing. When testing hypothermia on burns, Rizzo applied cold water blankets only when the animals were still under anesthesia (Rizzo et al. 2013). Eski applied an agent with a bath of the still anaesthetized rat while no lasting exposure to the local therapeutic was performed (Eski et al. 2012). Wang et al. repeatedly applied a lotion every 8 hours onto the burn comb wound for 3 days. The group used swaps covered with the lotion and did not cover the wound area (Wang et al. 2015). They did not report any problems of running down of the lotion or manipulation of the rats but saw BWP-saving effects in histology and macroscopically.

Sun and colleagues used Tegaderm™ (3M™, St. Paul, MN, USA) and sealed the dressing with Vetbond (3M™, St. Paul, MN, USA), both offered commercially, to apply local treatment with a conjugate solution containing anti-TNFa-Hyaluronic acid over a week. Tegaderm™ is a transparent foil dressing and Vetbond is an animal tissue glue. The group reported a moist wound milieu and no tissue lost in dressing changes (Sun et al. 2012, Friedrich et al. 2014). The Tegaderm™ dressing was also used by Sakamoto and his coworkers combined with an elastic adhesive bandage tape (Sakamoto et al. 2016). After a scald injury, Tagkalakis and group applied nitroglycerin ointment or prilocaine/lidocaine cream onto the wound in rats (Tagkalakis et al. 2015) and covered the wound area with Tegaderm™, cleaned the wound before every measurement and then reapplied the agent and dressing. Follow-up was 180 minutes (Tagkalakis et al. 2015) so no assertion can be made how well rats would tolerate the wound and local application for longer. Also in a study assessing a carbomer hydrogel in burn wounds, Hayati et al. used Tegaderm™ for topical administration and wound protection (Hayati et al. 2018). The group performed daily dressing changes, cleaning with swaps, repeated LDI measurements and did not report any wound mutilation. Repeated dressing changes seem elaborate for continuous perfusion and wound measurements.

We did not assess Tegaderm™ dressing on the burn wounds. The experience with Varihesive© dressing in our preliminary animals did not lead to the desired results, we therefore wonder that none of the groups using the Tegaderm™ dressing reported any problems. The Tegaderm™ dressing seems promising and further application and reporting of mutilation are necessary in upcoming studies. We plan on applying Tegaderm™ in further tests to review durability. However, we argue that wound manipulation in rodent models is underreported since quite a few studies do not mention impairments at all. The first wound protection devices were described more than 30 years ago but apparently not all research groups are aware of the problem.

In conclusion, most studies using topical agents in burn wounds avoid lasting exposure and the risk of wound manipulation in rats. A save and reliable way to apply local agents seems therefore urgently needed. Until further results, we argue that the proposed frame dressing is a cheap, flexible and safe alternative when using burn models and topical drug application. The model is convenient in the first days after burn induction, which are relevant for BWP, but has several limitations.

10.5 Further Research

10.5.1 Further Planned Modifications to Dressing

While this model did prove to be useful to inspect and measure changes after an intermediate burn, further modifications to the shown rat model are needed in order to use this model on a broad basis. As laid out, we plan to modify the aluminium frame by adding stapling sutures and combine it with shortening of teeth and nails as described (Komorowska-Timek et al. 1999), hopefully avoiding the need for collars in the future. Also an evaluation over a longer time period with Tegaderm™ seems reasonable, since most groups have not reported wound manipulation using this dressing.

10.5.2 Further Evaluation of LSCI in Burn Wounds and Burn Comb Models

Laser-Speckle-Contrast-Imaging still is a relatively new technique to measure perfusion in burn wounds. It seems necessary to further evaluate this technique in pre- and clinical studies. The shorter measurement time make LSCI a possible candidate for broader use. While we used the LSCI only on anesthetized animals, since we performed 60 seconds LSCI recordings per time point, the fast image acquisition could possibly avoid animal anesthesia. Measurement times of less than a second are described (Zötterman et al. 2017). Further evaluation is needed to promote this approach, in rodent as well as in human scientific issues. Continued studies to compare the well-established Laser Doppler with LSCI in burn models are warranted. Since LDI has proven to be even useful in assisting burn depth diagnosis in clinical settings, LSCI seems a promising alternative. We call for reporting animal and stamp weight, as wells as measuring stamp temperature over the application time. When using burn comb models, both - interspaces and burn fields - and possible hindering eschar, should be evaluated with the used measurement modality.

10.5.3 Early Changes in Burn Wound Progression in Non-Full-Thickness Burns

Non-full-thickness burns seem to be underrepresented in burn research. We emphasize more research on superficial burns and propose a model for BWP up to the intermediate dermis. Further evaluation of differences between full- and non-full-thickness burns and BWP seems to be necessary and research is needed to verify early perfusion changes in the zone of stasis. Since we did not perform any

biochemical or molecular tests, early changes in mediators and reactive oxygen species could be probed, especially on these early time points.

10.5.4 Possible Drugs To Administer Topically

This model was developed for topical administration of potential agents to reduce BWP. The proposed frame makes local treatment with lotions, gels and hydrogels possible. Agents like Infliximab (Sun et al. 2012), cerium nitrate (Eski et al. 2012), EDTA (Wang et al. 2015), keratin biomaterial hydrogel (Poranki et al. 2016), a bromelain-derived agent (Singer et al. 2010), GM-CSF (Fu et al. 2017) or carbomer 940 (Hayati et al. 2018) have already proven to be successful when applied locally on a burn wound. More agents have proven successfully but were administered systemically with potential drawbacks of adverse reactions (see 6.7.1).

Among them, erythropoietin and derived molecules reduced BWP (Tobalem et al. 2012, Tobalem et al. 2013). Unpublished data from our group also showed reduced BWP after certain EPO regimens. Other formulations of EPO have also been used locally in wound healing studies (Bader et al. 2012), ischemic flaps (Schmauss et al. 2019) and a study has been published to evaluate EPO in human IIb° and III° burns (Gunter et al. 2018). While the primary endpoint of 100% re-epithelialization was not achieved (Gunter et al. 2018), continuing evaluation of possible use in more superficial burns is necessary. Additionally, modifications to the EPO molecule have exposed tissue protective properties via different receptors (Brines et al. 2004): A derived EPO-molecule peptide, known as ARA 290, has been shown to attenuate thrombosis and inflammation in burns (Bohr et al. 2013). Similarly, carbamylated erythropoietin, known as CEPO, has also shown several tissue protective properties (Fantacci et al. 2006, Patel et al. 2011). While these derivates could be promising via systemic application (Hand and Brines 2011, Murua et al. 2011), more research in topical administration is warranted to further individualize treatment strategies. Topical administration could potentially avoid impairments such as impaired blood rheology and capillary dysfunction (Ehrenreich et al. 2009, Schmauss et al. 2019). These issues could be addressed in pre-clinical models, as shown in this study. Other hydrogels have been tested in burn wound care and wound healing but have not been examined regarding attenuating BWP. These topical agents such chitosan gel (Degim et al. 2011) or dextran-based hydrogel (Shen et al. 2015) could also be assessed with the proposed model. Agents such as Rapamycin (Xiao et al. 2013) or Beraprost

sodium (Battal et al. 1996) which have been proven to reduce BWP when given systemically, but have not been tested through local topical administration and could be used in a higher doses while avoiding systemic adverse effects.

While throughout the literature, multiple agents have been described, few have been thoroughly examined and none has found its way into everyday clinical practice.

11 Conclusion

This rat model offers a research tool for assessing superficial burns which reach the intermediate dermis after secondary burn wound progression - a well described but poorly understood process - which leads to horizontal and vertical injury extension. We were able to show gross and histological BWP following 10sec non-full-thickness burns using a common burn comb. We demonstrated significant differences in comparison to 60sec full-thickness burns; especially vertical BWP within 24 hours in interspaces and burn fields, as well as lesser interspace necrosis. We could observe changes in Laser-Speckle-Contrast-Imaging, a promising fast technology to assess perfusion in wounds similar to the widespread applied Laser Doppler. Baseline interspace and burn field perfusion was reached earlier after a 10sec burn. The model allowed for easy, quick and repeated wound assessment including inspection, perfusion evaluation and histology workup. The presented 8-component-frame dressing seems sufficient to be used over a period of up to 4 days, bearing the need for repeated re-suturing and attaching an Elizabethan collar, but modifications have been proposed. We believe to offer a universal research tool to assess multiple agents in their ability to attenuate BWP in superficial and intermediate burns in rats.

12 Bibliography

Abdullahi, A., S. Amini-Nik and M. G. Jeschke (2014). "Animal models in burn research." Cell Mol Life Sci **71**(17): 3241-3255.

Alharbi, Z., A. Piatkowski, R. Dembinski, S. Reckort, G. Grieb, J. Kauczok and N. Pallua (2012). "Treatment of burns in the first 24 hours: simple and practical guide by answering 10 questions in a step-by-step form." World Journal of Emergency Surgery **7**(1): 13.

American Burn Association. (2016). "Burn Incidence and Fact Sheet 2016." Retrieved 09/23/17, 2017, from http://www.ameriburn.org/resources_factsheet.php.

Arbeitsgemeinschaft der Wissenschaftlichen Medizinischen Fachgesellschaften. (1999, 01/2010). "S1 Leitlinie der Deutschen Gesellschaft für Verbrennungsmedizin: Thermische und Chemische Verletzungen." Retrieved 10/09/2017, from http://www.awmf.org/uploads/tx_szleitlinien/044-001l_S1_Thermische_und_Chemische_Verletzungen_2011-abgelaufen.pdf.

Bader, A., S. Ebert, S. Giri, M. Kremer, S. Liu, A. Nerlich, C. I. Gunter, D. U. Smith and H. G. Machens (2012). "Skin regeneration with conical and hair follicle structure of deep second-degree scalding injuries via combined expression of the EPO receptor and beta common receptor by local subcutaneous injection of nanosized rhEPO." Int J Nanomedicine **7**: 1227-1237.

Basak, K., M. Manjunatha and P. K. Dutta (2012). "Review of laser speckle-based analysis in medical imaging." Med Biol Eng Comput **50**(6): 547-558.

Battal, M. N., Y. Hata, K. Matsuka, O. Ito, H. Matsuda, Y. Yoshida and T. Kawazoe (1996). "Reduction of progressive burn injury by a stable prostaglandin I2 analogue, beraprost sodium (Procylin): an experimental study in rats." Burns **22**(7): 531-538.

Battal, M. N., Y. Hata, K. Matsuka, O. Ito, H. Matsuda, Y. Yoshida and T. Kawazoe (1997). "Reduction of progressive burn injury by using a new nonselective endothelin-A and endothelin-B receptor antagonist, TAK-044: an experimental study in rats." Plast Reconstr Surg **99**(6): 1610-1619.

Bohr, S., S. J. Patel, D. Sarin, D. Irimia, M. L. Yarmush and F. Berthiaume (2013). "Resolvin D2 prevents secondary thrombosis and necrosis in a mouse burn wound model." Wound repair and regeneration : official publication of the Wound Healing Society [and] the European Tissue Repair Society **21**(1): 35-43.

Bohr, S., S. J. Patel, K. Shen, A. G. Vitalo, M. Brines, A. Cerami, F. Berthiaume and M. L. Yarmush (2013). "Alternative erythropoietin-mediated signaling prevents secondary microvascular thrombosis and inflammation within cutaneous burns." Proc Natl Acad Sci U S A **110**(9): 3513-3518.

Briers, J. D. (2001). "Laser Doppler, speckle and related techniques for blood perfusion mapping and imaging." Physiol Meas **22**(4): R35-66.

Bibliography

Briers, J. D. and A. F. Fercher (1982). "Retinal blood-flow visualization by means of laser speckle photography." Invest Ophthalmol Vis Sci **22**(2): 255-259.

Briers, J. D. and S. Webster (1996). "Laser speckle contrast analysis (LASCA): a nonscanning, full-field technique for monitoring capillary blood flow." J Biomed Opt **1**(2): 174-179.

Brines, M., G. Grasso, F. Fiordaliso, A. Sfacteria, P. Ghezzi, M. Fratelli, R. Latini, Q. W. Xie, J. Smart, C. J. Su-Rick, E. Pobre, D. Diaz, D. Gomez, C. Hand, T. Coleman and A. Cerami (2004). "Erythropoietin mediates tissue protection through an erythropoietin and common beta-subunit heteroreceptor." Proc Natl Acad Sci U S A **101**(41): 14907-14912.

Bucky, L. P., N. B. Vedder, H. Z. Hong, H. P. Ehrlich, R. K. Winn, J. M. Harlan and J. W. May, Jr. (1994). "Reduction of burn injury by inhibiting CD18-mediated leukocyte adherence in rabbits." Plast Reconstr Surg **93**(7): 1473-1480.

Choi, M. and H. P. Ehrlich (1993). "U75412E, a lazaroid, prevents progressive burn ischemia in a rat burn model." Am J Pathol **142**(2): 519-528.

Choi, M., H. Rabb, M. A. Arnaout and H. P. Ehrlich (1995). "Preventing the infiltration of leukocytes by monoclonal antibody blocks the development of progressive ischemia in rat burns." Plast Reconstr Surg **96**(5): 1177-1185; discussion 1186-1177.

Clark, J. A., Jr., P. H. Myers, M. F. Goelz, J. E. Thigpen and D. B. Forsythe (1997). "Pica behavior associated with buprenorphine administration in the rat." Lab Anim Sci **47**(3): 300-303.

Crouzet, C., J. Q. Nguyen, A. Ponticorvo, N. P. Bernal, A. J. Durkin and B. Choi (2015). "Acute discrimination between superficial-partial and deep-partial thickness burns in a preclinical model with laser speckle imaging." Burns **41**(5): 1058-1063.

Dahiya, P. (2009). "Burns as a model of SIRS." Front Biosci (Landmark Ed) **14**: 4962-4967.

Daigeler, A., N. Kapalschinski and M. Lehnhardt (2015). "[Therapy of burns]." Chirurg **86**(4): 389-401.

Degim, Z., N. Celebi, C. Alemdaroglu, M. Deveci, S. Ozturk and C. Ozogul (2011). "Evaluation of chitosan gel containing liposome-loaded epidermal growth factor on burn wound healing." Int Wound J **8**(4): 343-354.

Deniz, M., H. Borman, T. Seyhan and M. Haberal (2013). "An effective antioxidant drug on prevention of the necrosis of zone of stasis: N-acetylcysteine." Burns **39**(2): 320-325.

Devgan, L., S. Bhat, S. Aylward and R. J. Spence (2006). "Modalities for the Assessment of Burn Wound Depth." Journal of Burns and Wounds **5**: e2.

Dorsett-Martin, W. A. (2004). "Rat models of skin wound healing: a review." Wound Repair Regen **12**(6): 591-599.

Bibliography

Dunn, A. K., H. Bolay, M. A. Moskowitz and D. A. Boas (2001). "Dynamic imaging of cerebral blood flow using laser speckle." J Cereb Blood Flow Metab **21**(3): 195-201.

Ehrenreich, H., K. Weissenborn, H. Prange, D. Schneider, C. Weimar, K. Wartenberg, P. D. Schellinger, M. Bohn, H. Becker, M. Wegrzyn, P. Jahnig, M. Herrmann, M. Knauth, M. Bahr, W. Heide, A. Wagner, S. Schwab, H. Reichmann, G. Schwendemann, R. Dengler, A. Kastrup and C. Bartels (2009). "Recombinant human erythropoietin in the treatment of acute ischemic stroke." Stroke **40**(12): e647-656.

Enlimomab Acute Stroke Trial Investigators (2001). "Use of anti-ICAM-1 therapy in ischemic stroke: Results of the Enlimomab Acute Stroke Trial." Neurology **57**(8): 1428-1434.

Enoch, S., A. Roshan and M. Shah (2009). "Emergency and early management of burns and scalds." BMJ **338**.

Eriksson, S., J. Nilsson and C. Sturesson (2014). "Non-invasive imaging of microcirculation: a technology review." Med Devices (Auckl) **7**: 445-452.

Eski, M., F. Ozer, C. Firat, D. Alhan, N. Arslan, T. Senturk and S. Isik (2012). "Cerium nitrate treatment prevents progressive tissue necrosis in the zone of stasis following burn." Burns **38**(2): 283-289.

Evers, L. H., D. Bhavsar and P. Mailander (2010). "The biology of burn injury." Exp Dermatol **19**(9): 777-783.

Fantacci, M., P. Bianciardi, A. Caretti, T. R. Coleman, A. Cerami, M. Brines and M. Samaja (2006). "Carbamylated erythropoietin ameliorates the metabolic stress induced in vivo by severe chronic hypoxia." Proc Natl Acad Sci U S A **103**(46): 17531-17536.

Firat, C., E. Samdanci, S. Erbatur, A. H. Aytekin, M. Ak, M. G. Turtay and Y. K. Coban (2013). "beta-Glucan treatment prevents progressive burn ischaemia in the zone of stasis and improves burn healing: an experimental study in rats." Burns **39**(1): 105-112.

Fourman, M. S., B. T. Phillips, L. Crawford, S. A. McClain, F. Lin, H. C. Thode, Jr., A. B. Dagum, A. J. Singer and R. A. Clark (2014). "Indocyanine green dye angiography accurately predicts survival in the zone of ischemia in a burn comb model." Burns **40**(5): 940-946.

Fox, R. S. and W. H. Frazier (1980). "Wound Protection in Experimental Rats: A New Technique." Plastic and Reconstructive Surgery **66**(1): 141-142.

Friedrich, E. E., L. T. Sun, S. Natesan, D. O. Zamora, R. J. Christy and N. R. Washburn (2014). "Effects of hyaluronic acid conjugation on anti-TNF-alpha inhibition of inflammation in burns." J Biomed Mater Res A **102**(5): 1527-1536.

Fu, G. F., S. M. Tian, X. J. Cha, H. J. Huang, J. H. Lou, Y. Wei, C. D. Xia, Y. L. Li and X. H. Niu (2017). "Topically administered rhGM-CSF affects PPARbeta expression in the stasis zone." Exp Ther Med **14**(5): 4825-4830.

Bibliography

Fujimori, S., Y. Sawada, M. Sugawara and I. Hatayama (1990). "Repeatedly available rat vest." European Journal of Plastic Surgery **13**(4): 185-186.

Glick, D., S. Barth and K. F. Macleod (2010). "Autophagy: cellular and molecular mechanisms." The Journal of pathology **221**(1): 3-12.

Gravante, G., V. Filingeri, D. Delogu, G. Santeusanio, M. B. Palmieri, G. Esposito, A. Montone and G. Sconocchia (2006). "Apoptotic cell death in deep partial thickness burns by coexpression analysis of TUNEL and Fas." Surgery **139**(6): 854-855.

Griffiths, R. W. and N. L. Humphries (1981). "Isoxsuprine and the rat abdominal pedicle flap: a controlled study." British Journal of Plastic Surgery **34**(4): 446-450.

Gunter, C. I., H. G. Machens, F. P. Ilg, A. Hapfelmeier, W. Jelkmann, S. Egert-Schwender, S. Giri and A. Bader (2018). "A Randomized Controlled Trial: Regenerative Effects, Efficacy and Safety of Erythropoietin in Burn and Scalding Injuries." Front Pharmacol **9**: 951.

Guo, S. X., Y. Y. Jin, Q. Fang, C. G. You, X. G. Wang, X. L. Hu and C. M. Han (2015). "Beneficial effects of hydrogen-rich saline on early burn-wound progression in rats." PLoS One **10**(4): e0124897.

Hand, C. C. and M. Brines (2011). "Promises and pitfalls in erythopoietin-mediated tissue protection: are nonerythropoietic derivatives a way forward?" J Investig Med **59**(7): 1073-1082.

Harder, Y., M. Amon, D. Erni and M. D. Menger (2004). "Evolution of ischemic tissue injury in a random pattern flap: a new mouse model using intravital microscopy." J Surg Res **121**(2): 197-205.

Hayati, F., S. M. Ghamsari, M. M. Dehghan and A. Oryan (2018). "Effects of carbomer 940 hydrogel on burn wounds: an in vitro and in vivo study." J Dermatolog Treat **29**(6): 593-599.

Heimbach, D., L. Engrav, B. Grube and J. Marvin (1992). "Burn depth: a review." World J Surg **16**(1): 10-15.

Heimbach, D. M., M. A. Afromowitz, L. H. Engrav, J. A. Marvin and B. Perry (1984). "Burn depth estimation--man or machine." J Trauma **24**(5): 373-378.

Hettiaratchy, S. and P. Dziewulski (2004). "Pathophysiology and types of burns." BMJ : British Medical Journal **328**(7453): 1427-1429.

Hettiaratchy, S. and R. Papini (2004). "Initial management of a major burn: II--assessment and resuscitation." Bmj **329**(7457): 101-103.

Hinshaw, J. R. (1968). "EARLY CHANGES IN THE DEPTH OF BURNS." Annals of the New York Academy of Sciences **150**(3): 548-553.

Hop, M. J., J. Hiddingh, C. Stekelenburg, H. C. Kuipers, E. Middelkoop, M. K. Nieuwenhuis, S. Polinder and M. E. van Baar (2013). "Cost-effectiveness of laser Doppler imaging in burn care in the Netherlands." BMC Surgery **13**: 2-2.

Bibliography

Hop, M. J., S. Polinder, C. H. van der Vlies, E. Middelkoop and M. E. van Baar (2014). "Costs of burn care: a systematic review." Wound Repair Regen **22**(4): 436-450.

Hop, M. J., C. M. Stekelenburg, J. Hiddingh, H. C. Kuipers, E. Middelkoop, M. K. Nieuwenhuis, S. Polinder and M. E. van Baar (2016). "Cost-Effectiveness of Laser Doppler Imaging in Burn Care in The Netherlands: A Randomized Controlled Trial." Plast Reconstr Surg **137**(1): 166e-176e.

Horton, J. W. (2003). "Free radicals and lipid peroxidation mediated injury in burn trauma: the role of antioxidant therapy." Toxicology **189**(1-2): 75-88.

Ipaktchi, K., A. Mattar, A. D. Niederbichler, L. M. Hoesel, M. R. Hemmila, G. L. Su, D. G. Remick, S. C. Wang and S. Arbabi (2006). "Topical p38MAPK inhibition reduces dermal inflammation and epithelial apoptosis in burn wounds." Shock **26**(2): 201-209.

Isik, S., U. Sahin, S. Ilgan, M. Guler, B. Gunalp and N. Selmanpakoglu (1998). "Saving the zone of stasis in burns with recombinant tissue-type plasminogen activator (r-tPA): an experimental study in rats." Burns **24**(3): 217-223.

Jackson, D. M. (1953). "[The diagnosis of the depth of burning]." Br J Surg **40**(164): 588-596.

Jannasch, O. and H. Lippert (2012). Wunde, Wundheilung und Wundbehandlung. Chirurgie. 9. Auflage. J. R. Siewert and H. J. S. Stein. Berlin, Springer-Verlag Berlin Heidelberg.

Jarrett, M., M. McMahon and K. Stiller (2008). "Physical outcomes of patients with burn injuries--a 12 month follow-up." J Burn Care Res **29**(6): 975-984.

Jaskille, A. D., J. C. Ramella-Roman, J. W. Shupp, M. H. Jordan and J. C. Jeng (2010). "Critical review of burn depth assessment techniques: part II. Review of laser doppler technology." J Burn Care Res **31**(1): 151-157.

Jaskille, A. D., J. W. Shupp, M. H. Jordan and J. C. Jeng (2009). "Critical review of burn depth assessment techniques: Part I. Historical review." J Burn Care Res **30**(6): 937-947.

Jauch, K.-W., W. Mutschler, J. N. Hoffmann and K.-G. Kanz (2013). Chirurgie Basisweiterbildung, In 100 Schritten durch den Common Trunk, Springer-Verlag Berlin Heidelberg.

Jeschke, M. G., R. Pinto, R. Kraft, A. B. Nathens, C. C. Finnerty, R. L. Gamelli, N. S. Gibran, M. B. Klein, B. D. Arnoldo, R. G. Tompkins, D. N. Herndon, I. The and P. the Host Response to Injury Collaborative Research (2015). "MORBIDITY AND SURVIVAL PROBABILITY IN BURN PATIENTS IN MODERN BURN CARE." Critical care medicine **43**(4): 808-815.

Jin, J., X. Zheng, F. He, Y. Zhang, H. Zhou, P. Luo, X. Hu and Z. Xia (2018). "Therapeutic efficacy of early photobiomodulation therapy on the zones of stasis in burns: An experimental rat model study." Wound Repair Regen.

Bibliography

Johnson, R. M. and R. Richard (2003). "Partial-thickness burns: identification and management." Adv Skin Wound Care **16**(4): 178-187; quiz 188-179.

Kagan, R. J., M. D. Peck, D. H. Ahrenholz, W. L. Hickerson, J. t. Holmes, R. Korentager, J. Kraatz, K. Pollock and G. Kotoski (2013). "Surgical management of the burn wound and use of skin substitutes: an expert panel white paper." J Burn Care Res **34**(2): e60-79.

Kaiser, M., A. Yafi, M. Cinat, B. Choi and A. J. Durkin (2011). "Noninvasive assessment of burn wound severity using optical technology: a review of current and future modalities." Burns **37**(3): 377-386.

Kayapinar, M., N. Seyhan, M. C. Avunduk and N. Savaci (2015). "Saving the zone of stasis in burns with melatonin: an experimental study in rats." Ulus Travma Acil Cerrahi Derg **21**(6): 419-424.

Keck, M., D. H. Herndon, L. P. Kamolz, M. Frey and M. G. Jeschke (2009). "Pathophysiology of burns." Wien Med Wochenschr **159**(13-14): 327-336.

Knabl, J. S., W. Bauer, H. Andel, I. Schwendenwein, P. F. Dado, M. Mittlbock, W. Romer, M. S. Choi, R. Horvat, G. Meissl and M. Frey (1999). "Progression of burn wound depth by systemical application of a vasoconstrictor: an experimental study with a new rabbit model." Burns **25**(8): 715-721.

Kolokythas, P. and M. C. Aust (2011). Verbrennungsverletzungen. Praxis der Plastischen Chirurgie. 1. Auflage. P. M. Vogt. Berlin Heidelberg, Springer- Verlag Berlin Heidelberg New York.

Komorowska-Timek, E., L. Newlin, F. Zhang, T. Dogan, W. C. Lineaweaver and H. J. Buncke (1999). "Shortening of rat teeth prevents autocannibalization of surgical flaps." J Reconstr Microsurg **15**(4): 303-306.

Lanier, S. T., S. A. McClain, F. Lin, A. J. Singer and R. A. Clark (2011). "Spatiotemporal progression of cell death in the zone of ischemia surrounding burns." Wound Repair Regen **19**(5): 622-632.

Lindahl, F., E. Tesselaar and F. Sjoberg (2013). "Assessing paediatric scald injuries using Laser Speckle Contrast Imaging." Burns **39**(4): 662-666.

Macionis, V. (2000). "New protective system preventing self-mutilation of rat surgical sites." J Reconstr Microsurg **16**(8): 609-612.

Macri, L. K., A. J. Singer, B. R. Taira, S. A. McClain, L. Rosenberg and R. A. Clark (2013). "Immediate burn excision fails to reduce injury progression." J Burn Care Res **34**(3): e153-160.

Majno, G. and I. Joris (1995). "Apoptosis, oncosis, and necrosis. An overview of cell death." Am J Pathol **146**(1): 3-15.

Martin, N. A. and S. Falder (2017). "A review of the evidence for threshold of burn injury." Burns.

Bibliography

Martineau, L. and L. G. Chua Chiaco (2000). "Protective clear shield for dorsal surgical wound sites in the rat." Plast Reconstr Surg **105**(6): 2102-2104.

McGrath, M. H. (1981). "How topical dressings salvage "questionable" flaps: experimental study." Plast Reconstr Surg **67**(5): 653-659.

Meyerholz, D. K., T. L. Piester, J. C. Sokolich, G. K. Zamba and T. D. Light (2009). "Morphological parameters for assessment of burn severity in an acute burn injury rat model." Int J Exp Pathol **90**(1): 26-33.

Micheels, J., B. Alsbjorn and B. Sorensen (1984). "Laser doppler flowmetry. A new non-invasive measurement of microcirculation in intensive care?" Resuscitation **12**(1): 31-39.

Mileski, W., D. Borgstrom, E. Lightfoot, R. Rothlein, R. Faanes, P. Lipsky and C. Baxter (1992). "Inhibition of leukocyte-endothelial adherence following thermal injury." J Surg Res **52**(4): 334-339.

Millet, C., M. Roustit, S. Blaise and J. L. Cracowski (2011). "Comparison between laser speckle contrast imaging and laser Doppler imaging to assess skin blood flow in humans." Microvasc Res **82**(2): 147-151.

Mirdell, R., S. Farnebo, F. Sjoberg and E. Tesselaar (2017). "Accuracy of laser speckle contrast imaging in the assessment of pediatric scald wounds." Burns.

Mirdell, R., F. Iredahl, F. Sjoberg, S. Farnebo and E. Tesselaar (2016). "Microvascular blood flow in scalds in children and its relation to duration of wound healing: A study using laser speckle contrast imaging." Burns **42**(3): 648-654.

Mitsunaga Junior, J. K., A. Gragnani, M. L. Ramos and L. M. Ferreira (2012). "Rat an experimental model for burns: a systematic review." Acta Cir Bras **27**(6): 417-423.

Monstrey, S., H. Hoeksema, J. Verbelen, A. Pirayesh and P. Blondeel (2008). "Assessment of burn depth and burn wound healing potential." Burns **34**(6): 761-769.

Moritz, A. R. and F. C. Henriques (1947). "Studies of Thermal Injury: II. The Relative Importance of Time and Surface Temperature in the Causation of Cutaneous Burns." The American Journal of Pathology **23**(5): 695-720.

Murua, A., G. Orive, R. M. Hernandez and J. L. Pedraz (2011). "Emerging technologies in the delivery of erythropoietin for therapeutics." Med Res Rev **31**(2): 284-309.

Nguyen, J. Q., C. Crouzet, T. Mai, K. Riola, D. Uchitel, L. H. Liaw, N. Bernal, A. Ponticorvo, B. Choi and A. J. Durkin (2013). "Spatial frequency domain imaging of burn wounds in a preclinical model of graded burn severity." J Biomed Opt **18**(6): 66010.

Nissen , S. E. and K. Wolski (2007). "Effect of Rosiglitazone on the Risk of Myocardial Infarction and Death from Cardiovascular Causes." New England Journal of Medicine **356**(24): 2457-2471.

Oremus, M., M. D. Hanson, R. Whitlock, E. Young, C. Archer, A. Dal Cin, A. Gupta and P. Raina (2007). "A systematic review of heparin to treat burn injury." J Burn Care Res **28**(6): 794-804.

Ozkan, O. and H. E. Ozgentas (2006). "Combination of rat vest, teeth shortening, and nail cutting to prevent autocannibalization and protect surgical flaps." Plast Reconstr Surg **117**(5): 1671.

Pallua, N. and S. von Bülow (2006). "Behandlungskonzepte bei Verbrennungen." Der Chirurg **77**(1): 81-94.

Papini, R. (2004). "Management of burn injuries of various depths." BMJ : British Medical Journal **329**(7458): 158-160.

Parvizi, D., M. Giretzlehner, P. Wurzer, L. D. Klein, Y. Shoham, F. J. Bohanon, H. L. Haller, A. Tuca, L. K. Branski, D. B. Lumenta, D. N. Herndon and L. P. Kamolz (2016). "BurnCase 3D software validation study: Burn size measurement accuracy and inter-rater reliability." Burns **42**(2): 329-335.

Patel, N. S., K. K. Nandra, M. Brines, M. Collino, W. F. Wong, A. Kapoor, E. Benetti, F. Y. Goh, R. Fantozzi, A. Cerami and C. Thiemermann (2011). "A nonerythropoietic peptide that mimics the 3D structure of erythropoietin reduces organ injury/dysfunction and inflammation in experimental hemorrhagic shock." Mol Med **17**(9-10): 883-892.

Pfurtscheller, K., T. Petnehazy, W. Goessler, I. Wiederstein-Grasser, V. Bubalo and M. Trop (2013). "Innovative scald burn model and long-term dressing protector for studies in rats." J Trauma Acute Care Surg **74**(3): 932-935.

Ponticorvo, A., D. M. Burmeister, R. Rowland, M. Baldado, G. T. Kennedy, R. Saager, N. Bernal, B. Choi and A. J. Durkin (2017). "Quantitative long-term measurements of burns in a rat model using Spatial Frequency Domain Imaging (SFDI) and Laser Speckle Imaging (LSI)." Lasers Surg Med **49**(3): 293-304.

Ponticorvo, A. and A. K. Dunn (2010). "How to build a Laser Speckle Contrast Imaging (LSCI) system to monitor blood flow." J Vis Exp(45).

Poranki, D., C. Goodwin and M. Van Dyke (2016). "Assessment of Deep Partial Thickness Burn Treatment with Keratin Biomaterial Hydrogels in a Swine Model." Biomed Res Int **2016**: 1803912.

Prindeze, N. J., H. A. Hoffman, J. G. Ardanuy, J. Zhang, B. C. Carney, L. T. Moffatt and J. W. Shupp (2016). "Active Dynamic Thermography is a Sensitive Method for Distinguishing Burn Wound Conversion." J Burn Care Res **37**(6): e559-e568.

Proano, E., L. Svensson and L. Perbeck (1997). "Correlation between the uptake of sodium fluorescein in the tissue and xenon-133 clearance and laser Doppler fluxmetry in measuring changes in skin circulation." Int J Microcirc Clin Exp **17**(1): 22-28.

Pynn, B. R., N. H. McKee, C. A. Nigra and C. R. Howard (1983). "A protective rat vest." Plast Reconstr Surg **71**(5): 716-717.

Bibliography

Qin, J., R. Reif, Z. Zhi, S. Dziennis and R. Wang (2012). "Hemodynamic and morphological vasculature response to a burn monitored using a combined dual-wavelength laser speckle and optical microangiography imaging system." Biomedical Optics Express **3**(3): 455-466.

Reddy, A. S., A. Abraham, S. A. McClain, R. A. Clark, P. Ralen, S. Sandoval and A. J. Singer (2015). "The Role of Necroptosis in Burn Injury Progression in a Rat Comb Burn Model." Acad Emerg Med **22**(10): 1181-1186.

Regas, F. C. and H. P. Ehrlich (1992). "Elucidating the vascular response to burns with a new rat model." J Trauma **32**(5): 557-563.

Reggiori, F. and D. J. Klionsky (2002). "Autophagy in the eukaryotic cell." Eukaryot Cell **1**(1): 11-21.

Rizzo, J. A., P. Burgess, R. J. Cartie and B. M. Prasad (2013). "Moderate systemic hypothermia decreases burn depth progression." Burns **39**(3): 436-444.

Rowan, M., L. Cancio, E. Elster, D. Burmeister, L. Rose, S. Natesan, R. Chan, R. Christy and K. Chung (2015). "Burn wound healing and treatment: review and advancements." Critical Care **19**(1): 243.

Sakamoto, M., N. Morimoto, S. Ogino, C. Jinno, A. Kawaguchi, K. Kawai and S. Suzuki (2016). "Preparation of Partial-Thickness Burn Wounds in Rodents Using a New Experimental Burning Device." Ann Plast Surg **76**(6): 652-658.

Salibian, A. A., A. T. D. Rosario, L. A. M. Severo, L. Nguyen, D. A. Banyard, J. D. Toranto, G. R. D. Evans and A. D. Widgerow (2016). "Current concepts on burn wound conversion-A review of recent advances in understanding the secondary progressions of burns." Burns **42**(5): 1025-1035.

Schabauer, A. M. A. and T. W. Rooke (1994). "Cutaneous Laser Doppler Flowmetry: Applications and Findings." Mayo Clinic Proceedings **69**(6): 564-574.

Scheinfeld, N. (2004). "A comprehensive review and evaluation of the side effects of the tumor necrosis factor alpha blockers etanercept, infliximab and adalimumab." J Dermatolog Treat **15**(5): 280-294.

Schmauss, D., F. Rezaeian, T. Finck, H. G. Machens, R. Wettstein and Y. Harder (2015). "Treatment of secondary burn wound progression in contact burns-a systematic review of experimental approaches." J Burn Care Res **36**(3): e176-189.

Schmauss, D., A. Weinzierl, F. Weiss, J. T. Egana, F. Rezaeian, U. Hopfner, V. Schmauss, H. G. Machens and Y. Harder (2019). "Long-term pre- and postconditioning with low doses of erythropoietin protects critically perfused musculocutaneous tissue from necrosis." J Plast Reconstr Aesthet Surg **72**(4): 590-599.

Schmauss, D., R. Wettstein, M. Tobalem, H. Machens, F. Rezaeian and Y. Harder (2014). "New treatment strategies to reduce burn wound progression." GMS Ger Plast Reconstr Aesthet Surg **4**(Doc01).

Bibliography

Sen, C. K., S. Ghatak, S. C. Gnyawali, S. Roy and G. M. Gordillo (2016). "Cutaneous Imaging Technologies in Acute Burn and Chronic Wound Care." Plast Reconstr Surg **138**(3 Suppl): 119s-128s.

Senarathna, J., A. Rege, N. Li and N. V. Thakor (2013). "Laser Speckle Contrast Imaging: theory, instrumentation and applications." IEEE Rev Biomed Eng **6**: 99-110.

Sharar, S. R., R. K. Winn, C. E. Murry, J. M. Harlan and C. L. Rice (1991). "A CD18 monoclonal antibody increases the incidence and severity of subcutaneous abscess formation after high-dose Staphylococcus aureus injection in rabbits." Surgery **110**(2): 213-219; discussion 219-220.

Shen, Y. I., H. G. Song, A. Papa, J. Burke, S. W. Volk and S. Gerecht (2015). "Acellular Hydrogels for Regenerative Burn Wound Healing: Translation from a Porcine Model." J Invest Dermatol **135**(10): 2519-2529.

Sheridan, R. L. and P. Chang (2014). "Acute burn procedures." Surg Clin North Am **94**(4): 755-764.

Shupp, J. W., T. J. Nasabzadeh, D. S. Rosenthal, M. H. Jordan, P. Fidler and J. C. Jeng (2010). "A review of the local pathophysiologic bases of burn wound progression." J Burn Care Res **31**(6): 849-873.

Singer, A. J. and A. B. Dagum (2008). "Current Management of Acute Cutaneous Wounds." New England Journal of Medicine **359**(10): 1037-1046.

Singer, A. J., S. A. McClain, A. Romanov, J. Rooney and T. Zimmerman (2007). "Curcumin reduces burn progression in rats." Acad Emerg Med **14**(12): 1125-1129.

Singer, A. J., S. A. McClain, B. R. Taira, J. L. Guerriero and W. Zong (2008). "Apoptosis and necrosis in the ischemic zone adjacent to third degree burns." Acad Emerg Med **15**(6): 549-554.

Singer, A. J., S. A. McClain, B. R. Taira, A. Romanov, J. Rooney and T. Zimmerman (2009). "Validation of a porcine comb burn model." Am J Emerg Med **27**(3): 285-288.

Singer, A. J., S. A. McClain, B. R. Taira, J. Rooney, N. Steinhauff and L. Rosenberg (2010). "Rapid and selective enzymatic debridement of porcine comb burns with bromelain-derived Debrase: acute-phase preservation of noninjured tissue and zone of stasis." J Burn Care Res **31**(2): 304-309.

Singer, A. J., B. R. Taira, F. Lin, T. Lim, R. Anderson, S. A. McClain and R. A. Clark (2011). "Curcumin reduces injury progression in a rat comb burn model." J Burn Care Res **32**(1): 135-142.

Singer, D. D., A. J. Singer, C. Gordon and P. Brink (2013). "The effects of rat mesenchymal stem cells on injury progression in a rat model." Acad Emerg Med **20**(4): 398-402.

Singh, V., L. Devgan, S. Bhat and S. M. Milner (2007). "The pathogenesis of burn wound conversion." Ann Plast Surg **59**(1): 109-115.

Singh-Joy, S. D. and V. C. McLain (2008). "Safety assessment of poloxamers 101, 105, 108, 122, 123, 124, 181, 182, 183, 184, 185, 188, 212, 215, 217, 231, 234, 235, 237, 238, 282, 284, 288, 331, 333, 334, 335, 338, 401, 402, 403, and 407, poloxamer 105 benzoate, and poloxamer 182 dibenzoate as used in cosmetics." Int J Toxicol **27 Suppl 2**: 93-128.

Spies, M. and P. M. Vogt (2008). Verbrennungen. Duale Reihe Chirurgie. 3. Auflage. D. Henne-Bruns, B. Kremer and M. Dürig. Stuttgart, Germany, Thieme**:** 906-925.

Stewart, C. J., R. Frank, K. R. Forrester, J. Tulip, R. Lindsay and R. C. Bray (2005). "A comparison of two laser-based methods for determination of burn scar perfusion: laser Doppler versus laser speckle imaging." Burns **31**(6): 744-752.

Stewart, C. J., C. L. Gallant-Behm, K. Forrester, J. Tulip, D. A. Hart and R. C. Bray (2006). "Kinetics of blood flow during healing of excisional full-thickness skin wounds in pigs as monitored by laser speckle perfusion imaging." Skin Res Technol **12**(4): 247-253.

Stone Ii, R., S. Natesan, C. J. Kowalczewski, L. H. Mangum, N. E. Clay, R. M. Clohessy, A. H. Carlsson, D. H. Tassin, R. K. Chan, J. A. Rizzo and R. J. Christy (2018). "Advancements in Regenerative Strategies Through the Continuum of Burn Care." Front Pharmacol **9**: 672.

Sun, L. T., E. Friedrich, J. L. Heuslein, R. E. Pferdehirt, N. M. Dangelo, S. Natesan, R. J. Christy and N. R. Washburn (2012). "Reduction of Burn Progression with Topical Delivery of (Anti-Tumor Necrosis Factor-α)-Hyaluronic Acid Conjugates." Wound Repair and Regeneration **20**(4): 563-572.

Tagkalakis, P., A. Dionyssopoulos, G. Karkavelas and E. Demiri (2015). "Topical use of Rectogesic® and Emla® to improve cutaneous blood perfusion following thermal injury. A comparative experimental study." Annals of Burns and Fire Disasters **28**(2): 134-141.

Taira, B. R., A. J. Singer, S. A. McClain, F. Lin, J. Rooney, T. Zimmerman and R. A. Clark (2009). "Rosiglitazone, a PPAR-gamma ligand, reduces burn progression in rats." J Burn Care Res **30**(3): 499-504.

Taira, B. R., A. J. Singer, H. C. Thode, Jr. and C. Lee (2010). "Burns in the emergency department: a national perspective." J Emerg Med **39**(1): 1-5.

Tan, J. Q., H. H. Zhang, Z. J. Lei, P. Ren, C. Deng, X. Y. Li and S. Z. Chen (2013). "The roles of autophagy and apoptosis in burn wound progression in rats." Burns **39**(8): 1551-1556.

Tenenhaus, M. and H. O. Rennekampff (2012). "Surgical advances in burn and reconstructive plastic surgery: new and emerging technologies." Clin Plast Surg **39**(4): 435-443.

Thallmair, M. (2015, 10/09/2017). "Merkblatt 04/2015: Analgesie Buprenorphin Ratte." from http://www.tierschutz.uzh.ch/dam/jcr:ffffffff-a9e4-863e-0000-0000462fb202/Merkblatt_Dosierungsempfehlung_BuP_Ratte_27_04_2015_Englisch.pdf.

Bibliography

Tiwari, V. K. (2012). "Burn wound: How it differs from other wounds?" Indian Journal of Plastic Surgery : Official Publication of the Association of Plastic Surgeons of India **45**(2): 364-373.

Tobalem, M., Y. Harder, F. Rezaeian and R. Wettstein (2013). "Secondary burn progression decreased by erythropoietin." Crit Care Med **41**(4): 963-971.

Tobalem, M., Y. Harder, T. Schuster, F. Rezaeian and R. Wettstein (2012). "Erythropoietin in the prevention of experimental burn progression." Br J Surg **99**(9): 1295-1303.

Tobalem, M., Y. Harder, E. Tschanz, V. Speidel, B. Pittet-Cuenod and R. Wettstein (2013). "First-aid with warm water delays burn progression and increases skin survival." J Plast Reconstr Aesthet Surg **66**(2): 260-266.

Tobalem, M., R. Wettstein, E. Tschanz, J. Plock, N. Lindenblatt, Y. Harder and F. Rezaeian (2019). "The burn comb model revisited." Burns.

Ueda, M., S. Torii and T. Oka (1981). "A new device for free skin grafting in rats." Plastic and reconstructive surgery **67**(5): 671-672.

Uraloglu, M., M. Livaoglu, O. Agdogan, S. Ersoz and N. Karacal (2018). "The effect of low molecular weight heparin on salvaging the zone of stasis in an experimental burn model." Turk J Med Sci **48**(3): 653-660.

Uygur, F., R. Evinc, M. Urhan, B. Celikoz and A. Haholu (2009). "Salvaging the zone of stasis by simvastatin: an experimental study in rats." J Burn Care Res **30**(5): 872-879.

Wachtel, T. L., C. C. Berry, E. E. Wachtel and H. A. Frank (2000). "The inter-rater reliability of estimating the size of burns from various burn area chart drawings." Burns **26**(2): 156-170.

Waitzman, A. A. and P. C. Neligan (1993). "How to manage burns in primary care." Can Fam Physician **39**: 2394-2400.

Wallace, A. B. (1951). "The exposure treatment of burns." Lancet **1**(6653): 501-504.

Wang, C. Z., A. E. Ayadi, J. Goswamy, C. C. Finnerty, R. Mifflin, L. Sousse, P. Enkhbaatar, J. Papaconstantinou, D. N. Herndon and N. H. Ansari (2015). "Topically applied metal chelator reduces thermal injury progression in a rat model of brass comb burn." Burns **41**(8): 1775-1787.

Wang, W. Y., P. W. Hsieh, Y. C. Wu and C. C. Wu (2007). "Synthesis and pharmacological evaluation of novel beta-nitrostyrene derivatives as tyrosine kinase inhibitors with potent antiplatelet activity." Biochem Pharmacol **74**(4): 601-611.

Wiechman, S. A. and D. R. Patterson (2004). "Psychosocial aspects of burn injuries." BMJ : British Medical Journal **329**(7462): 391-393.

Wilkinson, E. (1998). "The epidemiology of burns in secondary care, in a population of 2.6 million people." Burns **24**(2): 139-143.

Bibliography

Xiao, M., L. Li, Q. Hu, L. Ma, L. Liu, W. Chu and H. Zhang (2013). "Rapamycin reduces burn wound progression by enhancing autophagy in deep second-degree burn in rats." Wound Repair Regen **21**(6): 852-859.

Xiao, M., L. Li, C. Li, L. Liu, Y. Yu and L. Ma (2016). "3,4-Methylenedioxy-β-Nitrostyrene Ameliorates Experimental Burn Wound Progression by Inhibiting the NLRP3 Inflammasome Activation." Plastic and Reconstructive Surgery **137**(3): 566e-575e.

Xiao, M., L. Li, C. Li, P. Zhang, Q. Hu, L. Ma and H. Zhang (2014). "Role of autophagy and apoptosis in wound tissue of deep second-degree burn in rats." Acad Emerg Med **21**(4): 383-391.

Yuan, J., C. Wu, A. J. Holland, J. G. Harvey, H. C. Martin, E. R. La Hei, S. Arbuckle and T. C. Godfrey (2007). "Assessment of cooling on an acute scald burn injury in a porcine model." J Burn Care Res **28**(3): 514-520.

Yuhua, S., L. Ligen, C. Jiake and S. Tongzhu (2012). "Effect of Poloxamer 188 on deepening of deep second-degree burn wounds in the early stage." Burns **38**(1): 95-101.

Zötterman, J., R. Mirdell, S. Horsten, S. Farnebo and E. Tesselaar (2017). "Methodological concerns with laser speckle contrast imaging in clinical evaluation of microcirculation." PLOS ONE **12**(3): e0174703.

13 Acknowledgements

I would like to thank my supervisor Prof. Dr. med. Yves Harder for entrusting me with the responsibility of this project and his support in the research group after my work on another model (mouse skin flap) did not succeed as hoped. His patience, ongoing support and academic reasoning helped me not only to master the used burn comb model but also learn scientific project design and examination of results and their interpretation. I also thank Univ.-Prof. Dr. med. Hans-Günther Machens for allowing me to use the scientific environment of his department.

I also express my gratitude to PD Dr. med. Daniel Schmauss who was a great and reliable mentor. He chaperoned my work from beginning to end including the study design, discussing results as well as giving constructive feedback while writing and presenting my work. Without his outstanding support, his prompt availability and his personal advice, I would not have been able to finish this project.

I am extremely thankful for the help of the two histopathologists PD Dr. med. Melissa Schlitter and Dr. med. vet. Katja Steiger who assessed the burn depth. Especially Dr. Schlitter took several hours of her valuable time to rate slides, explain the findings and help with digitalizing. I'd also like to thank Petra Meyer from the Pathology Institute who helped me with staining and cutting the slides in an extraordinary quality.

I would also like to thank the other group members Anna Schuldt, Kariem Agua and Andrea Weinzierl without whom the laboratory work would not have been as interesting or as intellectually challenging. As much as I enjoyed thinking outside the box on their research projects, even more, I am thankful for their mutual support and helping hands when working with animals. This thank also goes to the ZPF-team of vet nurses, animal keepers and veterinarians whose daily animal care lightened not only my work but also the animal's quality of life.

I also express my thanks to Ursula Hopfner and Manuela Kirsch who introduced me to the laboratory work outside the animal facilities and offered their advice on all kinds of research tools. I also thank José Tomás Egaña for the financial support by allocating funds for experimental animals.

Additionally, I gratefully acknowledge Dr. Bernhard Haller and Dr. Alexander Hapfelmeier who offered the biweekly "Statistisches Kolloquium". They patiently explained correct data input and assisted exceedingly with the development of the applied statistic model.

Acknowledgements

I'm thankful for scientific peer group offered by the TUM Graduate School and the doctoral program "Translationale Medizin" through which I matched this research group. The gained interdisciplinary qualifications also inspire to put scientific results into context. I'm honored to be a part of this program and would like to thank the numerous involved teachers and professors.

Last but not least, I would like to thank my parents Martha and Erwin. I dedicate this work to them since without their love and support I would not have been able to study, start this project or have the endurance to finish it. Danke!

14 Attachments

Anesthesia Dosage Table Rats (ZPF Klinikum rechts der Isar München)

Tierart: Ratte

Wirkstoff	Medetomidin	Midazolam	Fentanyl		Wirkstoff	Atipamezol	Flumazenil	Naloxon	
mg/ml	1	5	0,05		mg/ml	5	0,1	0,4	
Anmischung für 5 kg (ml)	0,8	2	0,5	3,3	Anmischung für 5 kg (ml)	0,75	10	1,5	12,25
Gewicht in g	mg/kg	mg/kg	mg/kg	Mischung in ml	Gewicht in g	mg/kg	mg/kg	mg/kg	Mischung in ml
100	0,15	0,2	0,0005	0,07	100	0,075	0,02	0,012	0,25
125	0,1875	0,25	0,000625	0,08	125	0,09375	0,025	0,015	0,31
150	0,225	0,3	0,00075	0,1	150	0,1125	0,03	0,018	0,37
175	0,2625	0,35	0,000875	0,11	175	0,13125	0,035	0,021	0,43
200	0,3	0,4	0,001	0,13	200	0,15	0,04	0,024	0,49
225	0,3375	0,45	0,001125	0,15	225	0,16875	0,045	0,027	0,55
250	0,375	0,5	0,00125	0,16	250	0,1875	0,05	0,03	0,61
275	0,4125	0,55	0,001375	0,18	275	0,20625	0,055	0,033	0,67
300	0,45	0,6	0,0015	0,2	300	0,225	0,06	0,036	0,74
325	0,4875	0,65	0,001625	0,21	325	0,24375	0,065	0,039	0,8
350	0,525	0,7	0,00175	0,23	350	0,2625	0,07	0,042	0,86
375	0,5625	0,75	0,001875	0,24	375	0,28125	0,075	0,045	0,92
400	0,6	0,8	0,002	0,26	400	0,3	0,08	0,048	0,98
425	0,6375	0,85	0,002125	0,28	425	0,31875	0,085	0,051	1,04
450	0,675	0,9	0,00225	0,29	450	0,3375	0,09	0,054	1,1
475	0,7125	0,95	0,002375	0,31	475	0,35625	0,095	0,057	1,16
500	0,75	1	0,0025	0,33	500	0,375	0,1	0,06	1,23
525	0,7875	1,05	0,002625	0,34	525	0,39375	0,105	0,063	1,29
550	0,825	1,1	0,00275	0,36	550	0,4125	0,11	0,066	1,35
575	0,8625	1,15	0,002875	0,37	575	0,43125	0,115	0,069	1,41
600	0,9	1,2	0,003	0,39	600	0,45	0,12	0,072	1,47
625	0,9375	1,25	0,003125	0,41	625	0,46875	0,125	0,075	1,53
650	0,975	1,3	0,00325	0,42	650	0,4875	0,13	0,078	1,59
675	1,0125	1,35	0,003375	0,44	675	0,50625	0,135	0,081	1,65
700	1,05	1,4	0,0035	0,46	700	0,525	0,14	0,084	1,72
725	1,0875	1,45	0,003625	0,47	725	0,54375	0,145	0,087	1,78
750	1,125	1,5	0,00375	0,49	750	0,5625	0,15	0,09	1,84
775	1,1625	1,55	0,003875	0,5	775	0,58125	0,155	0,093	1,9
800	1,2	1,6	0,004	0,52	800	0,6	0,16	0,096	1,96
825	1,2375	1,65	0,004125	0,54	825	0,61875	0,165	0,099	2,02
850	1,275	1,7	0,00425	0,55	850	0,6375	0,17	0,102	2,08
875	1,3125	1,75	0,004375	0,57	875	0,65625	0,175	0,105	2,14
900	1,35	1,8	0,0045	0,59	900	0,675	0,18	0,108	2,21
925	1,3875	1,85	0,004625	0,6	925	0,69375	0,185	0,111	2,27
950	1,425	1,9	0,00475	0,62	950	0,7125	0,19	0,114	2,33
975	1,4625	1,95	0,004875	0,63	975	0,73125	0,195	0,117	2,39
1000	1,5	2	0,005	0,65	1000	0,75	0,2	0,12	2,45